POLITECNICO DI MILANO

SCHOOL OF INDUSTRIAL AND INFORMATION ENGINEERING

DEPARTMENT OF AEROSPACE SCIENCE AND TECHNOLOGY (DAER)

MASTER OF SCIENCE IN SPACE ENGINEERING

Precision Farming and Sustainability: Optimisation of a Radar Microsatellites Constellation for Italian Agriculture

---

Supervisor
Camilla COLOMBO
Co-Supervisors
Luca SOLI
Franco BERNELLI ZAZZERA

Author
Vittorio SARTORETTO
Student ID 903452

A.A. 2020-2021

This content is original, written by the Author, Vittorio Sartoretto. All the non-originals information, taken from previous works, are specified and recorded in the Bibliography. This work has been developed as a collaboration between Politecnico di Milano and Thales Alenia Space Italia S.p.A..

When referring to this work, full bibliographic details must be given, i.e.

Vittorio Sartoretto, "Precision Farming and Sustainability: Optimisation of a Radar Microsatellites Constellation for Italian Agriculture". 2021, Politecnico di Milano, Faculty of Industrial Engineering, Department of Aerospace Science and Technologies, Master in Space Engineering, Thales Alenia Space S.p.A., Supervisors: Camilla Colombo, Luca Soli, Franco Bernelli Zazzera

Printed in Italy

Abstract

Satellites are proving to be more and more useful in several areas, not only telecommunications; one of these is agriculture. Current social, economic and environmental changes require agriculture to become more productive and efficient while decreasing the environmental footprint and the cultivated area. Precision farming, which is a modern concept using digital techniques to monitor and optimise agricultural production processes, has proven to be the correct solution. Precision farming relies on several measurements of the crop status to guide decision-making. However, huge fields and crop phenology requires an instrument with large access area, that do not need continuous human piloting and capable of providing recursive passages, even over a single day. Therefore, satellites are very suitable platforms for carrying the sensors needed in agriculture, thanks to their altitude and intrinsic characteristics. Moreover, satellites can be arranged in a constellation, and this allows providing several measurements of the same site in a short period. As the number of satellites increases in a constellation, their dimension can decrease, decreasing the overall cost as well, while maintaining high performances. However, designing a constellation is a challenge, as there are no general rules. The high expenses, the safety treat to space and the design and computational effort increase the difficulty. The design shall take into account several drivers in a trade-off manner. There are two types of sensors for Earth observation, optical and infrared sensors and microwave sensors. In this work, a model capable of computing the main characteristics of a microsatellites constellation with synthetic aperture radar sensors has been designed. This model has then been used through a multi-criteria constellation design, where several properties are assessed. Each of these properties represents a constellation performance or cost. In particular, a multi-objective optimisation based on a genetic algorithm has been employed in order to find few optimal constellations that satisfy the mission requirements of the Italian agriculture use case. Part of the work has been devoted to retrieving the requirements starting from the state of the art and the user needs (Italian farmers and Italian agriculture as a whole). A final effort has been made in estimating the economic, social and environmental benefits that precision farming, through satellites data, can provide. This work finds itself in the context of the new European project called *A Green New Deal*, which pushes for the use of space data in the context of agriculture because of their huge applicability. Moreover, thanks to the European project called *Recovery plan for Europe* the Italian government might fund the project of a mixed optical-radar constellation of remote sensing of the Italian territory. This work has been developed as a collaboration between the Polytechnic University of Milan and Thales Alenia Space Italia S.p.A..

Keywords: Earth Remote Sensing, Low Earth Orbit, Constellation Design, Agriculture, Synthetic Aperture Radar, Multi-Objective Optimisation

Contents

List of Tables

List of Figures

Chapter 1

Introduction

1.1 Background

The dramatic increase in population, experienced worldwide between the second part of the last century and the first part of the ongoing century, will most probably continue in the upcoming future. This grows put huge stress on the food market, as the number of people continuously increases. At the same time, social changes are shifting the diets of many people. The number of malnourished and undernourished people is constantly decreasing, but it is still high in developing countries. On the other side, the climate change issue requires lower emissions, lower energy consumption and lower land exploitation. Finally, water consumption is becoming more and more important as water shortages are happening more frequently in all countries. These facts have several consequences on the food production process, especially on agriculture, which is the first big step in the food production chain. Essentially, a strong effort is required from agriculture to meet the increasing demand and the constraints imposed by the environment. In general, agriculture shall increase its production and efficiency while decreasing the land exploited, the environmental impact and water consumption. This means to produce more while consuming less, respecting the environment and especially reducing the intake of chemicals. Some countries are already moving in this direction, in particular, the European Union with its Green New Deal [107]. During this change, agriculture is strongly supported by technology. Digitalisation is more and more central in agriculture, and even with recent tools as artificial intelligence and the internet of things. In particular, there is an approach for agriculture that exploit digital and mechanical technologies in order to increase efficiency. This is called precision farming or precision agriculture. It is a different way of growing a crop, where each action is measured and based on scientific data. Each characteristic of a crop is constantly measured, then the data acquired feed a digital crop model that in turn tells the farmer what to do, when and how. This procedure allows them be very efficient, treating each plant according to their actual needs and health. In the end, the yield is maximised, the quality of the products is higher, the number of inputs are reduced, especially chemicals and water, and the soil is not under constant stress. The farmer is not the only one who benefits from these improvements. Everybody can get something, as the quantity and quality of food are higher and the environmental footprint is reduced. Many years of precision farming have finally proved that it is a possible solution for the increasing stress that is put on agriculture by the world

population and for the stress that agriculture puts on the environment. Mechanical devices, such as machinery and tractors, are part of this process, as they allow the farmer to take very accurate actions in the filed. As the precision of these tools is constantly increasing, they require more and more precise data that feed the digital models that determine the instruction to command them. Otherwise, their capabilities are simply wasted and the farmer cannot exploit the maximum potentialities of the field. Therefore, the request for more and more accurate data about the agricultural filed is increasing and is also needed to tackle all the problems that agriculture is facing. There are a couple of instruments that can measure the properties, such as the health, of a crop. These can be electric or chemical in situ-sensors, optical and infrared sensors and microwave sensors. The last two are usually carried by aeroplane, a UAV or even a satellite. Optical and microwave sensors are both valid information providers, however, microwave sensors, in particular a SAR, has the advantage that it can operate any time during any weather condition. Moreover, it can also penetrate the target, allowing to study its internal conditions. A satellite can carry onboard a microwave sensor. The advantage, with respect to a UAV or an aeroplane, is that it can access a larger area and it can operate for years without continuous piloting as an aeroplane requires. Due to the high power consumption, that depends on the distance from the ground, a satellite that carries a microwave sensor is almost forced to fly on a low Earth orbit. SAR instrument are available even at small size (less than 100 kg), and this makes them suitable to be carried in small satellites. In addition, satellites can be organized in a constellation. Despite the increasing number of satellites, a constellation usually leads to high performances. The advantage of using a small satellites, rather than massive ones, is that the total number of space segments can be easily increased, making it possible to arrange them in a constellation, without skyrocketing the price. Although the small SAR has lower performances than a bigger one, the small but higher number of satellites allow compensating. Therefore, a constellation of small satellites in LEO (low Earth orbit) is a good alternative to few big satellites for Earth observation (more precisely it is complementary). On the other hand, a constellation has also some drawbacks. It became clear that constellations of small satellites embedded with a synthetic aperture radar, that produce images for agriculture, is a central topic of this work. Designing a constellation is a complex task, and there are no general rules that can drive the design process. One complication, that is maybe the biggest one, comes from the fact that there are several parameters to be selected. A small change in some parameters can have a huge impact on the final result. Therefore, the number of possibilities for the final design is very high (in the order of millions and even more). Exploring all of them is impossible, and then a different solution shall be found, in order to reach a final design that is compliant with the requirements and is not oversized. The multi-criteria constellation design through property assessment used in this work is based on the research done by Huang et al. [62]. It is the core of this work to define a method capable of designing a constellation of SAR microsatellites that produces images for Italian agriculture. We will start this process by analysing more deeply the power of precision agriculture and why satellites (in particular SAR satellites) are such a useful part of precision agriculture. Then, throughout the analysis of the state of the art, in terms of current SAR missions, and user needs we will draw the mission requirements. The central and last part of this work is devoted to the definition and implementation of the tool for constellation analysis and optimisation. By the end of the thesis, we will find some possible constellations that satisfy our requirements. This work has

been developed as a collaboration between Thales Alenia Space Italia S.p.A. and Politecnico di Milano.

1.2 State of the art

Some constellations, civilian and commercial, that acquire SAR images are already available. Most of them produce images for agriculture as well. Sentinel-1 satellites of the European Copernicus programme provide free access to all of its products [27]. On the other side, commercial constellations offer high-quality images but not for free. This distinction between commercial and civilian missions, and their products, lays at the basis of the requirements definition. The analysis of the current SAR missions is deepened in Chapter 4. On the other side, constellation design is a complex task and no general rules exist. Few tools allow analysing the performances of a constellation, one of them is the STK (Systems Tool Kit) platform [4]. Although its high reliability, this tool allows the user to compute one configuration at a time. In the case of small satellites constellations, where the number of possible configurations explodes rapidly, it is not feasible to test all of them. The fastest way to solve this issue is to use numerical optimisation. However, it may not be easy to find a reliable and free tool that joins the constellation analysis and its optimisation. Finally, few attempts were made for estimating the profitability of precision agriculture on a national scale and this contributes to increase the value and, the complexity of the analysis we have done

1.3 Scope of the thesis

The scope of this work is bivalent. First, we want to build a model that computes the set of optimal solutions, in terms of constellation design, that respect the requirements we impose, throughout multi-objective genetic algorithm optimisation. This model will comprise an orbital propagator and a SAR model so that we have a high degree of control on both. This customised model allows us to tune the input parameters and have full control over the design of the constellations. The second scope is a direct result of the first one. Indeed, though the implementation of the model we build, we will find optimal constellation designs. These are of particular interest to the space industry, and the results we will find, represent a first mission analysis for the case study. Moreover, we will derive the requirements from the user needs and the current state of the art. Considering the actual offer in terms of SAR images from LEO satellites and constellation (civilian and commercial) we will be able to understand which are the current services and their limits or complications. This analysis will be complemented with the analysis of the user needs, based on the study of Italian agriculture. In this way, the requirements will be specifically tailored for the use case under consideration. In the end, we will also try to estimate the advantages (under several levels) that such a constellation of SAR microsatellites can bring, in particular to Italian agriculture.

1.4   Structure of the thesis

The first three chapter, after this one, recall the facts exposed in the *Background* section above. Indeed the second chapter presents which the main global issues connected with agriculture and present precision farming as a possible solution. Within the same chapter, the connection between precision farming and satellites is shown. Chapter 3 introduces the basics of synthetic aperture radar and its application in agriculture. The main missions for Earth observation that exploit a SAR are described in Chapter 4. At the end of this chapter, there is a small part that analyses which are the lacks, complication and limits of the current SAR mission, contextualised in the agriculture applications. Chapter 5 describes and analyses the main features of Italian agriculture from several points of view. This analysis is reflected in Chapter 6, along with that done in Chapter 4. Indeed, Chapter 6 lists the requirements that originate from the needs of Italian agriculture and the current offer in terms of SAR images from other satellites and constellation. Chapter 7 presents and describe the theory behind the model we have built, in order to compute the main properties of a constellation. Chapter 8 clarifies how we have exploited the multi-objective genetic algorithm optimisation and in particular, is clearly states the cost functions used. The results of the optimisation are presented in Chapter 9. These are differentiated in a Sun-synchronous case and a general case. Finally, the last chapter tries to compute and estimate the economic, social and environmental advantages brought by improvements in agriculture as a direct consequence of the SAR images produced by the constellation of satellites.

Chapter 2

World agriculture and problems statement

During the 21st century, agriculture will face several challenges. None of them should be neglected as they lead to dramatic socio-economic and environmental effects. We will try to sum up some of the fundamental characteristics of agriculture, then the crucial challenges it is expected to undergo and define which are their implications and what is required in order to answer these challenges. According to FAO, in 2016 global agricultural land area was 4.9 billion hectares, about 32% of the Earth's terrestrial surface. 1.6 billion ha of this land was cropland, increased by 0.3% over the previous ten-year period, and 3.3 billion ha were used for permanent meadows and pasture, decreased by 0.1% over the previous ten-year period [48]. Globally, only 62% of the crop production is allocated to human food while the rest is used to produce food indirectly, about 35%, and for bioenergy [48]. Agriculture has a strong impact on the environment as well. It is responsible for more than 30% of the global greenhouse emissions, irrigation exploits 70% of global freshwater withdrawals and rain-fed agriculture represents the world's largest employment of water [47]. Agriculture emissions of CO_2 overcame 5 million gigagrams per year, and they are expected to grow. In addition, the usage of fertilizer and pesticides increased by more than 30% between 2000 and 2017. The trend of some of the most important parameters for agriculture during the time span starting from 2000 is shown in Figure 2.1. The data shown in Figure 2.1 are retrieved from FAO data centre [49].
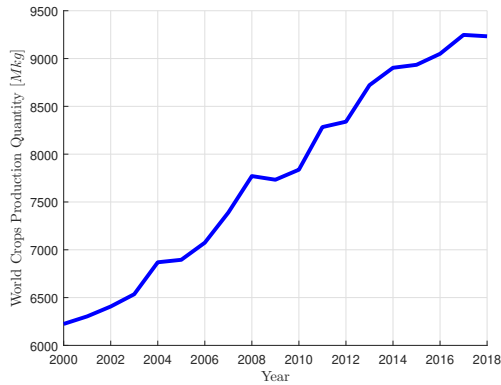
(a) World crops production quantity over time
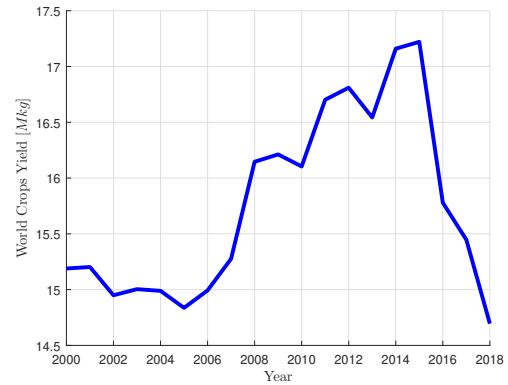
(b) World crops yield quantity over time
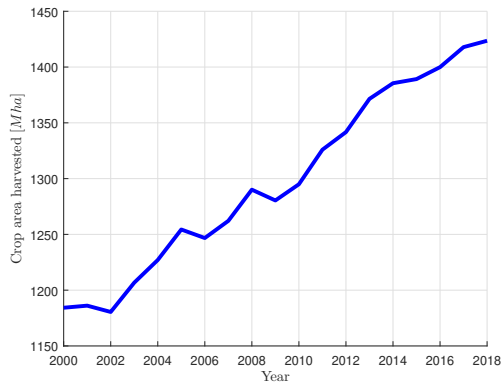
(c) World area harvested over time
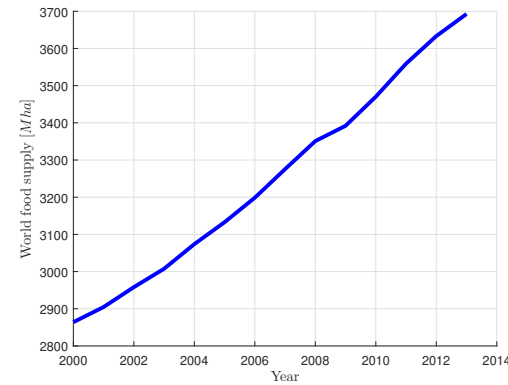
(d) World food supply over time
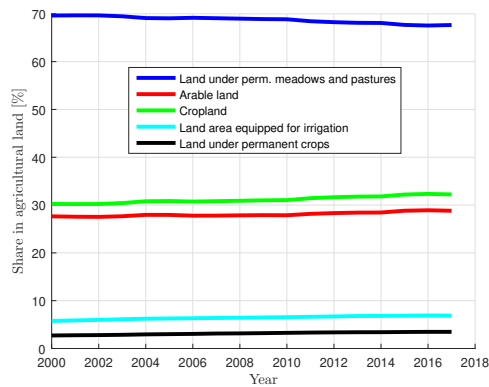
(e) World land indicators over time
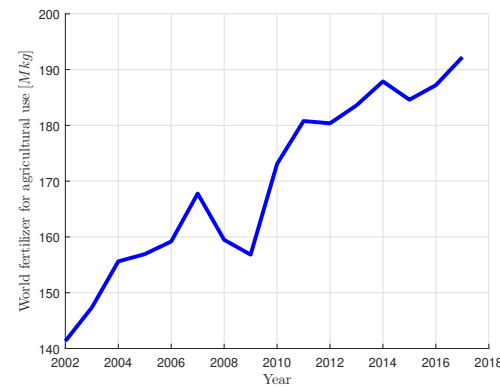
(f) World fertilizers use in agriculture over time
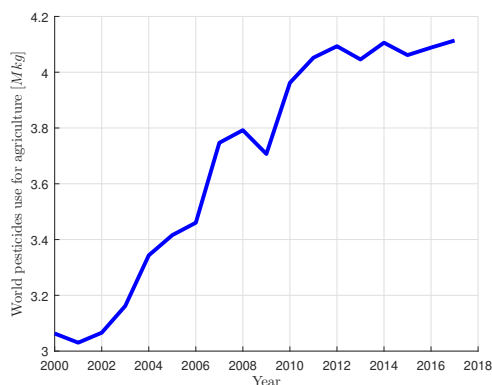
(g) World pesticides use in agriculture over time
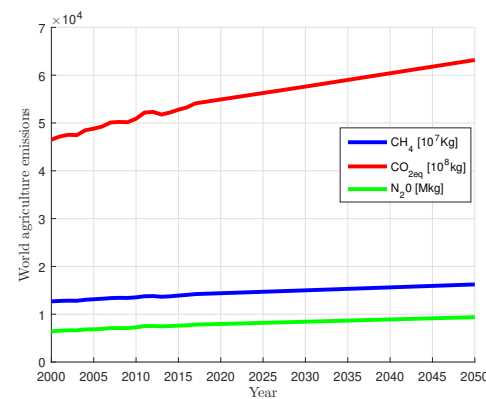
(h) World agriculture CO_2, CH_4, and N_2O emissions over time
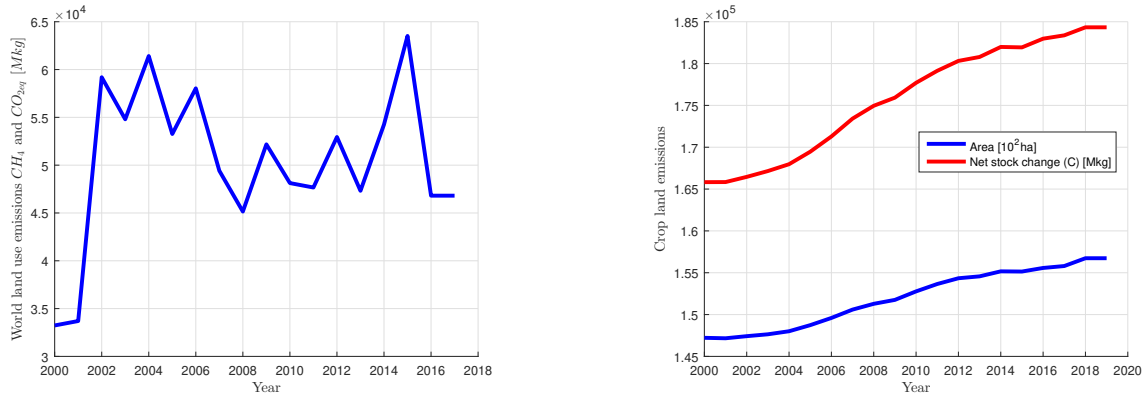
(i) World land use CO_2 emissions over time

(j) World net stock change from cropland over time

Figure 2.1: World agriculture indicators and main features in time [49]

First of all, global population will grow from the actual 7.79 billion in 2020 to 9.7 billion in 2050 [50]. This growth is relatively lower compared to the one experienced during the second half of the 19th century, but it is still remarkable. This trend is depicted in Figure 2.2. More
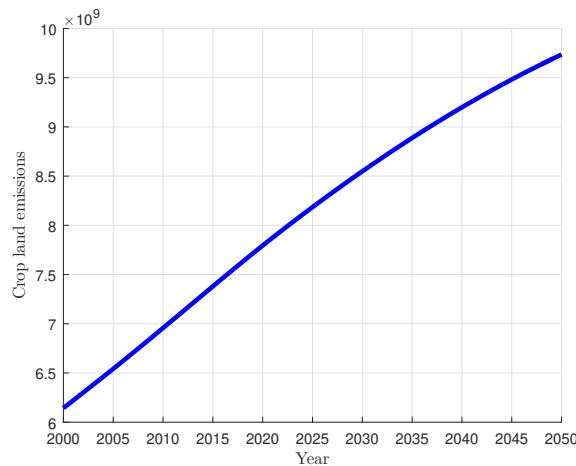
Figure 2.2: World population from 2000 to 2050. Data from [49]

people means a greater amount of food and an increase in overall production. At the same time, more than one billion people were undernourished and malnourished in 2009 [46]. This number is expected to decrease by 2050 to about 370 million people. This lack of food requires an increase in production to feed properly the people who need a healthy diet. Speaking of diet, a dietary change is taking place especially in the most developed countries. As we increase our kcal/day energy supply and shift our diet to a higher amount of meat, fat, sugar, and salt, an increase in agricultural production is required due to the high cost in terms of crop production for the less efficient animal feed. The world income is expected to grow as well, particularly in developing countries where access to food is not guaranteed for everybody. A greater income has a direct impact on the global demand for food [47]. A much more flourishing agriculture sector is key for development and poverty reduction. Agriculture is also a source of fuels, it is the case

of biofuels. Biofuels consumption has been increasing for the last fifteen years and it represents a real risk for food security. Roughly 10% of coarse grain is devoted to the production of biofuels. Overall, it is calculated that these improvements in people lives and the increasing population will require a 70% increase in global food production by 2050 [45]. Up to now, we have seen socio-economic changes but they are not the only ones likely to happen. Most of the natural resources exploited worldwide by agriculture are threatened. The intensification of agricultural production has always come along with soil nutrient depletion, erosion, desertification, depletion of freshwater reserves, damage of tropical forests, biodiversity loss and many others. When agriculture expands, it usually replaces grassland, savannah or forest as it mainly expands in the tropics. This degradation of natural resources has a direct drawback on agriculture. Luckily, this degradation is significantly slowing down and the availability of natural resources seems to be enough to compensate for the world future demand [46]. Nevertheless, shortages might arise in those countries where high growth of demand will face luck of commercial import, water and yield levels. Indeed, freshwater reserves are not evenly distributed around the globe. Biodiversity is a fundamental input in agriculture but it is mined by the agriculture side effects. Only four crop species furnish half of the plant-based calories in the human diet. Climate change is one of the major threats ever faced by humankind. It is powered by agriculture pollution as well and it is affecting agriculture. Weather is changing, temperature and carbon dioxide concentration are increasing and weed, pests and disease might spread easily. One of the biggest concerns is the enormous increase in demand for irrigation water. As stated above, agriculture contributes to around one-third of the greenhouse gas emissions and the massive exploitation of water, soil and chemicals enhance the change in world climate conditions. Finally, the outbreak of the world pandemic covid-19 in 2020 is posing new unexpected challenges. Just to mention one, during the first quarter of 2020, the Russian Federation has announced the stop of the export of wheat for security issues. Russia is one of the major producer and exporter of wheat. Those countries, that up to now were relying on the exportation of wheat from Russia, have to figure out new ways to compensate for this lack. Being able to completely supply the demand for food on its own has become a real scenario that some countries will face [6].

The result of so many changes is firstly the need for higher production of food, in particular of those foods necessary to ensure nutrition security and of those food products that are more responsive to higher incomes. The so-called yield gap (the difference between crop's potential yield and crop's actual yield), if closed without environmental degradation may substantially increase food supplies [45]. Small changes in diet, bioenergy usage and food waste could improve food delivery with no environmental harm. Higher production must be followed by reducing agriculture's environmental damages. In synthesis: greenhouse gas emission, biodiversity and habitat loss, unsustainable water withdrawals and water pollution from chemicals shall be cut. Ceasing the expansion of agriculture will be essential for moving onto a sustainable path [7]. Smarter management of water, superior irrigation efficiency and chemicals reduction would benefit the availability and quality of water. These guidelines shall be translated into actions in order to solve the incoming problems. Deriving system solutions and tactics from recommendations require a huge effort from the government, institutions and technology developers. Fortunately, potential solutions that move in the direction of higher production and lower environmental impact have already been found. Intensification leads to higher yield through improved practices and innovations. Within this context, we will discuss one such tactic that

has been found to be powerful and respectful of the guidelines listed above. It is the case of Precision and Smart Farming.

2.1 Precision farming

Let us first clarify the difference between precision farming, often referred to as precision agriculture and smart farming. The European Parliament's report on Precision agriculture and the future of farming in Europe defines precision agriculture as: "a modern farming management concept using digital techniques to monitor and optimise agricultural production processes" [93]. By exploiting precise measurements and predictions one can optimize several phases of the production process, improving the quality, quantity and efficiency of inputs and outputs. It is a technology-based approach. On the other hand, smart farming relies on the application of information and data technologies. Data are processed in order to improve farm operations. Farmers can access data in order to improve their decisions [5]. In the following, for the seek of clarity, we will consider only precision agriculture as it is connected with the scope of this work.

Some early definition of precision agriculture is: "that kind of agriculture that increases the number of (correct) decisions per unit area of land per unit time with associated net benefits". The benefits include social and environmental benefits: an increase in quantity and quality of production with the same or fewer inputs [78]. A nice example by Herring [61] describes the scenario like this: a farmer simply pushing a button, connects her/his tractor with Global Positioning Systems (GPS), then read on a display the state of the soil and the remote sensing data about the crop collected just yesterday. A cloud server crunches all this data and by pushing "send" the farmer can happily look at the tractor that applies, with meter accuracy, fertilizer and pesticides. Another definition by the National Research Council (NRC,1997) says: "Precision agriculture is a management strategy that uses information technologies to provide and process data with a high spatial and temporal resolution, for decision-making with respect to crop production". The use of precise agriculture essentially leads to increase farming yield; reduce farming costs; early detect farming problems; predict harvest. Precision agriculture technologies focus on spatial and temporal variations. It is based on defining the variability of some agricultural factors, like soils, pests and moisture. Precision agriculture is made by three main phases: the retrieval of data in time and space, analysis of the data and implementation of precise actions. The distinction between spatial and temporal management leads to the definition of respectively site-specific and development-specific technologies. Within the site-specific management, there are four components: Geographic Information Systems (GIS), GPS, Variable Rate Application (VRA), input systems and sensing technologies. The first simply connect spatially data with field characteristics. GPS localizes any kind of equipment. VRA can spatially vary the inputs, based on maps or real-time analysis. Farmers can rely on a yield map in order to identify problems in the crop or the need for special treatments. Some technologies, based on analytical models, helps in predicting the time evolution of several parameters. Farmers may know in advantage the crop growth, pest damage and how the crop will respond to the applied treatments. These tools help the farmer in taking important decisions at the right time. Up to now, the adoption of precision agriculture technologies has been

driven by profitability reasons, increasing yields, decreasing outputs, yield risks reduction and environmental benefits [87]. In order to properly understand the capabilities and applications of precision agriculture, we will focus our attention on some of the projects that involve and exploit precision farming. For the seek of consistency, we will mainly consider European and Italian projects. Further details about the profitability of precision agriculture are given in Chapter 10.

The Monitoring Agricultural ResourceS (MARS) started in 1988 as a European project under the guidance of the Joint Research Centre (JRC). It began with the goal of exploiting space technologies for studying crop areas and yields. Then, its activities enlarged, first it joined the development of the common agricultural policy (CAP) and since 2000 its services has been applied outside the EU. The JRC develops methods, tools, systems and assessments that cover the MARS thematic areas: agricultural monitoring, crop yield forecasting, global food security, agricultural biodiversity, rural development, climate change and Earth observation. Agricultural monitoring consists of distinguishing, identifying and measure crop production areas, estimating production and checking farmers' application validity for EU funds. Most of these tasks are carried out by means of remote sensing. Within agricultural monitoring, there are four main instruments. The first is the digital land parcel identification system (LPIS). LPIS was developed to implement the CAP's first pillar, allowing direct payment to farmers once their land has been identified and quantified. The main aim is to discover double applications of funds for the same piece of land. The measurements are taken using satellite remote sensing and satellite GPS. The second instrument is image acquisition and storage. Images are acquired with satellites and aircraft in the context of feasibility studies and CAP implementation. The third instrument is the support of agricultural policy. It is used to develop sustainable agriculture and to adapt CAP to social needs. It deals with issues on soil, maintenance, water resources, pasture areas and greenhouse gases emissions. The last instrument is the water supply to agriculture that studies the impact of agriculture on the quantity and quality of water resources. The second thematic area of MARS is crop yield forecasting. Estimates of crop production help EU's CAP decision makers in the growing season but also trade policies and humanitarian issues. Near real-time crop growth and yield, forecasting are provided by the JRC which monitors cereal, oil seed crops, protein crops, sugar beet, potatoes, pastures, and many more. JRC can also estimate the short-term effects of meteorological events on crop production. These predictions are mainly based on satellites data. The crop production is estimated also under the effects of several climate change scenarios so that CAP can be adapted to the incoming challenges. Another thematic area is agricultural biodiversity. It helps in understanding the link between agriculture and biodiversity and the impact of agriculture on the environment. Global food security means increasing the availability of food in the world via technology innovations, support of small-scale farming systems and international trade [38]. The Group on Earth Observations Global Agricultural Monitoring Initiative (GEOGLAM) was developed in 2011 by the Group of Twenty (G20) Agricultural Ministers. Its purpose is to improve market transparency and food security by collecting and sharing information on agriculture and production. GEOGLAM is also researching a response to the UN Sustainable Development Goals, the Paris Accord on Climate Change and the Sendai Framework on Disaster Risk Reduction [55]. Some of the signs of progresse made during the last three years 2017-2019 include: monthly reports on near-real-time global crop conditions, national and regional crop monitors,

crop outlook, rangeland and pasture conditions monitoring and definition of observation requirements for satellite-based observations. The operations carried out by GEOGLAM are strongly dependent on Earth observation activities [56]. Sentinels for Common Agricultural Policy (Sen4CAP) is a European project that aims at enriching and improving the CAP and its management by means of satellite-derived data. In particular, it wants to stress out how Sentinel exploitation may modernize and simplify the CAP. Sentinel is the name of the ESA's satellite missions that belong to the Copernicus programme. Sentinel satellites provide information as vegetation status, cultivated crop type map, grassland mowing product, monitoring activities and many other remote sensing products. Satellite data are processed with in-situ data as well [95] [73]. SATURNO is the name of the Italian project developed by "Distretto Agricolo delle Risaie Lomelline" founded by the European Agricultural Fund for Rural Development. The goal is to spread new methodologies and techniques that improve the distribution of fertilizer by means of satellite technologies and precision farming. The project involves rice farms in the Lomellina territory, in Lombardy. SATURNO wants to show the value of precision agriculture and its applications. The project is composed also of a series of lectures for the farmers on the new technologies introduced by precision farming. By means of satellite data and agricultural modelling, the farmer can access the phenological states of rice, and handle the fertilizer according to the real need of the plant. The farmer will be able to access yield maps to judge the efficiency of her/his actions during the most critical phases of the growing season. The satellite can exactly pinpoint where, when and how much the farmer has to operate [66]. TalkingFields was a demonstration study by ESA in Food & Agriculture, concluded in 2009 and now fully operational. The objective was to improve agricultural production by introducing a set of precision farming tools for a series of crops, namely winter wheat, maize and sugar beet. The users can rely on a series of services: improved soil mapping, economic evaluation, biomass map and yield estimation. Then, the user can tailor her/his crop management measures according to the real necessity of the crop. The contribution of space assets is fundamental for delivering the services. The Earth observation sensors provide spatial information about the crop that enter a model which outputs the assessments on the crop. Then, the GNSS component allows conducting of precision farming operations. Up to now, TalkinFields has already processed more than 50000 ha with more than 60 customers in 8 countries [2], [103]. SatAgro is a Polish start-up that offers precision farming services. They integrate images from NASA, ESA and private satellites in order to deliver a series of services that the farmer can access simply using a smartphone application. With the app the farmer can monitor crop's development, effects of weather events and agronomic treatments, variable-rate maps for the exact use of fertilizer [92]. FruitLook is another completed demonstration project by ESA. It showed how integrated satellite technologies may be crucial for water management in grapes and deciduous fruits fields. The project was focused on the South Africa region. Correct use of inputs (water, fertilizer, pesticides, etc.) protects the environments and reduces costs. On a regular basis, FruitLook provides information about water use, crop growth and nutrient management. By knowing the exact soil moisture, the farmer can irrigate at the optimal moment. Then, the quality and quantity of the grapes and fruits increase, generating more revenues [3]. Finally, a project that supports precision farming is present also in the H2020 context, it is called EU-GENIUS. It consists of a series of tools that promote Earth observation and its applications for agricultural and environmental usage, i.e. agriculture fields monitor, forest monitoring,

flood mapping, water quality monitoring [39]. EO4AGRI is a project whose main target is the improvment of operational agriculture monitoring based on Copernicus satellite-derived information and through geospatial and socio-economic information services. The project assists the implementation of the Common Agricultural Policy, it pushes for specifications of data-driven farming with investments into Copernicus data and information services, it addresses the food security issue and it assesses information about land-use and agricultural service potentially with Copernicus data [23]. GreenPatrol is a European precision farming project that aims at developing a robotic solution for integrated pest management in greenhouses. The robot will rely on satellites signal by Galileo. GreenPatrol is one of the first projects to use GNSS for indoor positioning [59]. EGNSS4CAP is a mobile application that digitises procedures for farmers in order to satisfy their reporting requirements under the Common Agricultural Policy [102]. Farmers can provide geo-localised pictures of their crop in order to support their request for funds.

2.2   Satellites use in precision farming

We can notice that mainly all of the precision farming projects exposed in the previous section rely on data acquired by means of satellites. The satellite collects a set of data that are then processed to obtain the assessments required. There are other options rather than satellites. It is possible to exploit aircraft, drones and other vehicles and tools for in-situ measurements. Each of these has its own benefits and drawbacks. It is not possible to say which one is better with respect to the others since it is the specific case study that leads to the choice of one over the others. One way is to couple two or more of them, but this comes with higher costs. Anyway, the massive exploitation of satellites within the last two decades has demonstrated that it is a viable option. There are some benefits that have brought to the almost indispensable use of satellite in agriculture. In the following, we list and analyse some of the most important ones:

- unbiased information, measurements are strongly reliable and it is known which kinds of errors may affect a particular measure and it is known how to correct them

- information amount, in principle a satellite can measure a variety of physical parameters. However, since the scientific capabilities of a satellite heavily depend on the satellite's payloads, this part will be deepened later on

- near real-time information, the data collected by satellites can be downloaded almost in real-time to the ground station. This depends on the location of the ground stations that communicate with the satellite and on the position on the orbit of the satellite, however, as we will see in Chapter 4, some constellations are capable of providing services with maximum timeliness of 3 hours

- large access area, this parameter depends on the satellite's payload as well, anyway, we can just mention that some instruments can access area of hundreds of km simultaneously. Such a wide area would not be accessible for example with a drone

- high spatial resolution, satellites can reach a sub-meter resolution in many application and in the case of geo-localization the European GNSS Galileo reaches cm resolution

- high temporal resolution (short revisit time), this parameter is related to the orbits of the satellites and the configuration of the constellation, anyway, as we will see in Chapter 4, some constellations will have revisit time of the order of hours. A continuous passage with an interval of a few hours is something that would be infeasible by means of aircraft, drones or any other means

- data access, this property is only applicable to satellites that are driven by national agencies. In this case, the data produced can be accessed and exploited by anyone without paying. In the case of a private constructor, usually, data are available only after paying

- any weather and 24 h, the possibility to acquire data under any weather condition is something that applies only to certain types of instrument, as we will see later on. Anyway, strong wind or generally bad weather would threaten the possibility to employ a drone, or in some cases even an aircraft. Instead, a satellite would operate independently on the weather. Moreover, the satellite keeps acquiring data during the whole day; on the other hand, logistics and human reasons would make it impossible to operate continuously a drone, an aircraft or a tractor. For example, the cost to fly an aircraft or a drone on a holiday would be much higher than usual, while this does not apply to a satellite

- continuity of data, this is one of the requirements that are on the basis of the design of an Earth observation mission. The satellite is developed to grant continuity of data for a long time span (usually on the order of more than five years)

- interoperability (interface with other instruments), many of the equipment employed in agriculture are evolving in the direction of more and more connectivity, first between themselves and then also with the satellite that provides useful data. The most effective example is to think that any modern machinery in the farm embeds a GNSS receiver to monitor and report key information on its status [1]

- no continuous human supervision, this is something that has already been stressed out previously, but it is clear that during a whole flight an aircraft needs a pilot, a drone may not be driven during its operations but it needs assistance before and after, while a satellite operates autonomously

In the previous section we have implicitly seen some of the information that can be retrieved by a satellite. What a satellite can measure is strongly dependent on the payload it embarks. For Earth observation purposes there are basically two categories of sensors, each of them can then be active or passive [81]:

- Optical and infrared sensors

  i passive

    ◇ High-resolution
    ◇ Multispectral, hyperspectral

     ii active: Lidar

- Microwave sensors

     i passive (radiometers)

     ii active (radars)

         ⋄ Scatterometer, Altimeter
         ⋄ Synthetic Aperture Radar

A schematic model of remote sensing sensor types is shown in Figure 2.3. The basic difference between the two categories lies in the frequency band exploited by the sensors. Then, the difference between active and passive lies in the source of radiant energy, passive sensors rely on radiant energy from natural sources while active sensors provide their own artificial radiant source of illumination. Synthetic aperture radar is an active form of remote sensing. The target
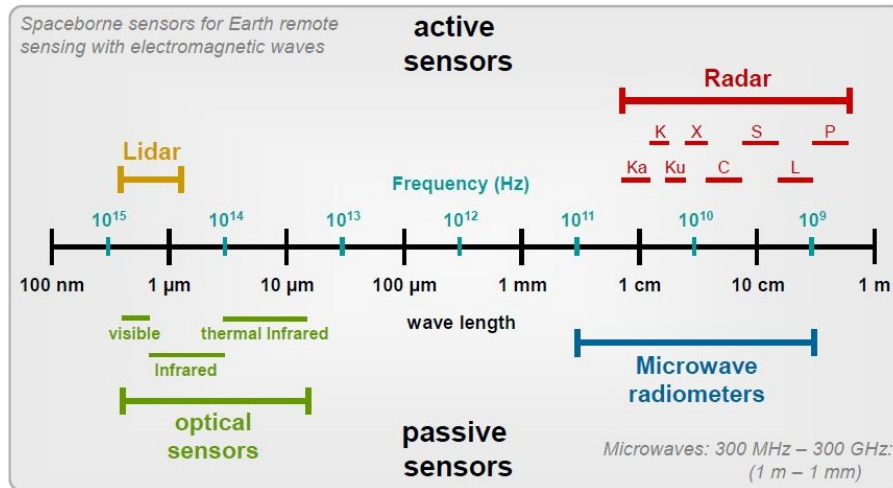
Figure 2.3: Types of remote sensing sensors [81]

surface is illuminated by a beam of energy with a fixed wavelength that can be anywhere from 1 cm (K band) to approximately 70 cm (P-band) [9]. In the next chapter, we will understand why SAR is a powerful sensor for agriculture applications and what are its advantages over other sensors.

2.3 A European green deal, from farm to fork and the common agricultural policy

The European Green Deal is the European Union plan to make the EU's economy sustainable [107]. Europe will be a resource-efficient economy where there are no net emissions of greenhouse gases by 2050, the economic growth is decoupled from resource use and no person and no place is left behind. This Green Deal provides an action plan to boost the efficient use of resources, restore biodiversity and cut pollution. The aim of being climate neutral in 2050 will

require action by all sectors of the European economy. Indeed the policy area spread all over these sectors. Two policy of interest for this work are the *From Farm to Fork* policy and the *Sustainable Agriculture* policy. Farmers will benefit from the EU Green Deal in several aspects: higher returns from sustainable business models, stronger role in the food supply chain, new business opportunity, lower costs and reduced inputs from innovations and technology (precision farming), stronger connection with consumers and new global markets [16].

The Farm to Fork strategy addresses the challenge of a sustainable food system. The strategy aims to reward the farmers that already employ sustainable practices. The strategy is also based on the need to reduce dependency on pesticides and antimicrobials, reduce excess fertilisation, increase organic farming, improve animal welfare, and reverse biodiversity loss [17]. The main objectives are: ensuring positive or neutral environmental impact of the food chain, ensuring food security, nutrition, health and preserving the affordability of food. It was stated that farmers should make use of nature-based, technological, digital and space-based solutions to deliver better climate and environmental results and reduce the use of inputs. The Commission wants to reduce the use and risk of chemical pesticides and nutrient losses by 50% by 2030. The Commissions will also work with the Member States to extend the application of precise fertilisation techniques and sustainable agricultural practices. Under Horizon 2020, the Commission prepared several calls for proposals for the Green Deal for a total of around EUR 1 billion. Under Horizon Europe, the Commission proposed to spend EUR 10 billion on R&I on food, bioeconomy, natural resources, agriculture, fisheries, aquaculture and the environment as well as the use of digital technologies and nature-based solutions for agri-food. The Commissions also stated the need for fast broadband internet to enable mainstreaming precision farming, use of artificial intelligence and full exploitation of satellite technology. This will result in a cost reduction for farmers, improve soil management and water quality, reduce the use of pesticides, fertilisers and GHG emissions. The common European agriculture data space will enhance the competitive sustainability of EU agriculture through the use of production, land use, environmental and other data, allowing precise application of production approaches and the monitoring of performances. The programme Copernicus will reduce the investment risks and facilitate sustainable practice [17].

The Common Agricultural Policy is a partnership between agriculture and society that, from 1962, aims to: support and safeguard farmers, help tackle climate changes, maintaining rural areas and landscape and keep the rural economy alive [18]. The CAP supports farmers income through direct payments and remunerate farmers for environmentally friendly farming. The new CAP, which the Commission proposed in June 2018, aims to help farmers to improve their environmental and climate performance through a more results-oriented model, better use of data and analysis, improved mandatory environmental standards, new voluntary measures and an increased focus on investments into green and digital technologies and practices [17].

Chapter 3

Introduction to synthetic aperture radar

The invention of radar is conferred either to Christian Huelsmeyer or Robert Watson-Watt, both dated back to the 20th century. It was first developed to detect objects in three-dimensional space. World War II contributed to its improvement up to the point that it became small enough to be carried on aeroplanes and soon its use spread into a range of new fields. The reason for this rapid development and employment lies in the all-weather and all-day capabilities of radar. A particular type of radar is the Side-Looking Airborne Radar where a radar sensor is mounted on an airborne. For this type of configuration, the azimuth resolution (direction parallel to the airborne track) is linearly degrading with the distance between the sensor and the ground. This problem was overcome in 1952 when Carl Wiley introduced the aperture synthesis principle. A given point on the Earth surface is imaged by many consecutive radar pulses and a particular postprocessing approach combine the data so that it looks like it was captured by a longer antenna. Basically, this principle allows to synthesis of a much longer antenna than the physical one. Resolution capabilities are linked to the antenna length and therefore Wiley's principle leads to high-resolution imaging from space as well. The image produced with this process is called a SAR image. What SAR essentially does is emit microwave signals and measure the backscattered portion of the signal in order to retrieve several characteristics of the imaged surface. This is expressed by the radar cross-section, the ratio between the received and incident signal intensity. This ratio is particularly influenced by:

- SAR wavelength, that is the wavelength of the radio waves emitted

- SAR polarisation, the property refers to the directions of the electric and magnetic field transmitted with the wave

- SAR incidence angle, the angle formed by the radar beam and a line perpendicular to the surface

- Surface dielectric properties, these govern how a microwave signal interacts with a scattering medium [44]

- Surface roughness relative to the wavelength, most bare and low-vegetation surfaces allow very little penetration such that the surface scattering dominates the response [44]

- Structure and orientation of the objects on the surface

Dielectric properties drive the amount of incoming radiation scattered at the surface, the amount of penetrated signal into the medium and the amount of absorbed energy by the medium. These interactions change according to the sensor wavelength λ. Typical SAR wavelengths and frequencies are shown in Figure 3.1 The penetration depth of the signal depends on the sensor wavelength and on the dielectric constant which in turn depends on sensor wavelength, soil density and moisture content of the medium. Generally, the longer the wavelength, the greater the penetration into the target. On the other hand, the roughness of a surface
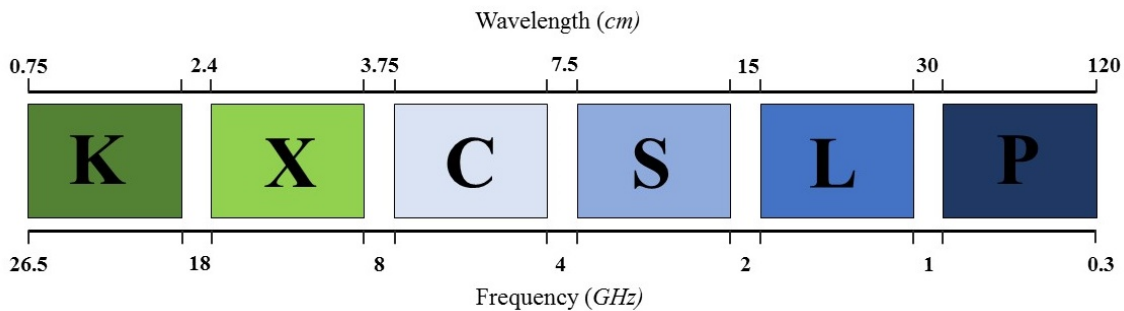
Figure 3.1: SAR wavelengths and frequencies spectrum

depends on the sensor wavelength and the amount of backscatter signal increases with the roughness. As we have seen, SAR is an active instrument that emits electromagnetic waves. The polarisation of a wave is the orientation of the plane of oscillation. Two signals at different polarisation interact differently with the imaged object and the backscattered signals change accordingly. Generally, a natural scene is composed of three types of scatterers: rough surface, double-bounce and volume. We can anticipate that the most important for agriculture are the rough surface scatterers (low-vegetation and bare soils) and volume scatterers (vegetation canopies). The observed radar reflectivity is the integration of single scattering mechanisms, such as surface, volume, and double bounce scattering. Each polarimetric channel produces a different scattering power for the three scattering types, and given the scattering, there is a certain polarimetric channel that produces the maximum scattering power [44]. The different types of polarisation exploited in SAR applications may be classified as:

i Single (One or Mono) polarisation; transmits horizontal (H) or vertical (V) polarised wave and receive H or V polarised wave

ii Dual polarisation; transmits H or vertical V polarised wave and receive H and V polarised wave

iii Full or Quad polarisation; transmitted and received waves are orthogonal pairs

Single, dual and full polarised waves are all linearly polarised waves. The Compact polarisation is slightly different, in this case, the instrument transmits circular waves and receives coherent dual circular waves. Finally, it is possible to mix compact and linear polarisation and produce a Hybrid polarisation, where circular waves are transmitted and orthogonal linear are received.

Different polarisations can determine the physical properties of the object observed. The polarisation state of a back-scattered wave from a natural surface can be linked to geometrical characteristics like shape, roughness and orientation and the intrinsic properties of the scatterer like humidity/moisture, salinity or medium density. The SAR range resolution is limited by the bandwidth of the transmitted pulse, increasing the bandwidth leads to a reduction of pulse duration and therefore of radiometric resolution. To preserve the radiometric resolution, SAR systems generate a long pulse with linear frequency modulation. Synthetic aperture processing is theoretically similar to the effect of a large antenna so that the resulting azimuth resolution is given by half of the physical aperture radar. The SAR pulse direction is never aligned with the platform-ground perpendicular direction but it is always inclined by an angle, usually called inclination angle or look angle. This is shown in Figure 3.2 along with the basic working principle of aperture synthesis. Returns from the scattered object are normally strong at low incidence angles and decrease with increasing incidence angle.
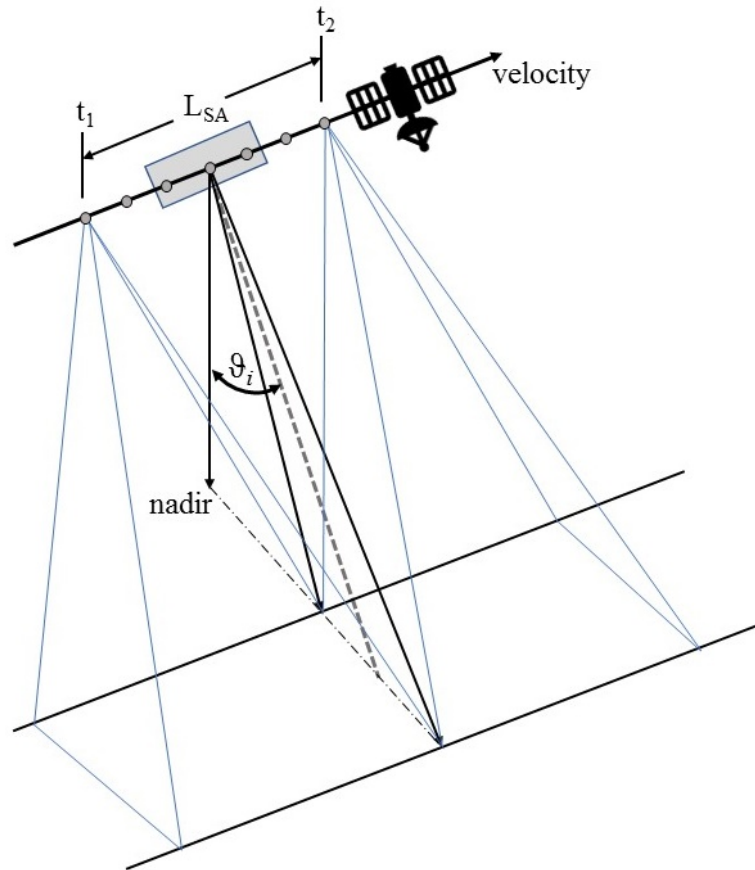
Figure 3.2: Basic principle of aperture synthesis and incidence angle. Adapted from [79]

Because of the misalignment of the SAR pulse direction and the nadir direction, data are affected by distortions as foreshortening, layover and shadow. Foreshortening produces a shorter slope than the real one for a sensor-facing object, it is the case of a mountain with a slope angle higher than the incidence angle where the mountain side looks shorter than it is. In areas of steep slopes lower than the incidence angle, the foreshortening becomes layover and

the top of the object is overlaid on the ground ahead. Finally, a large incidence angle produces shadow. SAR images are affected by a particular kind of noise, usually referred to as speckle. It is a granular 'noise' that inherently exists in and degrades the quality of SAR images. The scattering response from a resolution cell is the sum of thousands of single scattering events that means the sum of thousands of random vectors. Thus, summation vectors of different pixels will have different phase and amplitude producing a grainy signature [44].

SAR collects data in a series of different acquisition modes. The most commonly used is the Stripmap mode, where the antenna allows to tune the swath by changing the incidence angle. ScanSAR mode achieves a wider swath by steering the antenna in elevation. During Spotlight mode the sensor steers its antenna beam to continuously illuminate the terrain patch, allowing finer azimuth resolution, multiple viewing angles and imaging of multiple smaller scenes than Stripmap [91].

3.1   Advantages of synthetic aperture radar

The advantages of a Synthetic Aperture Radar can be summarised as follow:

- weather independent, the microwave portion of the electromagnetic spectrum allows overcoming clouds inhibition

- day and night imaging capability, the microwave portion of the electromagnetic spectrum allows to be independent of solar illumination

- penetration of radar waves, electromagnetic wave nature of SAR signal allows to penetrate the target up to a certain depth that depends on the wavelength allowing to study the target internal structure

- sensitivity to small surface roughness changes, the backscattered signal shows a certain degree of dependence from the surface roughness

- sensitivity to dielectric properties, the backscattered signal shows a certain degree of dependence from the dielectric properties of the target

- control over sensor's factors, such as power, frequency, phase, polarisation, incidence angle, spatial resolution and swath width allowing to precisely select what to look for

- geometric resolution independent from the distance, the synthesized aperture that is orders of magnitude larger than the transmitted antenna makes it possible to produce images with a meter resolution completely independent from target distance especially because of the signal processing technologies employed. Phase-preserving techniques make the SAR image independent of target range and wavelength

- minimal atmospheric effects

- complementary information to optical systems, combining SAR and optical data give a complete understanding of the target, collecting all the information that comes from different parts of the spectrum

3.2 Synthetic aperture radar in agriculture

The plant structure (leaves, stems, flowers, fruits/seed heads) size and orientation determine the interaction with the microwaves and the scattering from the soil surface is influenced by its roughness. The soil moisture and soil constituents influence the soil dielectric constant. The backscatter from a crop changes in time over the growing season and this temporal variation is exploited for example to distinguish one crop from another [110].

Radar backscatter from a crop is the combination of direct backscattering from the vegetation constituent, double-bounce reflection between the soil surface and crop canopy and direct backscattering from underlying ground. The major parameters that affect radar backscatter from crops may be classified into two groups:

- Sensor parameters

- Target parameters

There are three basics sensor parameters: frequency, polarisation, incidence angle. The selected wavelength implies a certain penetration into vegetation canopies and thus it limits the types of information that the radar can sense. Higher frequencies are usually dominated by canopy scattering while lower frequencies are dominated by soil backscatter. The radar will be able to discriminate between characteristics that are present within the depth it can travel; similarly, the soil moisture influence on backscatter comes from the moisture present within the layer that is sensed. The shape and orientation of the plant canopy relate with the signal polarisation that in turn changes the degree of penetration as well. Considering two typical polarisation, VV shows a strong interaction with vegetation structure while HH reveals more information about underlying soil. The radar incidence angle determines the path travelled by the signal through the canopy, influencing the penetration depth [110].

Other than sensor parameters, there are target parameters that affect radar backscatter from crops and in turn, these are the parameters that reveal information about the crop status. These are dielectric and geometrical characteristics of crops (plant/canopy parameters) as: crop type, phenological stage, water content, biomass, LAI, height, stem diameter, row orientation and distance, the orientation of plant constituents, plant surface water; and soil (soil parameters) as: soil moisture, surface roughness, soil texture. Finally, other parameters affecting the radar signal are ascribable to management practices as: tillage practices, row direction, row distance; and external factors as: rainfall, wind, weather in general. Each crop type has its own temporal signature, that is strongly dependent on radar parameters and external factors. Within the crop temporal signature it is also possible to detect the phenological stages of the crop.

SAR is employed in agriculture for three main applications, that are:

- Crop type mapping

- Crop management / biophysical parameter retrieval

- Soil parameter retrieval

SAR signal is able to build crop type maps that are exploited for estimation of crop surface coverage (in the context of management and administration it allows planning of distribution resources) and monitoring of crop productivity (production of yield models). These maps are strongly defined by the radar parameters, each frequency-polarisation-look angle combination leads to a different result and accuracy for different crops.

The second agricultural application after crop type mapping is crop management or bio-physical parameter retrieval. This application allows to:

    i map yield losses caused for example by lodging, flooding, pests

   ii estimate the yield (vital for economic and social reasons)

  iii precision farming (exact resources management)

   iv estimation of input parameter for crop growth model

Within the crop monitoring, high spatial resolution of the SAR product image is an essential data requirement as it helps discriminate small and irregular variations. Analysis of the SAR image can reveal several parameters of interest, useful to estimate the status and needs of the crop as: phenology, plant height, leaf area index, water content and plant biomass. A detailed list and description of many plant parameters that are available at several frequencies (even frequencies that belong to passive instruments) are presented in Table 1 in the Appendix.

Finally, SAR studies soil status through soil parameters. There are three main stages that characterize the agricultural field: soil covered by vegetation, covered by crop residue and bare soil. One of the most important soil parameters is the soil moisture, that has an economic value as it helps predict droughts, floods and contributes to hydrological models in general and is fundamental in the context of precision farming for accurate irrigation and management of crops. After soil moisture we find surface roughness, useful for estimation of harvest date, monitoring of residue cover and tillage practices. In general, multi-configuration SAR data (multi-temporal, multi-frequency, multi-angular, multi-polarisation) are needed to estimate soil moisture under vegetation [88].

3.3 Synthetic aperture radar and agriculture: literature analysis

We are briefly going to see some researches about the three main application of SAR in agriculture: crop type mapping, crop management / biophysical parameter retrieval and soil parameter retrieval.

3.3.1 Crop management / Biophysical parameter retrieval

The parameters collected by analszing the SAR data shall be inverted through mathematical models in order to get information about crop conditions. Some of these models are the Michigan Microwave Canopy Scattering (MIMICS) model, the Water Cloud Model (WTM), the vegetation microwave scattering models, the SAR interferometry technique, the polarimetric

interferometry technique and the SAR tomography technique. About crop height estimation, X-band showed a great potential especially in wheat and different single polarisation (HH and VV) lead to differences in height measurements. Regarding LAI, there is an empirical relationship between LAI of some crop types and backscattering coefficient for the P-, L-, and C-bands in HV; while alternating VV/HH polarisation can be used to estimate rice's LAI. Low frequency bands (L and C) were more correlated with LAI in corn and soybean. Basically, there are two methods for crop biomass estimation, a method that uses backscatter values and a method that use interferometric coherent properties. Combination of L- and C-bands with backscatter values at HV, circular and 45° cross polarisations exhibited good results in biomass estimation. L-band was more sensitive to large leaves crops (corn and sunflowers) while C- and X-bands were more sensitive to narrow leaves crops (wheat). Moreover, L-band was more sensitive to low plant density crops, while both L- and C-bands showed good results for high plant density crops. A strong correlation between multi-temporal C-band HH/VV backscatter ratios at 40° look angle and wheat biomass was found. X-band SAR data helped identify spatial heterogeneities in the wheat field and derive a time series of LAI maps that lead to improvement in the yield forecast of sugar beet and tomato crops [74].

3.3.2   Crop type mapping

Crop identification is strictly related to detection of phenology temporal variations. Crop identification accuracy can be improved with the use of multiple polarisations. In general, SAR images at multi-polarisation, multi-frequency at high temporal density are used to determine the crop types.

Classification of low biomass crops have been achieved with C-band data, while high biomass crops have been classified with L-band data. The fully polarimetric mode performed better than dual and single at C-, L-, P-bands over nine crops. HH polarisation was the most accurate to characterize alfalfa while HV for corn and wheat and VV was found to be more accurate than VH. Many studies demonstrated that multi-temporal data are always a source of improvement in classification accuracy [74].

Acquisitions from ERS C-band, VV polarisation, 23° and 12 m resolution were not enough to distinguish between individual fields in the Negev area, while fully polarimetric X-band SAR data were found to be very useful, marking the fields' boundaries very well [9].

C-band RADARSAT-1 SAR data were able to identify rice with an average accuracy between 80% and 90% with a peak of 98% in some regions. ENVISAT-ASAR cross HH/VV polarisation classified seven main crops with an overall precision of 80%. Single band, single phase showed poor results in crop recognition, while the combination of multi-bands and multi-polarisations SAR data can raise the accuracy to 87%. Fully polarised multi-bands data increased the results accuracy by almost 37% with respect to single-band data and RADARSAT-2 four polarisation band classified South China rice with a classification accuracy of almost 89% sun2018review .

Using VV and VH polarisations C-band SAR data performed better than L-band in crops classification even if for larger biomass crop the two frequencies are comparable. Using HH polarisation L-band performed better than C-band, with the exception of lower biomass crop. On the other hand, X-band outperformed the C-band and it provided completely higher accuracy for wheat. Finally, the benefits of using multi-frequency rather than single-frequency were

confirmed, adding an increase between 10% to 15%. However, the multi-temporal X-band was able to reach an accuracy of 85% in crops identification so that the integration of C-band data brought only small improvements. The study was conducted during the spring/summer period over some Canadian regions [97].

3.3.3   Soil parameter retrieval

Many current methods for surface roughness evaluation estimate a small range of surface roughness or identify only a particular type of cropland surface. In order to retrieve soil moisture accurately, multi-angle, multi-polarisation and multi-temporal SAR data shall be used. Pairs of low and high incidence angles have been used to retrieve soil moisture and rationing of the multi-temporal radar backscatter at C- and L-bands leads to decoupling the effect of soil moisture changes from other effects. Fully polarimetric L-band multi angular SAR data were investigated to estimate volumetric soil moisture under low agricultural vegetation. Combination of L-band VV and C-band HV plus VV showed good result for soil moisture inversion under a soybean canopy [74].

3.3.4   Results for specific crops

We will briefly go through some results present in the literature regarding specific types of crops. Backscatter coefficient from potato crop at L-band, HV polarisation, high angle is higher than other crops and bare soils [43]. Corn fields during plant growth show good response to L-, S-bands, HV polarisation, high angles [43].Good results for backscatter coefficient are usually achieved at HV polarisation, high angles and high frequency for sugarbeet citeferrazzoli2002sar. C-band, HV polarisation, high angles is a convinient radar configuration for rape [43]. C-, S- and X-bands at VV polarisation, low angles contain useful information for cycle monitoring of wheat [43]. Rice stem interacts more with VV polarisation than HH polarisation and L-band signatures are correlated with crop growth [43]. L-band SAR data show a clear response to irrigated rice growth with a strong HH double-bounce backscatter while HV response is dominated by volume scattering and so it is sensitive to rice plant biomass. C-band at dual polarisation is very accurate in monitoring rice, VV and VH backscatter are dominated by double.bounce and volume scattering; C-band is more sensible than L-band even at early growth stages [67]. Setiyono et al. [96] developed a rice yield estimation system based on the crop growth model ORYZA and X-, C-bands SAR data. Studying South and South-east Asian countries they found a positive correlation between SAR X-band and C-band (VV and VH polarisations) backscatter and LAI, and; the yield model was found to be robust in terms of capability to cover large yield variation and reliable. Estimation of rice yield requires three radar data in the growing period [101].

Chapter 4

Earth observation synthetic aperture radar missions, state of the art

In this chapter we are briefly going to see some EO missions, most of which carry a SAR. Their orbits, SAR parameters and spacecraft in general, will be compared in order to understand why some design choices were undertaken and which constraints drove those choices. Earth observation has the purpose of gathering of information about planet Earth's physical, chemical and biological systems. It involves monitoring and assessing the status of, and changes in, the natural and man-made environment. Among its objectives, Earth observation targets to mitigate the human civilisation's negative impact as well. Agriculture is one of the specific applications of Earth observation. Remote-sensing satellites have become fundamental in the development of Earth observation [22].

4.1 Copernicus programme

Copernicus is the name of the former Global Monitoring for Environment and Security, the European Earth observation programme. Copernicus goal is to develop operational information services on a global scale, using services components, in-situ components and space components, in support of environment and security policy needs. The Copernicus space component is represented by the Sentinels family [27]. Overall, there are six Sentinels but here we will go only through the first three as they are closer to the scope of this work. Plus, we will see some insights about a new mission that expands the Copernicus borders.

4.1.1 Sentinel-1, Sentinel-2 and Sentinel-3

Sentinel-1: Sentinel-1 is the first space component of Copernicus and it represents the European Radar Observatory. Sentinel-1 is composed of a constellation of two satellites, Sentinel-1A and Sentinel-1B. Sentinel-1 objective is to provide continuity of C-band SAR operational applications and services in Europe [32]. The key mission parameters are revisit time, coverage, timeliness combined with frequency band, polarisation, resolution and image quality parameters. The user consultation working groups of the European Union has defined three fundamental services for the Sentinel-1 mission: Marine Core Services, Land Monitoring and

Emergency Services. Mapping of land surfaces such as forest, water and soil and, agriculture, is an application of one of these services that is of interest for this work. The contract for building Sentinel-1 was given by ESA to Thales Alenia Space - Italia. The two satellites fly on a Sun-synchronous near-polar orbit, each satellite carries an imaging C-band SAR instrument capable of operating in five different modes. The satellites have been designed for surviving seven years of operations. The spacecraft is based on the Piattaforma Italiana Multi Applicativa (PRIMA) with a dedicated module for the payload. Each spacecraft weighs approximately 2200 kg, its dimensions are 3.4 m x 1.3 m x 1.3 m in a stowed configuration. Power generation relies on two solar arrays, with an overall surface of about 25 m^2, and a Li-ion battery with a 324 Ah capacity. Sentinel-1A was launched on April 3, 2014, while Sentinel-1B was launched two years later on April 25, 2016. On the 693 km altitude dawn-dusk orbit the two satellites share the same orbital plane, they are phased by 180° and their position is known within an accuracy of 10 m. Their orbit has been designed such that the ground track cycle repeats itself every 12 days and 175 orbits. The SAR instrument on board Sentinel-1 operates at 5.405 GHz and in four different observation/acquisition modes; each one with a different swath and resolution. This SAR instrument can support operations in dual polarisation, a programmable bandwidth and an incidence angle that ranges between 20° and 46°. The SAR antenna weighs 880 kg (40% of the total launch mass), measuring 12.3 m in length and 0.821 m in width. The total instrument mass, including the antenna, is 945 kg. The Sentinel-1 EO system support from 25 to 75 minutes per orbit of operations, depending on the acquisition mode. The maximum RF peak power is experienced during interferometric wide swath mode, 4368 W. The on-board data latency ranges from around 3 hours down to simultaneous acquisition and download (real-time data), ensuring a minimum data/product latency. A third satellite, Sentinel-1C will be launched in 2022 to ensure the continuity of services [32]. Sentinel-1 performances and main parameters are presented briefly in Table 4.3. *Sentinel-2* and *Sentinel-3*: Sentinel-2 and Sentinel-3 missions do not carry any SAR instrument similar to the one employed in Sentinel-1, however, we are briefly going to describe what these two missions are meant for. They belong to the Copernicus programme together with Sentinel-1, so that they are complementary and the data gathered by these missions can be put together. This complementary view shows the power of studying the same object with different points of view (in this case, different wavelengths) and in particular the power of combine SAR and optics data. Sentinel-2 has been developed to generate products like: generic land cover, land use and change detection maps; maps of geophysical variables. Sentinel-2 provides continuity of services like Land Fast Track Monitoring and Risk Fast Track, in the bigger context of Copernicus programme [33]. Sentinel-2 delivers data about vegetation health, plant indices, crop types and land changes. Again, Sentinel-2 is made by two satellites, flying on a 786 km altitude Sun-synchronous orbit, at an inclination of 98.5°. Each satellite weighs approximately 1200 kg and can produce up to 1700 W of electric power. Each satellite carries a 275 kg Multispectral Imager (MSI). The MSI is a telescope, based on the pushbroom observation concept. It covers 13 spectral bands spanning from the VNIR to the SWIR, with a swath of 290 km and a spatial resolution that ranges between 10 and 60 m [33]. The MSI requires around 170 W of power for operations. The operations of such an instrument are influenced by the presence of clouds. We can already see the differences in the spacecraft design and orbit design between Sentinel-1 and Sentinel-2, which depend especially on the two different payloads used. Sentinel-2 performances and main parameters are presented briefly

in Table 4.6. Sentinel-3 is designed to monitor ocean, land and ice surfaces as well as inland water surfaces and marine operations. The main observation objectives are: Ocean and land colour observation, ocean and land surface temperature, surface topography observation. In addition, Sentinel-3 can produce surface vegetation products. Like the previous two Sentinels, Sentinel-3 is made of 2 satellites, each of which weights 1150 kg consumes around 1100 W and flies on an 815 km altitude frozen sun-synchronous orbit at an inclination of 98.6° [34]. The payload consists on six instruments, divided into optical and topographic. The optical payload is made by an Ocean and Land Cover Instrument (OLCI), a medium resolution pushbroom imaging spectrometer with 21 bands between 400 and 1020 nm and a resolution of 300 m; a Sea and Land Surface Temperature Radiometer (SLSTR), designed for ocean and land surfaces temperature observation with 11 spectral bands and a swath width up to 1400 km. Then, there is the SAR Radar Altimeter, a dual-frequency (C-band and Ku-band) nadir-looking altimeter that can be operated in two modes and weighs 62 kg, absorbing 100 W. The SLAR antenna is a parabolic reflector. A Microwave Radiometer (MWR), a nadir looking sounder operating at K/Ku-band which measures water vapour and cloud water contents in the field of view of the altimeter. A Laser Retroreflector (LRR), a passive device that accurately locate the satellite from the ground via laser ranging techniques; and a Doppler Orbitography and Radiopositioning Integrated by Satellite (DORIS) which is a satellite tracking system. Finally, there is also a GNSS receiver [34]. Overall, the payload mass is about 370 kg. Sentinel-3 performances and main parameters are presented briefly in Table 4.6.

4.1.2 ROSE-L

ROSE-L is the name of a new ESA mission addressed to EU policy and gaps in Copernicus user needs, as well as to expand the current capabilities of the Copernicus component [25]. ROSE-L will be equipped with an L-band SAR, providing additional information to those gathered by Sentinel-1 C-band SAR. Some objectives include: forest management; subsidence and soil moisture monitoring and crop types discrimination for precision farming and food security; polar ice monitoring. In July 2020, ESA signed a contract with Thales Alenia Space as a prime contractor to build the satellite. ROSE-L performances and main parameters, derived from ROSE-L mission requirements document [21], are presented briefly in Table 4.4.

4.2 COSMO SkyMed

COSMO-SkyMed is a programme conceived by Agenzia Spaziale Italiana (ASI) and funded by the Ministry of Research and the Ministry of Defence, the most expensive Italian investment in space systems for Earth Observation. This programme has twofold object, civil and defence. Some applications of COSMO-SkeMed includes: defence and security; risk management; commercial services; and others (marine and coastal environments, agriculture, forestry, cartography, environment, geology and exploration, telecommunication, utilities and planning). TAS-I is the prime contractor of the system. The space segment is made by a constellation of four satellites. Each satellite is built on the PRIMA (the same as Sentinel-1) and weighs about 1700 kg, while producing a minimum 4 kW of power (BOL) with two solar arrays of 9.15 m^2 each. The EPS relies on a 336 Ah Li-ion battery as well. The satellite design life is 5 years.

The four satellites were launched between June 2007 and November 2010 on a Delta-2 launch vehicle. The final orbit selected for the satellites is a circular sun-synchronous dawn-dusk orbit at 619.6 km of altitude, inclined by 97.86°. This orbit is designed so that it repeats its ground track every 16 days [28]. The satellites are evenly spaced on the mentioned orbit so that the constellation has a revisit time at least lower than 60 h (worst case) that can go down to less than 12 h. The constellation can operate also in an interferometric configuration so that two satellites work in a tandem configuration in close proximity between each other even with the possibility of placing the two satellites in slightly different orbital planes. Each satellite carries an X-band SAR. The type of SAR allows for: very large bandwidth, multi-polarisation and full polarimetry support, electronic beam steering, programmable PRF, pulse width and bandwidth, multiple imaging modes, onboard calibration and data compression. The instrument is made by a phased array antenna and a central electronics module. The antenna has dimensions of 5.7 m x 1.4 m. Images can be acquired in three different modes: Stripmap, ScanSAR and Spotlight, with an incidence angle between 20 and 59.9° and a swath width between 10 and 200 km (extendible up to 1300 km for event monitoring and for achieving the best revisit time). Spatial resolution ranges between 1 and 100 m depending on the modes. The instrument calls for very high peak power loads of up to 14 kW. The continuous acquisition time depends on the mode and lies between 10 and 75 minutes [28]. COSMO-SkyMed Second Generation is the follow-up of COSMO-SkyMed (CSK). It was introduced with the idea of improving the quality and enhance the capability of CSK. Swath width, spatial and radiometric resolution, polarimetry and acquisition mode have been upgraded. In particular, a brand-new design of the SAR has been introduced and other changes have been made to several subsystems. CSK Second Generation's space segment is made of two satellites that will replace CSK satellites, ensuring the continuity of services. The two satellites are still based on the PRIMA, however, they are designed for an operational life of 7 years and to produce more power in order to satisfy the peak payload request of 18.6 kW. These two satellites are heavier than the previous four, the launch mass is about 2230 kg, however, the SAR antenna is of the same sizes. Launches happened in 2019 and 2020. The orbit is the same as CSK satellites. The new SAR instrument can provide up to 10 operative modes: four Spotlight (2 of which are available only for defence applications), one Stripmap, one Pingpong, one Quadpol and two ScanSAR. Polarisation, spatial resolution and swath depend on the mode; polarisation is available from single to quadruple, resolution ranges between less than 1 m to 40 m and the maximum swath is 200 km. The access angle can be modulated between 20° and 60° [29]. COSMO-SkyMed second generation performances and main parameters are presented briefly in Table 4.3.

4.3 RADARSAT constellation mission

RADARSAT Constellation Mission (RCM) is the follow-up of the RADARSAT programme [30]. The main scope is to provide continuity of C-band SAR data for the RADARSAT users while improving the quality of the services. Some RCM applications include: maritime surveillance and national security, disaster management, ecosystem monitoring (e.g. agriculture). Revisit time and timeliness have been improved since RADARSAT, being 4 days (that can be reduced down to 1 day in medium resolution) and from 24 hours to 10 minutes respectively. There are three main requirements that drove design choices: provide C-band data continuity to the users;

provide daily coverage of maritime approaches of Canada; meet a certain cost threshold [30]. This lead to the choice of three satellites to compose the constellation and other characteristics for the orbit and payload that we are going to briefly see. The three satellites were launched on June 2019 with a Falcon-9 rocket (a low-cost launch vehicle) onto a sun-synchronous circular orbit at 592.7 km of altitude at an inclination of 97.74°. The three satellites are equally spaced within the orbit. This orbit allows for a 12 days repeat cycle. Each spacecraft is box-shaped (based on the Magellan MAC-200 bus) with one single solar panel. The total spacecraft mass is about 1460 kg, while the 2.2 m x 1.7 m solar panel produce almost 1600 W, enough to power the SAR instrument for 15 minutes per orbit. The low-cost approach requires that the design of the SAR system is in terms of mass, power consumption, volume, and antenna size, in compliance with the constraints imposed by using a low-cost launch vehicle and a small spacecraft bus [30]. The SAR payload weights approximately 600 kg with a peak power consumption of 1270 W. The SAR antenna measures 6.75 m x 1.38 m. Swath width ranges between 20 km and 350 km (that can be increased to 500 km for accessible purposes) with a spatial resolution from 50 m to 5 m. The polarisation used by this SAR instrument is a hybrid polarisation, in addition, two multi-polarisation capabilities are provided: dual and quad-pol. The SAR antenna access angle is fixed to 37.5°. RCM performances and main parameters are presented briefly in Table 4.5.

4.4   ALOS-2

ALOS-2 is a JAXA mission that follows after ALOS and targets to provide continuity of services in: cartography, regional observation, disaster monitoring and environmental monitoring [26]. ALOS-2 provides specific data for agricultural monitoring, contributing to its sophistication and sustainability, especially for irrigated rice. The spacecraft weighs 2120 kg and it is embedded with two solar arrays that generate 5.2 kW of power (BOL). It was launched in May 2014 on a sun-synchronous orbit at 628 km of altitude and 97.9° of inclination. This orbit leads to a repetition of the satellite ground track every 14 days, which is also the satellite revisit time performance. ALOS-2 space segment is designed to survive for at least 5 years. ALOS-2 main payload is an L-band SAR based on an active phased array antenna. This particular instrument offers left-side and right-side looking observation and the possibility to change the incidence angle between 8° and 70°. This instrument is made by the antenna and an electronic unit. The antenna is quite big, as it measures 9.9 m x 2.9 m and weighs 547.7 kg. The electronic unit weighs 109.1 kg and absorbs from 3.3 kW to 6.1 kW of peak power. This SAR can acquire images in three different modes: Spotlight, Stripmap (with three different settings) and ScanSAR. Depending on the mode, the swath width increases from 25 km to 350 km (with an observation area of 1160 km) and polarisations from single to full are exploited (plus an experimental compact polarisation). ALOS-2 offers a ground resolution of his products from 100 m down to even 1 m according to the acquisition mode [26]. ALOS-2 performances and main parameters are presented briefly in Table 4.4.

4.5   SAOCOM-1

SAOCOM (SAtélite Argentino de Observación COn Microondas) is an Argentinian project for natural and anthropogenic disaster monitoring and agriculture, mining and ocean application monitoring services [31]. The objective is to provide high-quality, accurate and frequent data for the users. This project is a joint project between CONAE (Comisión Nacional de Actividades Espaciales) and ASI so that Argentine SAOCOM satellites operate together with Italian COSMO-SkyMed satellites to provide more frequent information, with a twice-daily coverage capability. The space segment is made of a constellation of two satellites, SAOCOM-1A and SAOCOM-1B. Each satellite weighs approximately 1600 kg and they are designed with an operative life of 5 years. The two satellites were launched in 2019 and 2020 on a sun-synchronous near-circular orbit at an altitude of 619.6 km and an inclination of 97.86°. The orbit repeat cycle is 16 days, the same as COSMO-SkyMed. Each SAOCOM satellites carry an L-band SAR in order to answer all the requirements in terms of services. This SAR operates in three different modes: Stripmap, TopSAR and ScanSAR with different polarisation, from single to quad. Swath width ranges between 40 km and 350 km, with resolution from 100 m to less than 10 m. The incidence angle varies between 20° and 50°. This instrument transmits a peak power of 3.1 kW. A single satellite acquires up to 450 minutes of images per day [31]. SAOCOM-1 performances and main parameters are presented briefly in Table 4.5.

4.6   ICEYE constellation

The Finnish company ICEYE Ltd is designing a constellation of SAR microsatellites in order to make SAR data much more available to support decision making in several areas [35]. Data produced by ICEYE constellation will be useful in trade, exploration, relief efforts, farming and environmental protection. It was anticipated that the constellation is going to be formed by approximately 18 satellites, each one carrying an X-band SAR. It is estimated that the new satellite and sensor design will cut the costs, almost 100 times less costly than comparable larger spacecraft. The satellites weighs 85 kg, and it is embedded a single solar panel. The sensor is side-looking and utilizes an active phased array antenna that measures 3.2 m x 0.4 m. The SAR instrument emits up to 4 kW of power (RF peak) and it can acquire images in 3 different modes: Stripmap, Spotlight, ScanSAR (which is currently under development). Depending on the acquisition mode, the ground swath varies between 5 km and 30 km, in the same fashion ground resolution ranges between 3 m and 1 m. Images are acquired only with a single VV polarisation and with a look angle between 10° and 30°. The first two satellites (ICEYE-X2) of the constellation (after the proof-of-concept first satellite) were launched in 2018 on a sun-synchronous circular orbit at 570 km and an inclination of 97.7°, with a repeat cycle of 17 days. Then, ICEYE-X3, ICEYE-X4 and ICEYE-X5 satellites were launched in 2019, still on sun-synchronous circular LEO. Finally, ICEYE-X6 and ICEYE-X7 have been launched in September 2020. At the moment of writing, ICEYE offers public access to radar satellite imagery and in March 2020 their satellites achieved the finest resolution class in commercial SAR [35]. ICEYE constellation performances and main parameters are presented briefly in Table 4.3.

4.7 Capella X-SAR constellation

Capella Space is an American startup that is designing a constellation of 36 microsatellites to provide global coverage with an average X-SAR imaging revisit time below one hour. The constellation will be fully operational in 2021 and it will be able to provide products that meet specific user demands all over the world. Each satellite has a mass lower than 40 kg, despite the small dimensions of the body, the SAR antenna span 8 m^2. The satellites are designed with a 3 years life, so that by launching 12 satellites every year the constellation will keep unchanged its imaging capability over time. An average 500 km altitude, polar orbit will be exploited by all the satellites. The SAR instrument on-board these small satellites is able to acquire images at one single polarisation (HH) but with different acquisition modes: Stripmap, multi-swath Stripmap, staring Spotlight and sliding Spotlight. Swath width varies between 10 km and 200 km according to the mode, while the resolution is always lower than one metre and in the best case it is of the order of some centimetres [24]. Capella X-SAR constellation performances and main parameters are presented briefly in Table 4.4.

4.8 PRISMA

PRISMA (PRecursore IperSpettrale della Missione Applicativa) is an ASI mission focused on the development and delivery of hyperspectral products and the qualification of the hyperspectral payload in space [36]. In this case, the payload is not a SAR, however, it is important to show what kind of information can be gathered with payloads different from SAR; even to understand what can be obtained by combining information from different instruments. Moreover, we can appreciate how different types of instruments drive some design choices, especially in the selection of the final orbit. Some mission objectives are: monitoring of natural resources (e.g. land cover and land crop status, soil mixture and carbon cycle) and atmospheric characteristics with a small satellite; provide data products with a short delay period; technologies demonstration. The satellite provides global observation capability with specific areas of interest being Europe and the Mediterranean region. The space segment weighs 830 kg at launch, it consumes a maximum 720 W and it is designed for a 5 years lifetime. In 2019 PRISMA was launched on a sun-synchronous circular orbit at 615 km with an inclination of 97.85°. The orbit repeat cycle is 29 days. The on-board sensor is an hyperspectral instrument based on a pushbroom type observation concept capable of generating hyperspectral imagery with a spatial resolution of 30 m on a ground swath of 30 km. The spectral resolution is lower than 12 nm in a range of 400-2500 nm. Overall, the PRISMA instrument acquires images at 237 different spectral bands. A panchromatic camera at 5 m resolution is also present. The instrument (included the panchromatic camera) weighs around 90 kg and on average requires 110 W of power. The design of the optical part consists of a telescope with two spectrometers and the panchromatic camera. These optical parts have a field of view of 2.45° [36]. PRISMA satellite performances and main parameters are presented briefly in Table 4.6.

4.9   Data comparison and analysis

Here, we will briefly try to sum up some of the most important characteristics of the space segments we have described above including their orbital characteristics. A comparison between them is performed with the idea of showing which are the implication in the space segment of employing different types of SAR. Table 4.1 compare the orbital main characteristics of the SAR missions we have analysed so far, while Table 4.2 compares the satellites and SAR characteristics in terms of mass, power and dimensions. It is worth stressing out that as the dimensions of the SAR increases, considering its mass and antenna dimensions, so does the dimensions of the spacecraft in order to host the massive payload. A bigger SAR antenna calls for more power as well and thus the bus shall be able to provide that power via its solar arrays. However, a bigger SAR instrument allows higher performances, in terms of swath, polarisation, operative modes and acquisition time, as we can notice from Table 4.2, Table 4.3, Table 4.4 and Table 4.5. Moreover, a bigger SAR can reduce the number of satellite in the constellation while obtaining similar revisit time performances; instead smaller SAR requires to increase in the number of satellites if one wants to get a low revisit time. A huge satellite is almost forced to fly on higher orbits than a small satellite, in order to reduce the drag produced by the Earth atmosphere, this is shown in Table 4.1. On the other hand, flying on higher orbits allows increasing the ground swath even if this costs in terms of power to be supplied. Finally, a massive satellite will lead to high launch cost, but this shall be considered together with the fact that the constellation will be made by fewer satellites.

It is worth underlining the limitations of the space segments just exposed in order to understand which are the complications that a farmer shall face once looking for satellite data. This is also useful for deriving user requirements. Understanding which are the current limitations and bottle-necks allows us to define the main characteristics of the constellation we want to draw. Moreover, we do not want just to overcome the technological limitations but we want to build something that is complementary at least with the current European programme Copernicus, not an alternative to it. This approach allows to maximise the final result and exploits all possibilities. Sentinel-1 satellites provide free access to their data, then these are free for the farmer. However, in the best case, the images produced by Sentinel-1 are at 10 m resolution. For some applications this may be enough but for some others, like VRT it is not. This poses a limit in the applications of Sentinel-1 data, as their resolution is not compatible with the agriculture machinery resolution. Moreover, Sentinel-1 data are available after a few days from their acquisition, again this is not compatible with some particular cases' urgency. Sentinel-1 revisit time is too low as well. It is not devoted only to agriculture applications and therefore it cannot provide images of the same place once a week or more frequently as it is required in some applications. Although Sentinels data are very useful and important, especially for their accessibility, they might not be enough. Another provider of SAR images is the Italian constellation COSM-SkyMed. COSMO overcomes all the technological limitations of Sentinel-1, resolution and revisit time are much better. However, its images are not accessible. These are owned by the Italian government, and they are not provided regularly to possible users. The last possibility for the farmer who is seeking SAR data is to look at the market. In these case, there are constellations that provide images with high enough resolution, revisit time and timeliness. However, these come with a price. Sozzi, et al. in [100] listed the characteristics

and the price of satellites' optical data. In particular, they underlined that there is a minimum order area that one can ask for. Order below that limit are not accepted. For agricultural use, the threshold of a minimum area is very high, 2500 hectares [100], and then, the corresponding price can be afforded only by a few farms. Finally, they computed that the use of satellites with a sub-meter spatial resolution is justified only with 370 to 470 hectares. This scenario is very meaningful as it shows that acquiring SAR images at high quality (resolution, revisit time, timeliness) is quite difficult (if not impossible) for a wide portion of farmers (especially those who own small fields). These are the first considerations that have driven us during the design of these constellations, overcoming the limits that do not let all the farmers access good satellites data. These aspects will be reflected in the requirements definition in Chapter 5.

MISSIONS	Altitude [km]	Inclination [deg]	Eccentricity [-]	Revisit cycle [days]	Particularities
COSMO-SkyMed II Generation	619.6	97.86	0	16	SSO dawn-dusk
Sentinel-1	693	98.18	near 0	12	SSO
RADARSAT Constellation	592.7	97.74	0	12	SSO dawn-dusk
SAOCOM-1	619.6	97.86	near 0	16	SSO dawn-dusk
ALOS-2	628	97.9	near 0	14	SSO
ICEYE Constellation	570 - 832	97.7 - 98.6	0	17	SSO
Capella X-SAR	485 - 525	near 90	0	NA	NA

Table 4.1: SAR constellations orbital parameters

MISSIONS	COSMO-SkyMed II Generation	Sentinel-1	RADARSAT Constellation	SAOCOM-1	ALOS-2	ICEYE Constellation	Capella X-SAR
# of satellites [-]	2 (II generation) + 2 (I generation)	2	3	2	1	18	36
S/C mass [kg]	2230	2157	1460	3050	2120	85	40
S/C power [kW]	NA	4.8 (EOL)	NA	NA	5.2 (EOL)	NA	0.4
SAR mass [kg]	810	945	600	NA	656.8	NA	NA
SAR power [kW]	18.6 (absorbed), 9 (RF peak)	4.368 (RF peak power)	1.270	3.1 (RF peak power)	6.1 (RF peak power)	4 (RF peak power)	NA
SAR antenna dimensions [m]	5.7 x 1.4	12.3 x 0.821	6.88 x 1.37	10 x 3.5	9.9 x 2.9	3.2 x 0.4	8
SAR acquisition time [min]	10 to 75	75 (wave) - 25 (Strip/Top)	15	15	NA	NA	10
Design life [years]	7	7.25	7	5	5	NA	NA

Table 4.2: SAR constellations, satellites technical features. Note: ICEYE altitude refers to ICEYE-X2, X3 and X4; while Capella altitude refers to the whole constellation

MISSION	Payload	Frequency	Acquisition mode	SAR Polarisation	Resolution [m]	Swath width [km]	Look angle [deg]	Revisit time	Data Access
COSMO SkyMed II Generation	SAR	X-band	Stripmap	Single (HH/HV, VV/VH) or dual (HH&HV+ VV&VH)	3x3 and 5x20 and 3x3	40x2500 and 30x2500 and 15x2500	20 - 60	12 hours	Commercial; limited proposal-based scientific
			Pingpong	Dual (HH+VV)	12 x 5	30 x 30	20 - 60		
			Quadpol	Quadruple (HH&HV& VV&VH)	3 x 3	40 x 16	20 - 45		
			ScanSAR 1	Single or dual	20 x 4	100 x 2500	20 - 60		
			ScanSAR 2	Single or dual	40 x 6	200 x 2500	20 - 60		
			Spotlight 1A	NA	NA	NA	NA		
			Spotlight 1B	NA	NA	NA	NA		
			Spotlight 2A	Single or dual	0.35 x 0.55-0.51-0.48	3.1-3.2-4.4 x 7.3	20 - 60		
			Spotlight 2B	Single or dual	0.63 x 0.63	10 x 10	20 - 60		
			Spotlight 2C	Single or dual	0.8x0.8	5x10	20 - 60		
Sentinel-1	SAR	C-band	Stripmap	Dual (HH+HV, VV+VH)	5x5	80	20 - 45	1-3 d depending on latitude (2 d Europe)	Free & Open
			Interferometric Wide swath	Dual (HH+HV, VV+VH)	5 x 20	250	>25		
			Extra wide swath	Dual (HH+HV, VV+VH)	25 x 100	400	>20		
			Wave	Single (HH or VV)	5 x 20	20	23 & 36.5		
ICEYE Constellation	SAR	X-band	Stripmap	Single VV	0.5-3	30	10 - 30	1-3 hours	Commercial
			Spotlight	Single VV	0.6-1	5	20 - 35		
			ScanSAR	Not available	NA	NA	NA		

Table 4.3: SAR main features of COSMO SkyMed, Sentinel-1 and ICEYE Constellation

MISSION	Payload	Frequency	Acquisition mode	SAR Polarisation	Resolution [m]	Swath width [km]	Look angle [deg]	Revisit time	Data Access
Capella X-SAR	SAR	X-band	Stripmap	Single HH	0.3	10-30x50, 40x40, 50-140x30, 150-780x20, 790-2100x10	10 - 50	Hourly	Commercial
			Multi-swath stripmap	Single HH	0.3	10-30x50, 40x40, 50-140x30, 150-780x20, 790-2100x10			
			Staring spotlight	Single HH	0.3-1	5x20, 10x010, 5x10, 5x30, 15x10			
			Sliding spotlight	Single HH	0.018-0.274	10-200			
ALOS - 2	SAR	L-band	Spotlight	Single pol (HH, HV, VH, or VV)	1x3	25x25 (1160 observation area)	8 - 70	14 days	Free & Open
			ScanSAR	Single pol (HH, HV, VH or VV) and Dual pol (HH+HV or VH+VV)	47.5x77.7, 95.1x77.7, 44.2x56.7	350.5x355, 489.5x355 (1160 observation area)			
			Stripmap	Single pol (HH, HV, VH or VV) and Dual pol (HH+HV or VH+VV)	3x3, 6x4.3, 9.1x5.3	55x70 (1160 observation area)			
			Full polarimetry	Full (Quad.) pol (HH+HV+VH+VV)	5.1x4.4, 8.7x5.3	40-50x70, 30x70 (1160 observation area)			
ROSE-L	SAR	L-band	/	Linear dual and full	<10	Sufficient to cover the spatial coverage of Sentinel-1	/	3 d (Europe) 6 d (global)	NA

Table 4.4: SAR main features of Capella X-SAR, ALOS-2 and ROSE-L

MISSION	Payload	Frequency	Acquisition mode	SAR Polarisation	Resolution [m]	Swath width [km]	Look angle [deg]	Revisit time	Data Access
RADARSAT Constellation	SAR	C-band	Low resolution	Single and dual and compact	100	500 x 10	37.5	4 d + daily global re-look	Commercial
			Medium resolution	Single (HH,VV,HV,VH),dual (HH+HV,VV+VH,HH+VV) and compact	16-50	30-350x10			
			High-very high resolution	Single and dual and compact	3-5	20-30 x 10			
			Low noise	Single, dual(HH+HV,VV+VH) and compact	100	350 x 10			
			Quad-pol	Quadruple (HH&HV&VV&VH)	NA	>20 x 10			
			Spotlight	Single, dual(HH+HV,VV+VH) and compact	1x3	20 x 5			
SAOCOM-1	SAR	L-band	Stripmap	Single pol (HH or HV or VH or VV) Dual pol (HH/HV or VV/VH) Quad pol (HH/HV/VH/VV)	<10	>20-40	20 - 50	8 days	Distributed from the centre in Buenos Aires
			TopSAR narrow	Single pol (HH or HV or VH or VV) Dual pol (HH/HV or VV/VH) Quad pol (HH/HV/VH/VV)	<30-50	>100-150			
			TopSAR wide	Single pol (HH or HV or VH or VV) Dual pol (HH/HV or VV/VH) Quad pol (HH/HV/VV) Compact pol (RH/RV or LH/LV)	<50-100	>220-350			

Table 4.5: SAR main features of RADARSAT Constellation and SAOCOM-1

MISSION	Payload	Frequency	Acquisition mode	Resolution [m]	Swath width [km]	Look angle [deg]	Revisit time	Data Access
Sentinel-2	Multispectral imager	13 spectral bands spanning from the VNIR to the SWIR, featuring 4 spectral bands at 10 m, 6 bands at 20 m and 3 bands at 60 m spatial sampling distance	Systematic push-broom acquisitions / lateral mode capability	Ranging from 10 to 60 m on the ground, depending on the band	290	MSI FOV: 20.6	5 days	Free & Open
Sentinel-3	SRAL radar altimeter	C-band + Ku-band	Low resolution SAR	300	NA	/	1-2 days (depending on payload)	Free & Open
	MWR MicroWave radiometer	K-band + Ka-band	/	Accuracy <3K	23.5	/		
	OLCI Oceran and land color instrument	21 spectral bands in the range 0.4-1.0 μm	/	300	1270	/		
	SLSTR sea and land surface temperature radiometer	11 spectral bands in the range 0.555-10.85 μm	/	0.5-1 km	740 (dual) - 1400 (nadir)	/		
PRISMA	PRISMA, hyperspectral instrument	VNIR channel: 400-1010 nm spectral range, 66 bands; SWIR channel: 920-2505 nm spectral range, 171 bands; Pan channel: 400-700 nm spectral range, 1 band	/	VNIR and SWIR channels: 30 m. Pan channel: 5m	30 for all channels	/	29 days	Free & open for "research and development"

Table 4.6: Main payloads features of Sentinel-2, Sentinel-3 and PRISMA

Chapter 5

Italian agriculture

In this chapter, we will go through some of the peculiarities of Italian agriculture. First, we introduce it and then we will see why this sector is so important, not only for the Italian economy but also for the whole society. This will help us understand why there is such a large need to exploit precision agriculture technologies and satellites data. Moreover, after presenting the main Italian agriculture data we will be able to obtain the mission requirements on the basis of the user needs. Finally, the data that is going to be shown, provides a useful tool when we will assess the benefits produced by the exploitation of SAR satellites data.

First of all, it is necessary to locate the role of agriculture in Italy. In 2017, Italian's GDP figure was 1736592 million Euro [65]. During the same year, the value of the agri-food chain was 522169 million Euro [19], 30% of the national GDP. More than 2 million businesses were active in that sector. Still in 2017, agriculture, forestry and fishery together produced 73265 million Euro, 14% of the agri-food chain; with more than 1 million businesses and more than 1.2 million people employed [19]. Agriculture represents 94% of the agriculture-forestry-fishery branch value. In 2018 the agriculture-forestry-fishery branch has grown by 1.6% (added value), however, in 2019 production decreased by 0.7% and added value decreased by 1.6%. Agriculture decreased by 0.8% its production and by 1.7% its added value. Nonetheless, the agri-food chain added value is growing, by 1% from 2018 to 2019, and the employment rate in agriculture is stable [64]. By looking at the European Union scenario, in terms of agriculture, we can again stress out its value. In 2019 Italy was the European country with the highest added value in agriculture [64], 31.8 billion Euro, and almost one-fifth of the whole agricultural added value in Europe was generated in Italy, more than France, Spain and Germany. Moreover, this added value has been generated with relevant levels of production in terms of quantity and quality and with limited subsides. Indeed, Italian agriculture is the least subsidized in the EU. In terms of production value, Italy scored third place in the 2019 Europe ranking with 56.5 billion Euro [64]. It is already clear that agriculture, and the agri-food chain that depends on it, are two main pillars of the Italian economy and society. Thus, a huge effort shall be put in improving the quality of this sector, in maintaining its importance and in developing its potential even in the light of the low decrease of 2019. Just comparing the overall results of Italian agriculture with those of other European countries, even without comparing their features and characteristics, it is easy to recognize the main role of Italian agriculture in the larger European one. In 2017, there were more than 1.5 million economic units operating in the agricultural sector. On

Year	2011	2012	2013	2014	2015	2016	2017	2018	2019	2020
Arable Land	39390,3	36552,9	36155,7	39852,0	36580,6	37706,0	35534,1	35074,0	34775,7	30960,1
Woody and Shrub Crops	24973,4	22597,4	24437,3	22670,7	25421,8	25061,1	22952,6	25138,8	23996,8	24129,4
Total	64363,7	59150,3	60592,9	62522,7	62002,4	62767,1	58486,7	60212,8	58772,4	55089,5

Table 5.1: Italian agricultural production from 2011 to 2020, all values in millions of kg. Source: ISTAT

average, they employed 8.4 hectares with a standard output of 38.7 thousand € [70]. Now that we have seen why agriculture requires continuous effort from improving technologies and for higher and higher attention, we can analyse Italian agriculture in more details.

5.1 Production and surface

First of all, we should understand what is mostly produced in Italy and how much land is dedicated to that production. Table 5.1 presents the evolution of the total agricultural production from 2011 to 2020 regarding two classes: arable land and woody and shrub crops. The same data are visible in Figure 5.1 and 5.2 along with the total surface exploited for agriculture and the evolution of the Italian population, strongly correlated with the total production.

Agriculture is not only important for its economic and social value but also from a geographical standpoint. Indeed, more than 40% of the Italian surface is devoted to agriculture, with its 12723679 ha with respect to a total surface of 30207283 ha. This shall be considered together with the fact that Italian territory is made by 42% of hills, 35% of mountains and 23% of plain. Figure 5.3 shows the amount UAA over the total province surface. If we split the agricultural production into three main classes: arable land, permanent forage-permanent grassland and pastures, and woody and shrub crops it is possible to measure the portion of land devoted to each of these three classes in each of Italian regions. These data are visible in Table 5.2 and Figure 5.4. Sicilia, Puglia, Sardegna, Lombardia and Emilia-Romagna are the regions that devote most land to agriculture while Puglia is the region with the highest relative UAA, 79%. Arable lands are mostly cultivated in the North and South, the same trend occurs for permanent forage-permanent grassland and pastures, while woody and shrub crops are mostly cultivated in the South. Table 5.3 shows the total surface exploited for agricultural use in each region for different types of arable lands, and woody and shrub crops respectively. This table helps understand what is mainly cultivated in each region and therefore to retrieve which are the main needs of each region as different crops require different treatments. Among the agricultural enterprises, 97.4% of the total rely on crops as their main production [70].

5.2 Social and economical aspects

We have already seen some economical features of Italian agriculture as a whole, now we move deeper considering the single businesses scenario. Data regarding the number of units present in agriculture (farms, businesses and enterprises) and their size are shown in Table 5.4. Most

Region	Arable land [ha]	Permanent forage-permanent grassland and pastures [ha]	Woody and shrub crops [ha]	Total [ha]
Piemonte	531322	240770	85645	857737
Valle d'Aosta	183	54000	771	54954
Liguria	54303	36623	19248	110174
Lombardia	821131	207578	31715	1060424
Trentino Alto Adige	6023	326300	45590	377913
Veneto	421079	90032	110943	622054
Friuli-Venezia Giulia	257647	45863	27043	330553
Emilia-Romagna	776813	106956	112471	996240
Toscana	350032	107097	152301	609430
Umbria	187656	78800	40003	306459
Marche	301491	62420	27183	391094
Lazio	311021	302300	142177	755498
Abruzzo	166669	233244	79503	479416
Molise	97768	50200	21070	169038
Campania	256565	115479	162884	534928
Puglia	764477	227615	551882	1543974
Basilicata	212197	135589	43517	391303
Calabria	123563	152971	238439	514973
Sicilia	581921	473048	446884	1501853
Sardegna	310287	724391	80986	1115664

Table 5.2: UAA per region per crop class in 2018. Source: ISTAT

	Piemonte	Valle d'Aosta	Liguria	Lombardia	Trentino Alto Adige	Veneto	Friuli-Venezia Giulia	Emilia-Romagna	Toscana	Umbria
Arable land										
Cereals	349724	32	51343	334020	586	132883	159600	319260	156174	88940
Legumes	5899	0	69	9519	6	3339	659	21657	21230	6531
Roots, bulbs and tubers	1771	0	48	321	52	2243	19	5227	502	163
Potato	1247	150	708	604	670	3020	226	5274	979	400
Early potato	4	0	340	0	0	0	0	0	64	0
Sweet potato	0	0	0	0	0	251	0	0	5	0
Sugar beet	620	0	0	2323	0	9697	265	21503	0	0
Beet	94	0	3	6	5	7	4	327	143	0
Horticultural	5654	1	815	14950	497	14082	367	34259	6132	1496
Industrial crops	22248	0	0	56969	0	176442	61907	47168	20040	17706
Temporary fodder	144061	0	977	402419	4207	79115	34600	322138	144763	72420
Woody and shrub crops										
Grapevine	43593	470	1625	24610	15669	87030	24052	53305	59113	12311
Olive tree	116	0	17040	2423	392	5302	625	4023	89875	27001
Citrus fruit	0	0	57	0	0	0	0	0	9	0
Bearer	41936	301	526	4682	29529	18611	2366	55143	3304	691
	Marche	Lazio	Abruzzo	Molise	Campania	Puglia	Basilicata	Calabria	Sicilia	Sardegna
Arable land										
Cereals	152203	84096	89914	68520	111405	415321	159945	64613	289057	51165
Legumes	18264	3579	6515	2925	8403	13390	1484	3918	12585	7304
Roots, bulbs and tubers	181	2533	2225	158	2513	5850	521	1483	3519	967
Potato	141	2081	4543	230	5127	1060	106	4489	2032	291
Early potato	3	59	56	70	2487	1585	0	370	6852	1161
Sweet potato	13	47	0	0	0	60	0	2	0	0
Sugar beet	0	0	0	0	0	0	0	0	0	0
Beet	0	0	0	0	15	46	0	0	0	202
Horticultural	3569	16369	15420	3260	23785	80079	10017	17201	51095	14993
Industrial crops	41866	4793	4178	1595	4189	2134	530	86	1	13
Temporary fodder	85251	197464	43818	21010	98641	244952	39594	31401	216780	234191
Woody and shrub crops										
Grapevine	15865	21031	33202	5605	25678	112249	2516	9145	125759	27180
Olive tree	9606	83041	41895	14335	75663	383650	26086	184529	157861	40604
Citrus fruit	0	614	6	4	2962	9301	5814	37465	85324	3329
Bearer	1712	37491	4400	1126	58581	46682	9101	7300	77940	9873

Table 5.3: UAA per region per type of arable land and per type of woody and shrub crops, 2018. All values in hectares. Source: ISTAT
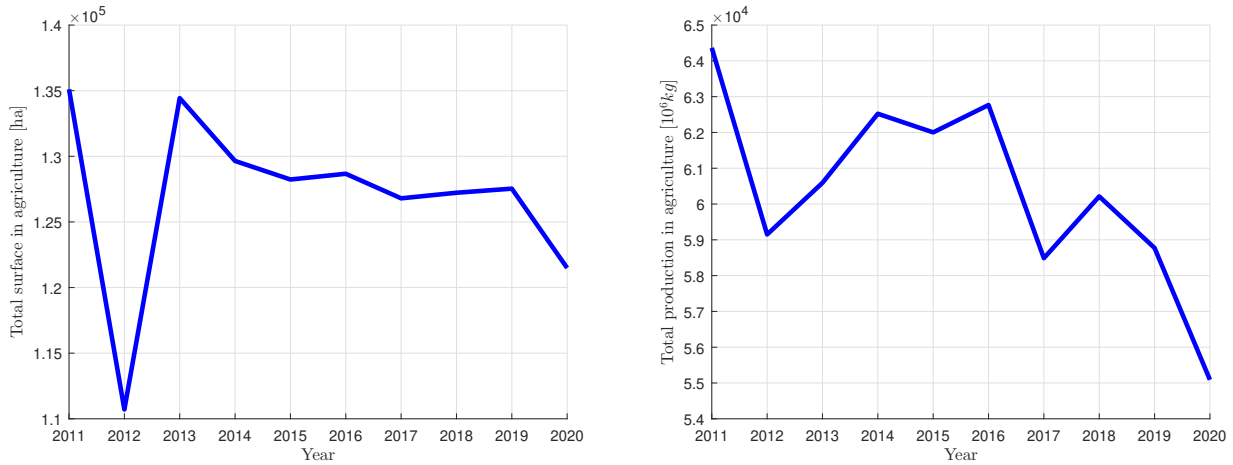
(a) Total surface for agriculture, from 2011 to 2020. Source: ISTAT [63]

(b) Agriculture production, from 2011 to 2020. Source: ISTAT [63]
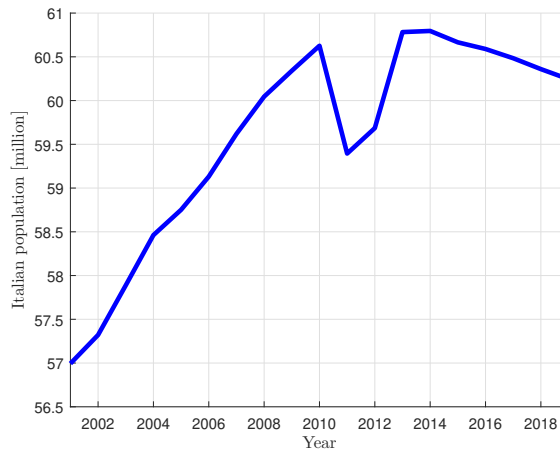
(c) Italian population evolution, from 2001 to 2019. Source: ISTAT [63]

Figure 5.1: Italian agriculture macro data. Source: ISTAT [63]

of the production units are present in South Italy: 46.9% of the total units (700 thousand enterprises) are in Puglia, Sicilia, Calabria and Campania. Again Puglia, Sicilia and Sardegna are the regions that show higher levels of UAA (over 1.3 million hectares) while Liguria has the least surface [70]. Among the 1.5 million economic units in agriculture, there are about 413 thousands agricultural enterprises (27.3%), who own over 65% of the UAA (average UAA is higher than 20 hectares). On the other side, there are 86 thousands agricultural enterprises (5.7%) owned by businesses that mainly operate in other sectors, public authorities and non-profit organizations. 550 thousand agricultural enterprises who are present on the market on occasion, they own 22% of the total UAA and, finally, 465 thousand agricultural enterprises (30.7%) that are a family business, more often with the only purpose of self-consumption and characterized by very small dimensions, 1.7 hectares on average [70]. The differentiation
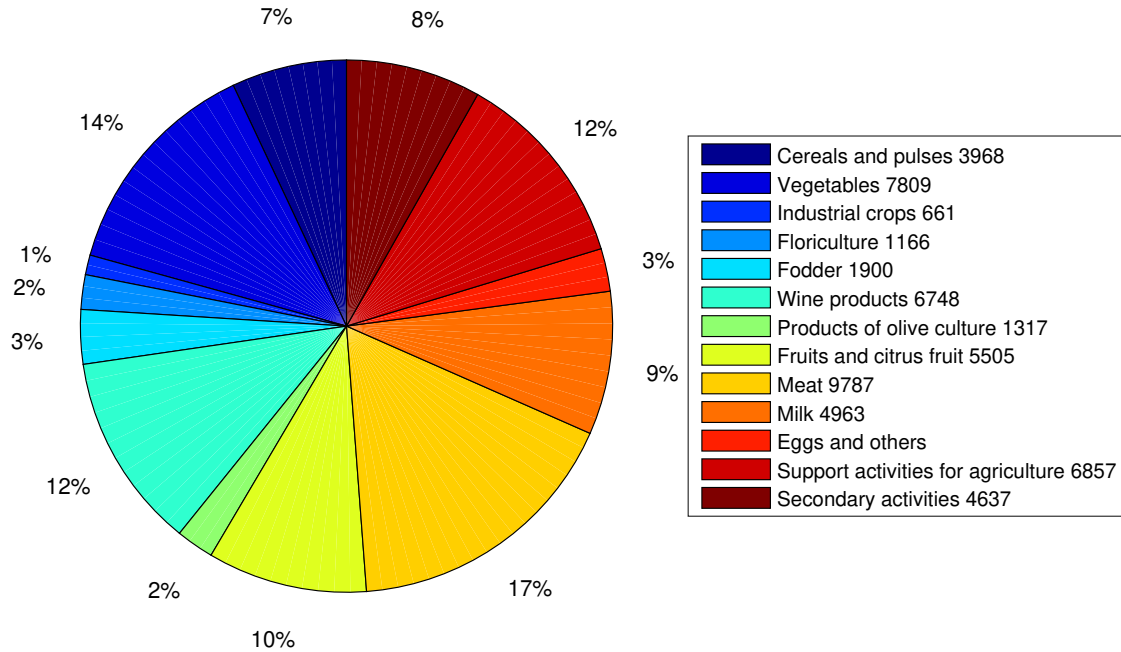
Figure 5.2: Production of goods and services at basic prices of the agricultural branch - Values at current prices (millions of Euro). Source: ISTAT [63]

of these types of enterprises along with their dimensions is shown in Figure 5.5. Agricultural enterprises are mainly present in North Italy while South Italy is mostly characterised by family businesses. The histogram of Figure 5.6a shows which kind of agricultural units are mainly spread in Italy, in terms of size. In 2017 in Italy there were more than 1.5 million units. In particular, 71% of the total units are characterized by a UAA lower than 5 ha and 46% of those units (almost 500000 units) own a parcel smaller than 1 hectare. This means that there is a strong presence of small farms, enterprises and businesses in Italy. This fact will lead to several considerations in the following as such small entities requires a lot of attention and precision in their production chain as they are much sensitive to small changes and unexpected events. The map of Figure 5.6b shows how the units are spread over the territory. In South Italy, there is a higher number of units but on the contrary, these are smaller compared to those of Northern Italy. There is a differentiation between the number and size of units from north to
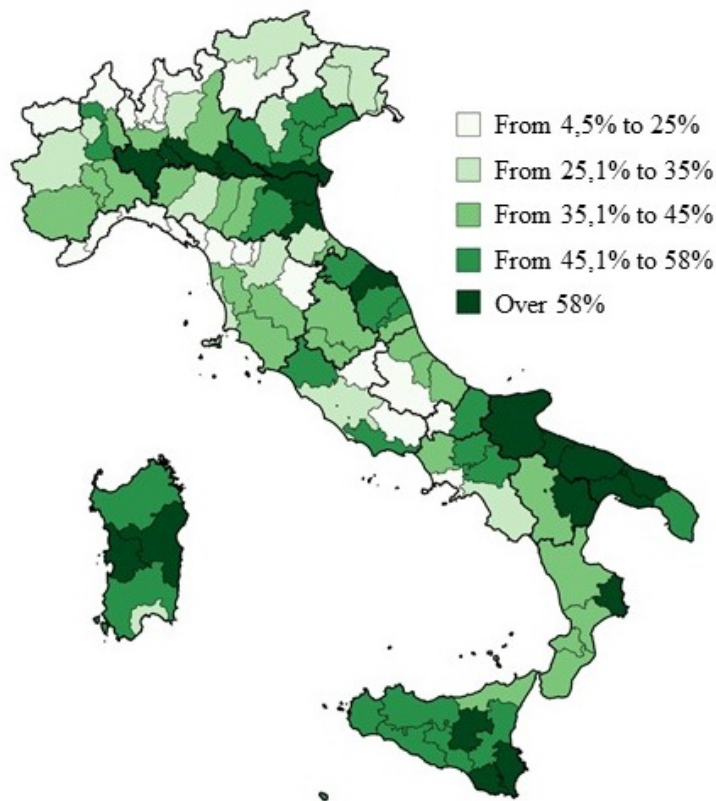
Figure 5.3: UAA over total province surface, 2017. Source: ISTAT

south. Table 5.5 and Table 5.6 depict some economical macro data about Italian companies. In Northern Italy, farms are larger in size and manage to produce more with respect to farms that operate in Southern Italy. On average, a farm owns a parcel of about 8 hectares and produce about 27 thousand Euro per year. Therefore, on average in Italy farms are small-medium sized and their turnover is contained. These two facts stress the need of putting higher effort into increasing the production and decreasing the costs while maintaining high quality. Almost 90% of Italian farms have a turnover lower than 49999.99 Euro, while 70% drops even down to 14999.99 Euro, confirming the scenario depicted above. Agricultural enterprises specialized in permanent crops represent 27.7% of the standard production while those specialized in farming represent 36% of the standard production [70]. Speaking about employment, the 413 thousand agricultural enterprises employ about 815 thousand people and 98.6% of those enterprises on average employ less than 10 people. There are only 5 thousands enterprises that employ more than 10 people and less than 50 while only 0.1% of the enterprises employ more than 50 people. 520 thousand people work in enterprises that cultivate crops. In 2019 the value of production made by agriculture, fishery and forestry was 61.6 B€, as we have seen agriculture made a little worse than in 2018 but the agri-food chain increased its added value. Also, the costs of production have increased in 2019, in particular, prices of seed, motive power, plant protection products, insurances, water, transportation and fertilizers increased [64]. Production decreased in all the regions except for those in the South where it increased by 2.3%.
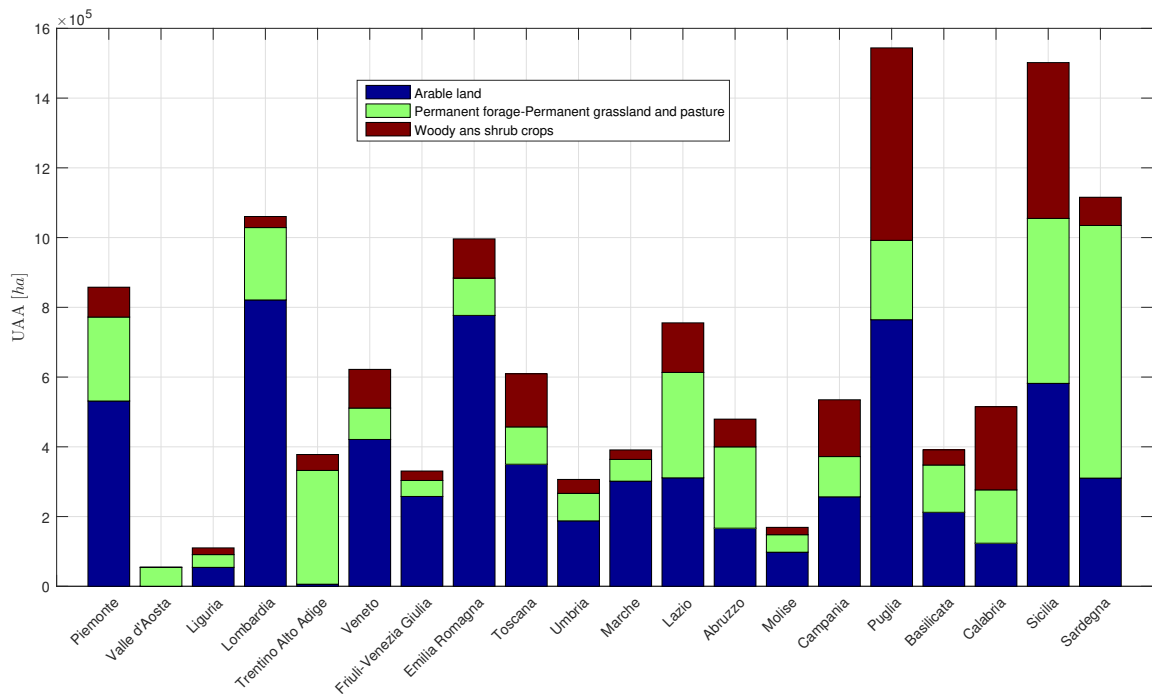
Figure 5.4: UAA per region per crop class, 2018. Sorce: ISTAT

5.3   Environmental aspects

The Coldiretti analysis on greenhouse emission in Italy [15] states that only 7% of the national greenhouse emission are produced by agriculture. Meanwhile, only 11.8% of the fine dust present in the air comes from agricultural soils and breeding. Overall, Italian agriculture is one of the most sustainable in Europe with 30 million tonnes of $C0_2$ equivalent; France, Germany, UK and Spain agricultures produce more CO_2 than Italy. These results are possible thanks to the 299 PDO, PGI, TSG specialities (European record), 524 DOC, DOCG and IGT wines, about 79000 operators in organic agriculture (European leadership), the highest number of young farmers under 35 and the highest number in the world of agri-food products that respect the limits of chemical residue. Italy holds the world record in the number of farmers' markets with the largest direct sales network of farmers. Finally, Italy is the fourth world producer of biogas with 77% of the total plants that process agricultural biomass waste. In general, there are many chemicals used in agriculture, such as fertilizers, pesticides and plant protection products. In case their amount is not exactly tuned with respect to the crop or soil actual need there are numerous drawbacks. In case the crop need has been excessed, the product's quality is altered and its high chemical content is absorbed by the person who will eat the crop product. The direct damages against human health are clear. Moreover, the high amount of chemicals will be absorbed by the soil and transferred to surface or groundwater. The resulting polluted water will be used again in agriculture, maintaining high the levels of the chemicals, or for human and animals supply, causing health issues. In the opposite case, when chemicals less than needed are applied, the harvest may not match the expectations in terms of quantity and quality, or even worse, much of the harvest may be damaged by insects or diseases. As it is

	Units	UAA [ha]	Average UAA [ha]		Units	UAA [ha]	Average UAA [ha]
Piemonte	65.847	847.627	12,873	Marche	43.838	480.178	10,953
Valle d'Aosta	3.289	68.703	20,889	Lazio	104.686	637.286	6,088
Lombardia	51.620	1.056.558	20,468	Abruzzo	56.441	358.108	6,345
Liguria	19.249	45.548	2,366	Molise	25.370	186.712	7,360
Trentino-Alto Adige	37.302	313.923	8,416	Campania	129.724	551.124	4,248
Veneto	88.206	747.969	8,480	Puglia	242.899	1.328.051	5,468
Friuli-Venezia Giulia	21.834	235.678	10,794	Basilicata	45.260	516.932	11,421
Emilia-Romagna	68.713	1.007.144	14,657	Calabria	145.824	628.558	4,310
Toscana	67.031	646.265	9,641	Sicilia	192.904	1.425.825	7,391
Umbria	39.719	360.858	9,085	Sardegna	66.379	1.333.999	20,097
Italia	1.553.437	13.090.968	8,427				

Table 5.4: Number of units and their size per region, 2017. Source: ISTAT

	Units	UAA [ha]	Average UAA [ha]	Production [M€]	Average production [€]	Average turnover [€]	Intermediate costs [€]
North	393362	4637072,2	11,78	22119	58500		
Center	255274	2124587	8,32	4723	19986		
South	904801	6329309	6,99	14060	16080		
Italy	1553437	13090968,2	8,42	40902	27473	25531	11323

Table 5.5: Main economic features of Italian agricultural units, 2017. Source: ISTAT [63]

clarified in Figure 5.9 Italy is already doing a great job in containing the fertilizer consumption with respect to other countries. In this graph, that compare the kg of fertilizer per hectare of cultivated land in Italy, Germany, Spain, France and Netherlands, only chemicals fertilizer have been considered. However, fertilizer consumption is very variable over Italian regions. The map of Figure 5.7a and the histogram of Figure 5.8 show that there is a relevant use in the northern regions that decreases going south. Lombardia, Emilia-Romagna and Veneto are the regions with the highest fertilizer consumption; in 2018 more than 70000 tonnes of fertilizer were employed in Lombardia, more than three times of the Sicilian consumption. This trend of higher consumption in the northern regions is stable during the years, as depicted in Figure 5.7b. In the following, we will see that this imbalance led to environmental damages. Overall,

Italy	Units	Average economic values for companies by turnover class				
	1553437	Up to 14999,99 €	15000 - 49999,99 €	50000 - 99999,99 €	100000 - 449999,99 €	Over 500000 €
Companies %		70,7%	18, 4%	5,8%	4,6%	0,5%
Production, average [€]		3472	29220	71920	203890	1232782
Turnover, average [€]		2706	27310	68993	192947	1156741
Intermediate Costs, average [€]		1743	10749	24930	73388	664084

Table 5.6: Economic features and division for companies, 2017. Source: ISTAT [63]
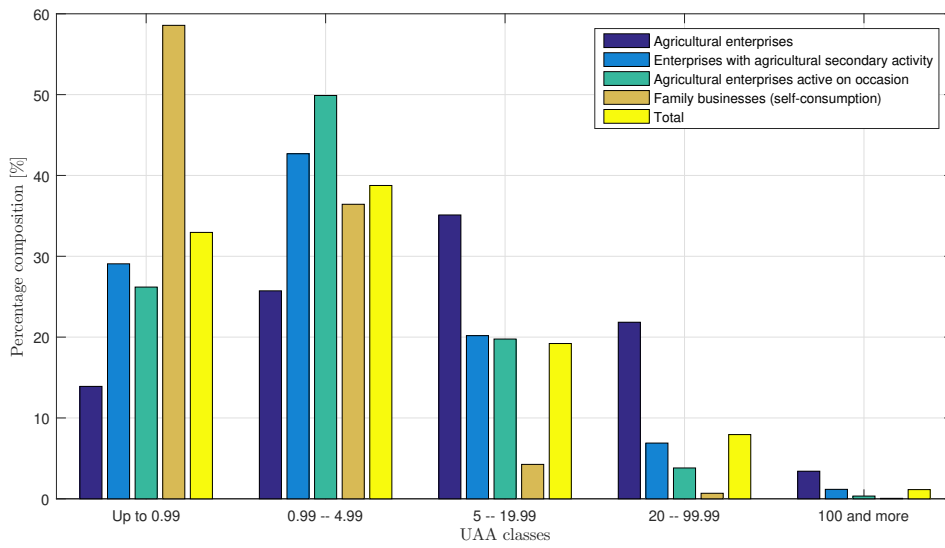
Figure 5.5: Production units per type per UAA classes, 2017. Source: ISTAT [63]
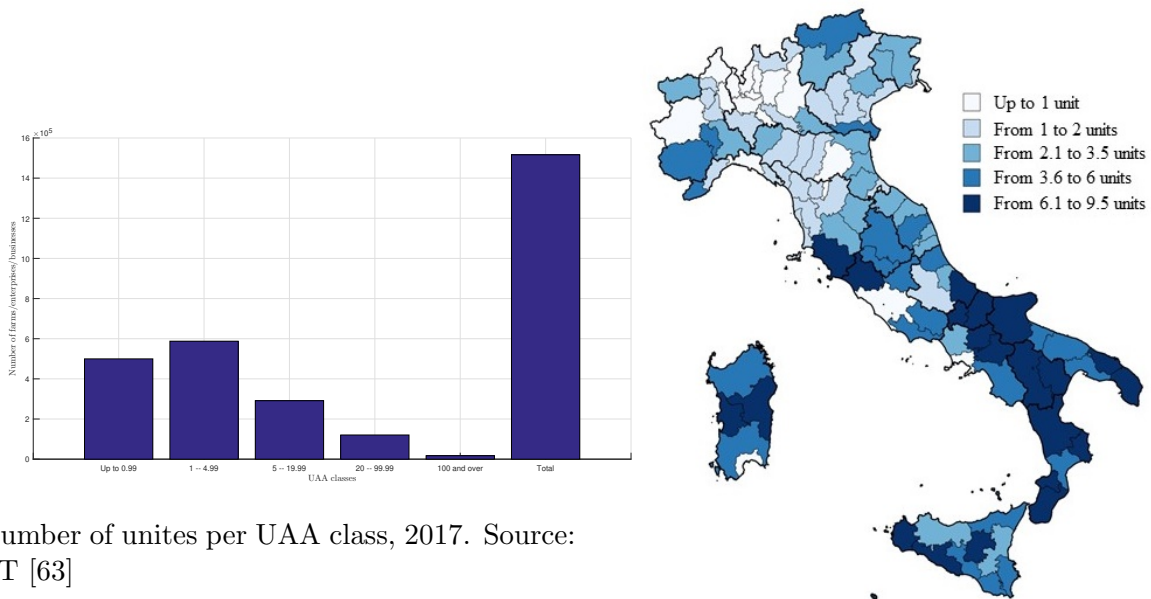
(a) Number of unites per UAA class, 2017. Source: ISTAT [63]

(b) Agriculture production, from 2011 to 2020. Source: ISTAT [63]

Figure 5.6: Distribution of units fro UAA classes and over the territory, 2017. Source: ISTAT [63]

in Italy, about 4.3 millions tonnes of fertilizer have been spread for agriculture in 2019 [63].

Considering plant protection product, the scenario is similar to that shown for fertilizer. Northern regions, Veneto and Emilia-Romagna, are those who make use of more plant protection products. However, considerable amounts are exploited in Puglia, Sicilia and Campania as
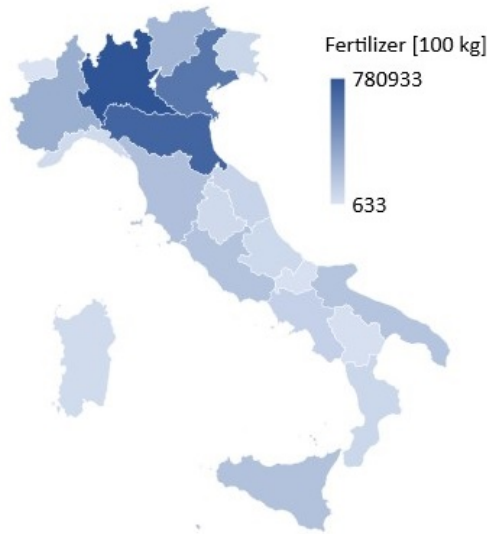
(a) Map of fertilizer consumption, 2018. Source: ISTAT [63]
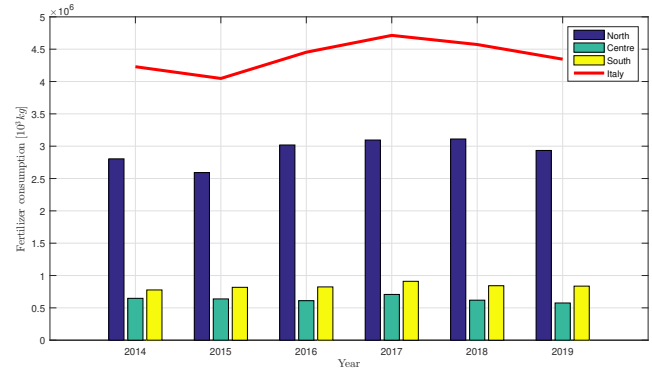
(b) Fertilizer consumption over the 2014 - 2019 period. Source: ISTAT [63]

Figure 5.7: Fertilizer consumption per region and over the years

well, even more than Lombardy and comparable to Piemonte. The plant protection products use in 2018 over the 20 Italian regions is shown in Figure 5.10. In particular, 120000 tonnes of plant protection products have been used in 2018 [63], this number is slowly decreasing over the years as depicted in Figure 5.10b.

According to the national report on pesticides in water by ISPRA [86], the researches conducted during the 2015-2016 period, indicated a widespread of pesticide presence and contamination. Herbicides were still the most commonly found substances, above all a cause of direct use on the soil. Compared to the past, the presence of fungicides and insecticides has increased, above all because the number of substances sought has increased and their choice is more targeted to the uses on the territory. Overall, contamination is more widespread in the Po-Veneto plain, due to its intense agricultural use. In surface waters, 23.9% of the total, have concentrations above environmental limits, while in groundwater, 8.3% of the total have concentrations above the limits. The progressive increase in the territorial diffusion and presence of pesticides, in the period 2003-2016, has a direct correlation to the extension of the network and the number of substances sought. Veneto is one of the regions that employs more kg of pesticides per cultivated area, 10 kg/ha, against the national average of 4.6. The 2016 data reveals the presence of pesticides in surface waters in 67% of the total monitoring points. In groundwater, pesticides are present in 33.5% of the total monitoring points. Herbicides and some of their metabolites are still the most commonly found substances, especially in surface waters. The ISPRA suggests that preventive actions are envisaged at different levels of intervention, such as: agricultural practices compatible with the environment such as organic farming and defence integrated plant protection system with low pesticide input, favouring non-chemical methods; operator training; correct handling, storage and treatment of packaging and inventories; measures for the protection of the aquatic environment. The reduction in consumption of
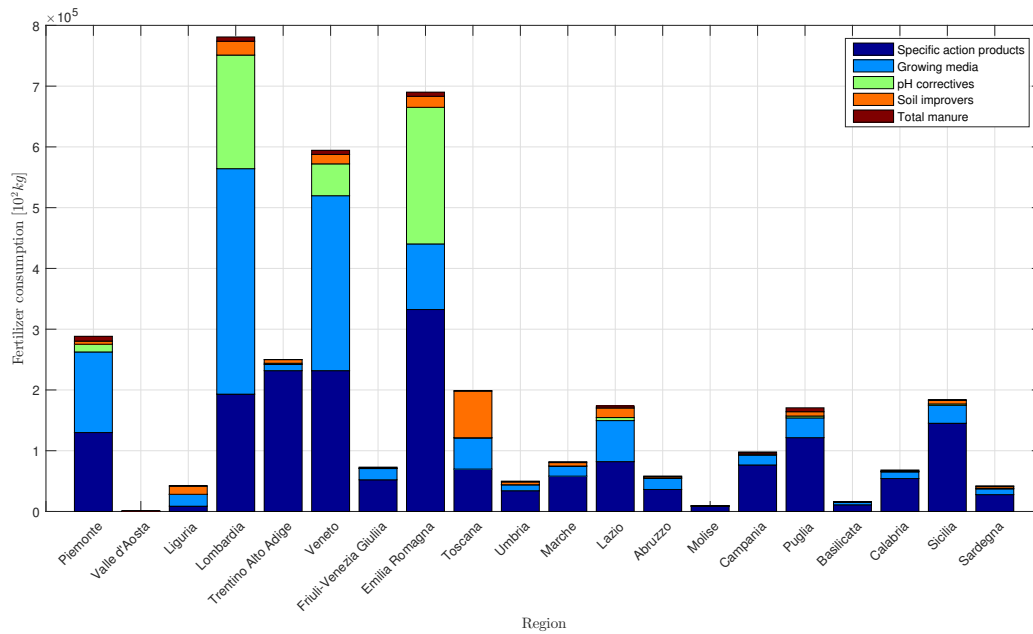
Figure 5.8: Fertilizer consumption per type in Italian regions, 2018. Source: ISTAT [63]

the most dangerous products would seem to highlight their more cautious use in agriculture. This trend is favoured by the orientation of the national and European agricultural policies and by the economic incentives granted within the Community for the purpose of adopting low impact techniques in agriculture and the enhancement of quality in productions.

Considering water usage, overall Italy has wide availability, on overage, it rains 1000 millimetres a year. However, there are regions where the actual number approaches 2000 millimetres and others where it gets down to 300. Of course, water is vital for agriculture but climate changes are reducing the number of rainfall while increasing their intensity. In 2016 there was a strong deficiency of snowfall in the Alps, unexpected snowfall and frost in central Apennines and southern regions, and strong rainfall and flooding in Sicily. Overall, in 2016, drought interested the whole country. Moreover, the water availability in agricultural dams has dropped from 2016 to 2017. Thus, it is more and more important to use techniques that reduce the water consumption and allow to select the perfect way, time and amount of dosing, sharing it with the farmers. The development of precision agriculture was selected as a major step to be taken, in 2017 five European countries (included Italy) gave birth to the *Irrigants d'Europe*, a project whose goal is to create an European strategy for water usage in agriculture while facing issues such as climate changes, power consumption, human health and food security [54]. According to [12] in 2020 Italy is undergoing the strongest water shortage of the last 60 years. Agriculture in Italy, exploits 70% of the available fresh water, one of the worst performance in Europe. In the last 20 years, water shortages have caused over 15 billions Euro damages in agriculture, especially in Puglia, Emilia-Romagna, Sicilia and Sardegna. Finally, it was calculated that precision agriculture could lead to saving up to 50% of water consumption.
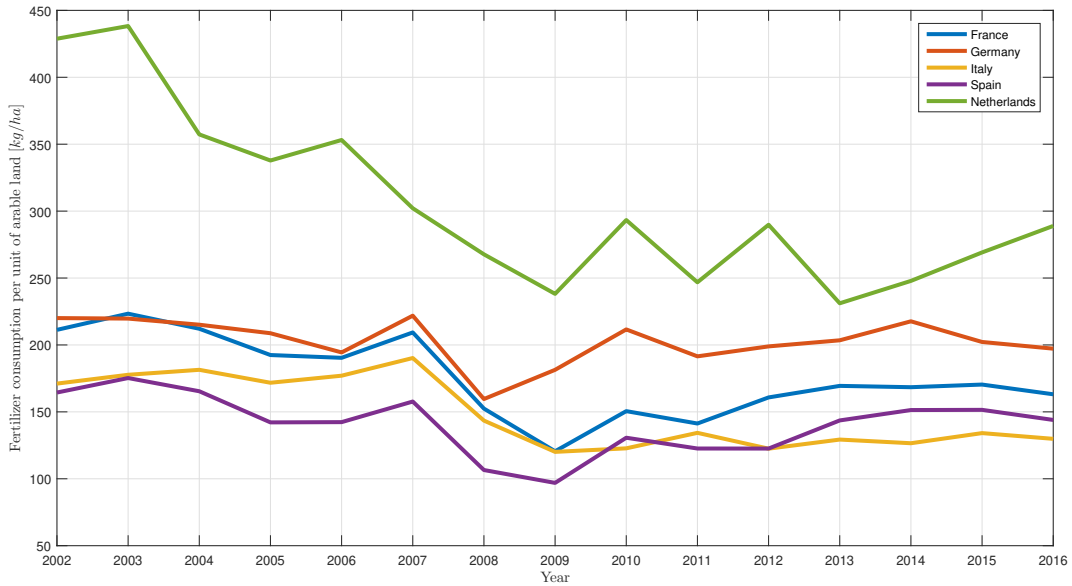
Figure 5.9: Relative fertilizer consumption from 2002 to 2016 in 5 European countries including Italy. Source: Knoema

(b) Plant protection products consumption over the 2014 - 2019 period. Source: ISTAT [63]
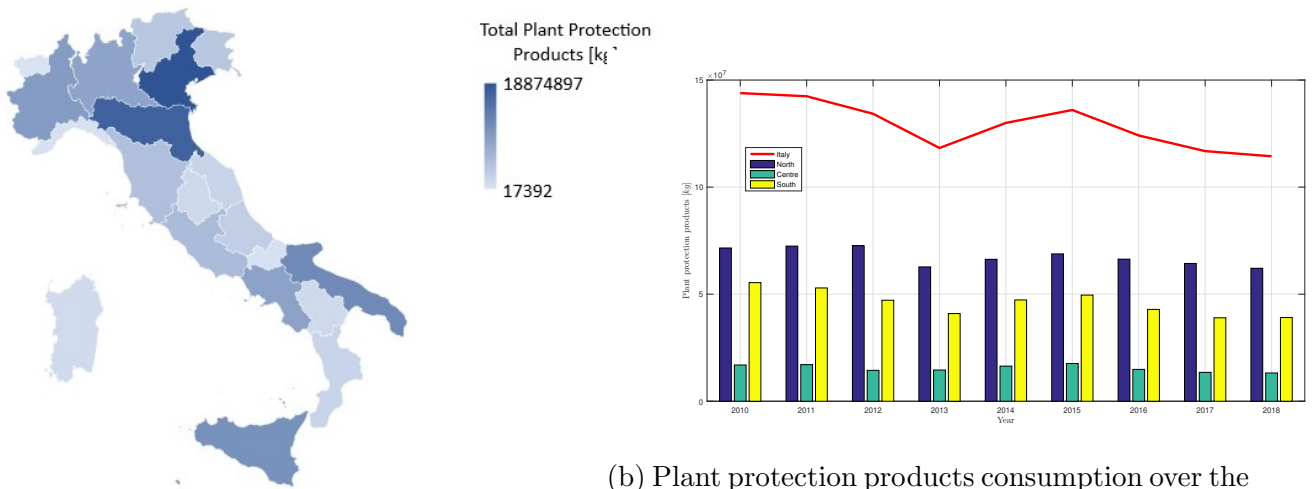
(a) Map of plant protection products consumption, 2018. Source: ISTAT [63]

Figure 5.10: Plant protection products consumption per region and over the years

5.4 Precision agriculture

According to a research conducted in 2015 by the Italian Ministry of Agricultural, Food and Forestry Policies, only 1% of the UAA were processed by means of precision agriculture technologies. The main applications were yield mapping, driving systems, ISOBUS, control of
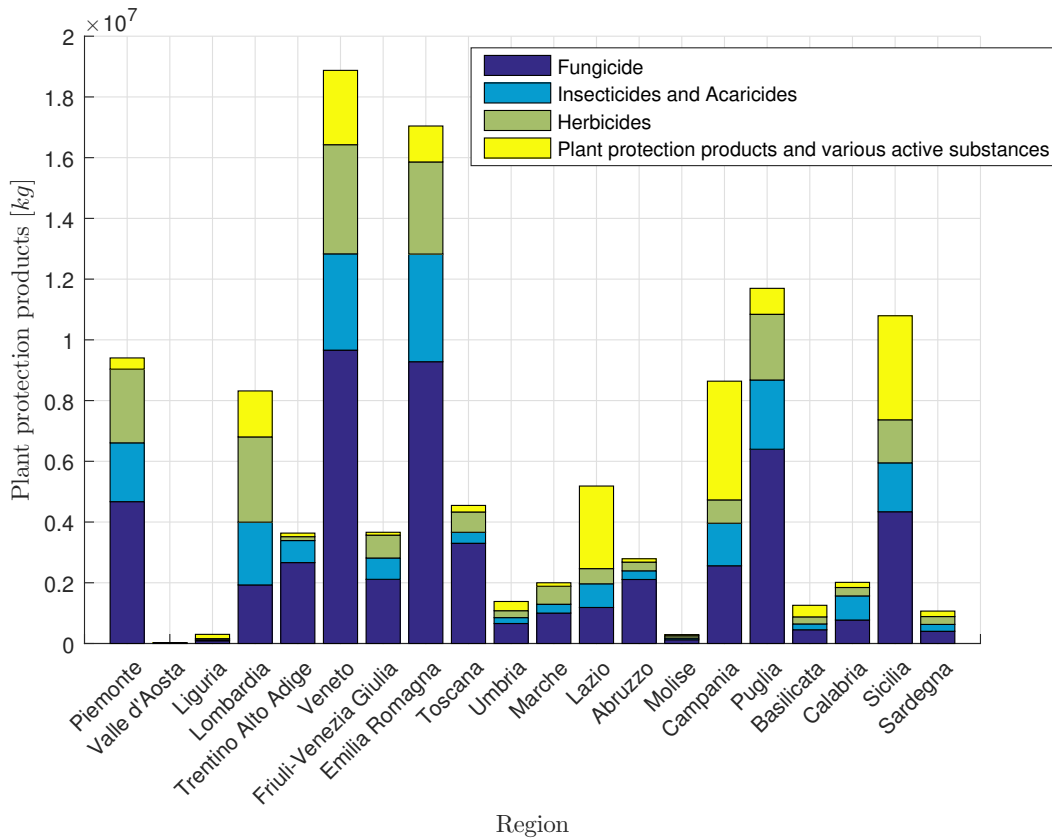
Figure 5.11: Plant protection products consumption per type in Italian regions, 2018. Source: ISTAT [63]

equipment, VRT. In September 2017 the Ministry of Agricultural, Food and Forestry Policies issued a document called *Guidelines for the development of precision agriculture in Italy* [8]. This document gives a very detailed introduction and description of precision agriculture. In the forthcoming scenario, the agricultural sector will be asked to face two challenges, one, the increase of production with the least possible environmental impact, and second, the increase of the production efficiency and input consumption efficiency with the least possible environmental impact. In both cases, precision agriculture is the most important available tool. Moreover, the strategic innovation plan, given by the EU, defines four bullet points that aim at sustainability and precision agriculture has been identified as a necessary step to the achievement of the previous. The technologies available on the market not always answer the farmers' needs because sometimes these do not meet the agriculture local conditions or because these are too expensive. Overall, the development of precision agriculture in Italy is consistent with the development over the European Union and, precision agriculture itself is undergoing its third acceptable time thanks to the cost reduction and new market models. According to this document, the benefits expected from precision agriculture are: optimisation of production and quality efficiency; cost reduction; inputs optimisation while reducing environmental impacts; creation of new business opportunities. The document goes on to describe many applications of precision agriculture and the technologies involved. It also depicts the Italian diffusion of pre-

cision agriculture with respect to the international scenario. Despite the outstanding benefits, precision agriculture in Italy is not diffused as much as in other countries. The causes can be identified in strongly heterogeneous environments; environment characteristics; age, education level and farms dimensions. Therefore, precision agriculture shall also target those farms that can reorganize themselves by means of small but effective actions. It is underlined that Italian territory is characterized by high-quality productions, and then the technological contribution should respect the processes and methods that give value to those productions. It is worth mentioning the importance of the technologies that trace the high quality-products that are more often subjected to counterfeiting (i.e. fake *made in Italy*). The research conducted established that despite the huge offer available on the market the situation is still in its first development phase. It was estimated that in the future the business volume for agronomic consulting and services provision is overcoming that of driving systems. Finally, precision agriculture is of fundamental importance in the context of CAP as it joins the two cores of the CAP, sustainability and innovation [8]. We have already seen some precision agriculture projects in Chapter 1, some of them based in Italy as well; we now go through some specific application. Within the ERMES project, it was developed a service to show the utility of using satellite maps to support variable rate fertilisation [10]. Very high resolution imagery, both optical and SAR, were used to produce prescription maps for nitrogen fertilisation to be used in VRT. The experiments, conducted in three different regions, including Italy, demonstrated the usefulness of satellite-based solutions for decreasing the costs through accurate use of fertilizers and improving yield through better management of intra-field variability. In the Italian context, it was shown that adopting VRT technologies leads to a rise in production with a possible income increase up to 72 €/ha [10]. At the same time, it helps avoid negative environmental impacts and farmers comply with European regulations.

Chapter 6

Requirements definition

The objective of the mission is to design a LEO constellation of microsatellites capable of providing SAR data for the Italian agriculture use case. In order to design the constellation, we draw some requirements that need to be satisfied. These are driven by the current offer of SAR data by other constellation (see Chapter 3) and by the user needs, that were derived from the characteristics of the Italian agriculture exposed in the previous chapter. Moreover, the requirements were written trying to put the constellation in a complementary position with respect to the Sentinel satellites. The requirements are listed in Table 6.1. In Table 6.1 we refer to the mission with the acronym MAESTRO (Microsatellites SAR conStellation for iTalian agRiculture Observation).

REQ.ID	Importance	Requirement	parent req	notes
MA-F-001	M	The mission shall be designed as an EO imaging radar mission providing continuity of data for user services		
MA-F-002	M	The payload shall include an imaging Synthetic Aperture Radar that is optimised for the mission objectives	MA-M-002	
MA-F-003	M	The mission shall aim at providing the following services: Precision Agriculture, Insurance, Food Security - Trading		If a requirement specifically refers to only one, or two of these services it will have the identifying code at the beginning: respectively PA, IN, FT

REQ.ID	Importance	Requirement	parent req	notes
MA-F-004	M	Within the services listed in MA-F-002 the MAESTRO mission shall provide the following low-level services: see Table 6.2	MA-F-002	see Table 6.2
MA-F-005	M	The mission shall provide assessments of the products listed in Table 6.2	MA-F-003	see Table 6.2
MA-F-006	M	The mission shall provide coverage of the following geographic area: 35.2° N up to 47.1° N, 6.5° E up to 18.5° E		Italian territory - see Table 6.2 for further details
MA-F-007	M	The mission shall ensure 3 h of timeliness after observation		
MA-F-008	M	The mission shall ensure the complete coverage of the area of interest in 7 days		see Table 6.2 for area of interest
MA-M-001	M	The mission shall provide the following hours of revisit time: see Table 6.2		see Table 6.2
MA-M-002	M	The mission shall operate in the following centre frequency: X-band		
MA-M-003	M	The services expressed in MA-F-003 shall be delivered with a minimum accuracy of: see Table 6.2	MA-F-003	see Table 6.2
MA-M-004	M	The mission shall operate in the following modes: Spotlight acquisition mode		
MA-M-005	M	The mission shall operate exploiting the following polarizations: single, dual, quad - pol		
MA-M-006	M	The geo-location accuracy of data shall be better or equal than 2 m		
MA-O-001	M	The mission shall be operational for at least 4 years		
MA-O-002	M	The mission shall operate in a systematic mode and provide "On Demand" operations as well		

REQ.ID	Importance	Requirement	parent req	notes
MA-O-003	M	Data quality and system performance of the mission shall be maintained		
MA-O-004	M	IN: The mission shall guarantee at least TBD h of geometrical accessibility (On Demand operations)	MA-O-002	
MA-P-001	M	Each satellite shall not exceed 200 kg of mass		Wet mass
MA-P-002	M	Each satellite shall carry a SAR payload that do not exceed 90 kg of mass		

Table 6.1: Requirements for the mission design

Precision Agriculture

Low-level services

Variable Rate Technology Applications

Products: Crop growth rate, Leaf Area Index, Normalized Difference Vegetation Index, Fraction of Vegetation Cover, Crop biomass

	Spatial Resolution	Temporal Resolution	Coverage	Period	Duration
Nominal - North/Center Italy	<3 m	≤ 7 days	8939210 ha	12 months	12 months
Nominal - Center/South Italy	<3 m	≤ 7 days	9825940 ha	12 months	12 months
Out of nominal / Emergency (water shortage)	-	-	-	-	-

Precision Irrigation

Products: Soil moisture, Leaf Area Index, Vegetation Drought Index

	Spatial Resolution	Temporal Resolution	Coverage	Period	Duration
Nominal - North/Center Italy	<5-10 m	5 days	8939210 ha	12 months	12 months
Nominal - Center/South Italy	<5-10 m	5 days	9825940 ha	12 months	12 months
Out of nominal / Emergency (water shortage)	<5-10 m	≤ 2 days	zone 1, 2 and 3	†	6 weeks

Yield Estimation

Products: Leaf Area Index, Crop biomass, Enhanced SAR Vegetation Index

Spatial Resolution	Temporal Resolution	Coverage	Period	Duration
6 m	weekly	8939210 ha	12 months	12 months
10 m	weekly	9825940 ha	12 months	12 months
6 m	≤ 2 days	zone 1, 2 and 3	†	6 weeks

Food security and Trading

Low-level service

Crop Land Estimation

Products: Leaf Area Index, Crop biomass, Fraction of Vegetation Cover

Spatial Resolution	Temporal Resolution	Coverage	Period	Duration
6 m	9 days	18765150 ha	12 months	12 months

Crop Yield Assessment

Products: Leaf Area Index, Normalized Difference Vegetation Index, Enhanced SAR Vegetation Index

Spatial Resolution	Temporal Resolution	Coverage	Period	Duration
8 m	weekly	18765150 ha	12 months	12 months

Insurance

Low-level service

Vegetation Condition & Crop Monitoring

Products: Leaf Area Index, Crop biomass, Fraction of Vegetation Cover

Spatial Resolution	Temporal Resolution	Coverage	Period
10 m	On Demand	18765150 ha	12 months

Table 6.2: Annex table to requirements. Note: zone 1, zone 2 and zone 3 are defined explicitly in the relative section. †: June–July–August and January–February–March for zones 1 and 2, and December–January–February–March for zone 3.

Let us now try to see what is the rationale behind the values that are present in 6.2.

6.1 Precision agriculture

Regarding precision agriculture, three low-level services were identified:

- Variable rate technology applications

- Precision irrigation

- Yield estimation

Each of these services is then split into a "nominal" case and an "out of nominal / emergency" case. The "out of nominal / emergency" case refers to the eventuality where data would be needed more frequently in order to minimize the effects of an emergency, which could be a water shortage period. This allows to discriminate from different scenarios and to avoid overestimation. Moreover, the "nominal" case is further divided into two geographical regions: a north/centre region (corresponding to the relative Italian regions) and a centre/south region. Then, for each of the three low-level services and for each of the three geographic-situation cases, five performance parameters are identified. They are:

i Spatial resolution: the resolution of the images produced by the SAR instrument

ii Temporal resolution: the constellation revisit time

iii Coverage: the area where the spatial and temporal resolutions shall be provided

iv Period: the period of the year when it is most likely that the satellites data would be needed

v Duration: the time span within the period when the previous performance parameters should be granted

We begin by considering the VRT Applications case. In both of the geographic regions, in the nominal scenario, the requirements for spatial resolution, temporal resolution, period and duration are the same. The requirement on the spatial resolution comes from the available technology currently used for variable rate application. Devices on board agriculture machinery are capable of spreading, spraying and operating within an accuracy of 3 to 5 m. It is fundamental that the operation carried out by these machineries are based on reliable and accurate data in order to fully exploit the potential of the available technology. The revisit time for precision agriculture has been set to an upper limit of 7 days. Period and duration requirements coincide as they strictly depend on the type of crop and its phenological cycle. In order to cover as many crops as possible, the service shall be provided during the whole year. The coverage requirement in the north/centre area comes from the UAA of those regions (Valle d'Aosta, Piemonte, Lombardia, Trentino Alto Adige, Friuli Venezia Giulia, Veneto, Liguria, Emilia Romagna, Toscana, Umbria, Marche). It is equal to 5717032 ha (35.5% of the total regions surface and 19% of the Italian surface). A 20% margin, of the total north/centre area, was added, in

order to avoid bad coverage where areas would remain out of the constellation passages. The coverage requirement in the centre/south area comes from the UAA of those regions as well (Lazio, Abruzzo, Molise, Campania, Puglia, Basilicata, Calabria, Sicilia, Sardegna). It is equal to 7006647 ha (49.7% of the total regions surface and 23.2% of the Italian surface). Again, a 20% margin, of the total centre/south area was added. We can now move to the precision irrigation service. All three cases have the same spatial resolution. $< 5 - 10$ m. This requirement is still driven by the accuracy of the latest technology employed in irrigation. This is able of spraying water, adjusting the output within around 5 m. Coverage, period and duration for the nominal cases are the same as the VRT Applications service since the same considerations still apply. The temporal resolution has been assessed considering the water need of different crops. Table 4 in the Appendix lists 21 different crops, and for each of them, the maximum and minimum water need during the growing period W_{need}, and the maximum and minimum duration of the growing period T_{crop}. These crops can be characterized as shallow rooting crops, medium rooting crops or deep rooting crops. Then, depending on the soil type, shallow and/or sandy, loamy or clayey; it is possible to define the approximate net irrigation depths d_{net} as a function of the root type. This is shown in Table 2. The water provided by rain shall be considered as well. Table 3 presents the average daily and monthly rainfall during the twelve months of the year in Italy. According to these data and the growing period of crops, it is possible to roughly retrieve the amount of water provided to the crops by rainfall. This is a variable parameter as it depends also on the geographic position, it may change year after year and it depends also on several field characteristics. Then, defining an efficiency for the field application ea, as part of the water is lost through deep percolation and run-off, yields to the calculation of an approximate gross irrigation depths for each of the root and soil types [41]:

$$d_{gross} = \frac{100 \ d_{net}}{ea} \tag{6.1}$$

where the efficiency has been set to 90%, a typical value for drip irrigation. Once the gross irrigation depths has been found, it is possible to retrieve the number of irrigation applications over the growing period N_{irr} and the irrigation interval t_{irr} as it follows [41]:

$$N_{irr} = \frac{W_{need}}{d_{gross}} \quad , \quad t_{irr} = \frac{T_{crop}}{N_{irr}} \tag{6.2}$$

The irrigation interval has been calculated considering all possible combinations of water need, growing period and soil type. The shortest irrigation interval was found for rice to be about 5 days. Then, the time resolution for precision irrigation, in the nominal north and south cases, is set to 5 days. The out of nominal / emergency case consists of a water shortage period. In this scenario, water provided by rainfall is missing and even water reserves may not be as available as usual. More than usual, it is required to irrigate the crops with their exact water need, to avoid waste; and it may be even required to estimate the crop that needs water the most as there may not be enough water for all crops. The process used is the same as above with the difference of absence of rainfall. The absence of rainfall during the whole growing period is a strong assumption but it allows to remain on the safe side and not to underestimate the scenario. With no rainfall, the shortest irrigation interval has been found with the minimum duration of the growing period, the maximum water need and a clayey soil for rice and potato;

2.14 days and 2.5 days respectively. Therefore, it is reasonable to assume that 2 days of revisit frequency for precise irrigation is a value with a certain safe margin, that allows the system to be robust enough. The procedure and values just used are based on [41] and [40]. Regarding the coverage requirement in the emergency case, three zones have been defined. Each zone is made by a set of contiguous regions that are more interested by water shortages [51]. Zone 1 comprises Puglia, Sicilia and Sardegna and it is the region with the highest water shortages risk [51]. Zone 2 comprises Marche, Abruzzo and Molise and finally zone 3 comprises Piemonte, Lombardia and Emilia-Romagna. The period required for emergency services is June-July-August and January-February-March for zones 1 and 2 and December-January-February-March for zone 3. These periods are based on the average rainfall per region, and they represent per each zone the time span with the lowest rainfall [51]. Data about rainfall per month per region are shown in Table 5. The duration requirement is set to 6 weeks, as an average water shortage duration, so that the spatial, temporal requirements and coverage shall be provided for 6 weeks in the periods defined. The remaining service for precision agriculture is yield estimation. Crop yield estimation refers to the capability of predicting crop yield. On one side it is fundamental for the farmer as she or he wants to be sure to at least produce enough to cover the costs, and this information is useful for decision making and improving the crop management maximizing the yield and the quality. On the other side, it is important on a national level to exactly know in advance the future yield as this will influence the products import and export and thus the market economy. Coverage, period and duration requirements are the same as in VRT applications and precision irrigation as the same considerations apply, both for nominal and out-of-nominal cases. The requirement on the temporal frequency, in the nominal case, is based on a series of scientific researches. Hadria et al. [60] investigated the performance of two approaches to test a crop model using remotely sensed estimates of LAI under various time revisit capabilities. The satellite revisit time frequency considered are: once a day, every 5 days, every 10 days and every 15 days. They found that in all cases the estimate of yield is acceptable, with an average error that is always lower than 10% of the reference value. The daily frequency always gave the best results, however, a good compromise for the satellite revisit capacity appeared to be the 10 days frequency. Zhang et al. [112] investigated the degree of vegetation phenology detection sensitivity to temporal sampling from satellite data, by means of daily EVI data. The temporal resolution used for data sampling were 2, 4, 6, 8, 10, 12, 16, 18 and 20 days. It was found that the absolute errors increase linearly with the temporal resolution of sampling and the error was lowest at a temporal resolution of 6 or 8 days. Myers et al. [82] investigated how changes in the temporal sampling rate affect the goodness of model fit and estimation of phenological transition timing for corn in the mid-Atlantic. Time series with average revisit intervals ranging from 3 to 24 days were considered and NDVI was selected as the index for temporal resampling tests. Results showed that, as the temporal sampling interval increases, estimates of all phenological transition dates vary more and more, becoming less precise. On average, a 3-day increase in temporal sampling, that means moving from one image every 3 days to one image every 6 days, will add one day of error onto estimates of crop phenological stages. Vintila et al. [105] investigated the main characteristics, including the revisit frequency, required for future space mission dedicated to monitoring crops at the field scale. This study used weekly LAI images at a spatial resolution between 10 to 20 meters. Six scenarios of satellite revisit frequency, 1, 2, 3, 7, 15, and 30 days, were considered. The results

indicated that the uncertainties of the weekly LAI estimates as compared to the reference LAI are very low and quite similar up to 7 days revisit frequency. These papers results lead to the selection of 7 days temporal resolution for yield estimation in the nominal case. Moreover, looking at the rice phenological phases, and the first phenological phase of wheat, germination and emergence, which lasts between 10 and 15 days; it is reasonable to assume that 7 days revisit time is a good compromise. An economic reason is at the of the spatial resolution requirement. The case of cereals has been analysed. For each of the twenty Italian regions, it was built a table showing the different cereals that are grown in that region, the surface devoted to agriculture and the average yield for each cereal. Then, considering the average prices of cereals over the year, the number of farms that grow those cereals and the surface they exploit, the average income of a farm, that grown cereals, has been retrieved. All these data are shown in Table 5. Usually, a farm face costs that cover from 70% up to 80% of the whole income depending on the year and also on the region. The idea behind the selection of the spatial resolution is that the farmer wants to obtain a yield that at least grants the full coverage of the expenses. This means that the farmer has to predict the yield with a certain accuracy. This accuracy is different for each region. The process used in order to estimate this accuracy is the following: in each region, it was constructed a field with a size equal to the average cereal field size of the region. That field has been subdivided into many pixels of size equal to 0.25 cm. Then, a random number has been assigned to each pixel, following a sine law along the rows, in order to simulate the spatial variability of the target physical parameters. A generic row assumes the values:

$$\zeta \, sin([0, \ 2\pi]) + \zeta \tag{6.3}$$

where ζ is a random number and $[0, 2\pi]$ is a vector of values between 0 and 2π. Given the spatial resolution of the platform, which is higher than the size of the pixels, it was assumed that the platform measures the value of one random pixel within those that lay inside the square defined by its spatial resolution. A simplified example of this process is given in Figure 6.1. The problem becomes the definition of the maximum instrument resolution capable of estimating the yield with an accuracy that allows being sure to cover the expenses. It can be simply solved by means of MATLAB *fsolve* function. The previous calculation was carried out for each region. In the case of the northern regions, it was found that a spatial resolution of 6 m is enough to estimate the yield with the requested accuracy. While, for southern regions, the same steps lead to a spatial resolution of 10 m. In the emergency case of yield estimation, the requirements are the same as the precision irrigation case but the spatial resolution. It was kept equal to that of the northern regions in the nominal case, due to the high sensitivity of the scenario.

6.2   Food security - Trading

We now move on to the second part of Table 6.2. The service food security and trading in made by two low-level services:

- Crop land estimation

- Crop yield assessment

Figure 6.1: Example spatial resolution definition. The blue box represents the field with its spatial variation inside the pixels, the red box represent the instrument pixel area of acquisition. In this particular case, the instrument measures a value of 25.2 with its resolution, while the real value of that area is 12.6

Crop land estimation refers to the possibility to recognize the type of crop that is being culti-vated and precisely estimate the size of the field devoted to that particular crop. This service has been found to be useful especially in the context of CAP, where the EU has to refund the farmer that claims an economic aid. Before refunding, the EU wants to check the validity of the declaration made by the farmer in terms of the size of her or his fields and the crops cultivated, as these define the amount of the refund. The possibility to carry out these operations via satellite may speed up the process and improve the accuracy. The revisit frequency has been set to 9 days, as suggested in [72] and [99]. Khaliq et al. in [72] found that a multi-temporal revisit frequency of 10 days from Sentinel-2 achieved an overall accuracy higher than 90% in crop classification. Skriver et al. in [99] found that the average classification error for cross-polarization is down to 3% at L-band and 6% at C-band, with a 9 days interval on SAR images acquisition. The choice for spatial resolution is driven by an economic consideration. In the context of the CAP, if the farmer application is eligible she or he may receive up to 425 €/ha if all the requisites are positively satisfied [83]. Considering an average Italian crop field, around 6.4 ha, the farmer can be refunded for a maximum of 2720 €. It is reasonable to suppose that the CAP commission wants to characterize the field, in terms of cultivated crop and size, as much accurately as possible. This allows the EU to allocate the exact amount of money and the farmer to receive for what he actually owns. Once the different crops within the field have been identified, if more than one, we can hypothesize that the field dimensions shall be retrieved with a maximum error of 2%. This error implies a maximum mistake of 8.5 €/ha, which results in a maximum mismatch of 54.4 € for the average Italian field. In order to link this economic margin with the spatial resolution, we introduce the hypothesis of a triangle-shaped field. So that we should be able to approximate the triangle area with squares (pixels of the instrument acquisition area), while satisfying the required tolerance of 2%. Two different triangles have been considered, an equilateral triangle and an isosceles triangle with an angle on the basis

of 30°, as depicted in Figure 6.2. The problem can be stated as: "find the square side l that
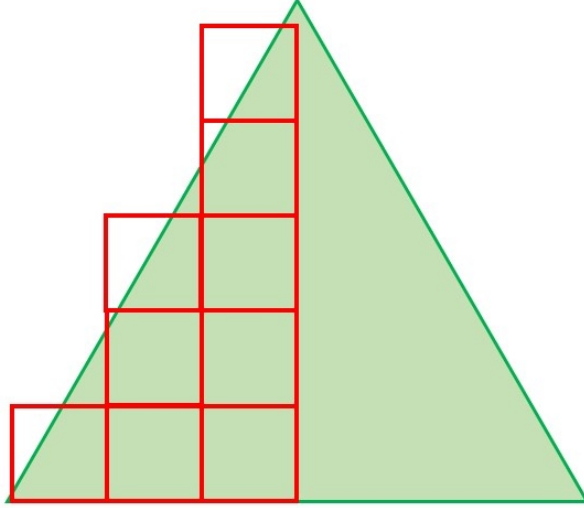
Figure 6.2: Example of spatial resolution assessment for crop estimation. In green the triangular filed and in red the instrument pixels

approximates the triangle are with a maximum error of $\pm 2\%$". The triangle area is known to be the average Italian field size, 6.4 ha. A basic algorithm to solve this problem starts with an initial guess (i.e. half of the triangle basis) and it computes the number of squares needed to cover the triangle surface. A square is considered as a valid square, that counts in the final area estimation, only if its area is covered for more than 80% by the triangle. Once the number of valid squares is computed, one can be evaluated the approximated area by simply taking the product between the number of squares and the square area. In order to find the square side that solves the problem one can define a cost function J as:

$$J = \left| N_{squares}(l)l^2 - A_{real} \right| \tag{6.4}$$

and employ a zero function finder such as MATLAB *fsolve*. As soon as the l value provides an area that is greater than $(A_{real} - 0.02 A_{real})$ and lower than $(A_{real} + 0.02 A_{real})$ the function J is set to zero and the problem is solved. The only small complication is that *fsolve* requires an initial guess that is quite close to the final value, otherwise, it will not converge. A couple of smart iteration at the beginning can immediately lead to a value that is accepted as a good initial guess by *fsolve*. Finally, 6 m is a resolution capable of providing the required accuracy in characterizing an average size Italian field. However, as fields dimensions in Italy are quite different from region to region, it is worth stressing out that a 6 m resolution can provide a maximum 5% error in estimating the average field size in Liguria, that is about 2.4 ha, the smallest in Italy. Crop yield assessment refers to the capability of predicting the crop yield, as we have seen above. In some country, assessing the yield is crucial to guarantee access to food for the whole population. The requirement on the temporal frequency is the same as in the precision agriculture service since the same considerations apply. The requirement on spatial resolution is an average between those in the case of precision agriculture in northern regions

and southern ones. Explicitly, 8 m is the average between the 6 m of yield estimation in the nominal case for north/centre Italy in precision agriculture and the 10 m of the nominal case for centre/south Italy. In this case, the coverage required is simply the sum of the two areas defined in the precision agriculture case, meaning we want to cover all the possible agricultural fields in Italy. The duration was simply set to 12 months, as this type of data may be required during the whole year.

6.3 Insurance

The remaining part of 6.2 is the central column, the one devoted to the insurance service. Vegetation condition & crop monitoring is the low-service offered. Insurance companies may rely on satellite data before repaying farmers after a meteorological event. This allows the insurance company to pay the exact amount of money corresponding to the entity of the damage and it also allows the farmer to be paid for what she or he has really lost. The satellites shall provide data about the condition, status and health of the crop in order to estimate the damage. The temporal resolution requirement says "On Demand", which means that once the farmer or the insurance company need to check the status of a crop, they can make a request for the service. The service is not provided during the whole year but just after the request, as it is a consequence of particular events that do not happen every day. Behind the spatial resolution requirement, there is an economic reason. The case of paddy rice was considered, as it is the cereal with the highest relative cost (see Table 6). We can compute the average revenue from rice in each region, starting from the production in terms of tonnes/ha, the average UAA for rice and its cost in terms €/tonnes. We can assume that the insurance company refunds up to 70% of the total value. The highest refund per hectare happens in Piemonte, equal to 1900 €/ha. We can also assume that the insurance company, and the farmer, do not want to mistake the refund by more than 95 €/ha. This implies a margin of 2% in Piemonte. We can calculate the same margin in all other region starting from the 95 €/ha maximum error. Once we have the margin of error for each region we can employ the algorithm used for the yield estimation case (summarised in Figure 6.1). The spatial resolution that brings an error lower than the margin in all the regions is 10 m. As for the food security case, the coverage required was set to the sum of the two areas defined in the precision agriculture case and the duration was set to 12 months for the same reasons.

Chapter 7

Mission analysis

The scope of this work is to design a constellation of SAR microsatellites able to provide useful imagery for application in agriculture in Italy. In this chapter, we first present the theory behind the orbital mechanics part of the work and the design of the orbital part of the constellation together with the model for SAR operations that defines the Earth coverage analysis. The real system under consideration is the constellation made by N satellites, where each satellite is described by an orbit that change in time due to the effect of perturbations. Then, each satellite is equipped with a SAR instrument that periodically acquires images of the Earth surface. This system is a very complex one, as it is composed of several subsystems that cooperate and work together. The satellite orbit, the SAR instrument, the power system, the propulsion system, the TT&C systems are just some examples of all the subsystems that compose the satellite system. Taking into account all the subsystems together would be a complex task that overcomes the scope of this work. This is why the physical model used within this work is made by an orbital part, the SAR instrument and the power subsystems. These three elements are enough to draw an accurate constellation analysis that meets the requirements defined for this work. The physical and mathematical models will be described deeply in the following.

7.1 Specialised orbits

7.1.1 Repeat-ground track orbit

There are some types of particular orbits that rise up under specific conditions and allow to perform unique analysis. One of these is the repeat-groundtrack orbit. It retraces their groundtrack over a certain time interval so that it allows to periodically revisit a particular point on the Earth [104]. We introduce the anomalistic period as the time required for the satellite to complete one revolution with respect to perigee considering the argument of perigee drift:

$$P_k = \frac{2\pi}{n} = 2\pi\sqrt{\frac{a^3}{\mu}} \tag{7.1}$$

The repeat-groundtrack orbit depends on the time span it takes the satellite to make two successive equator crossing, usually referred to as nodal period, and the period of the Earth's

rotation with respect to the ascending node referred to as the nodal period of Greenwich. It can be written as:

$$P_{\theta_G} = \frac{2\pi}{\omega_\oplus - \dot{\Omega}} \qquad (7.2)$$

The nodal period can be determined with [104]:

$$P_\Omega = \frac{2\pi}{\dot{M} + \dot{\omega}} = \frac{2\pi}{n + \dot{M}_0 + \dot{\omega}}$$

$$\dot{M}_0 = \frac{-2nR_\oplus^2 J_2 \sqrt{1-e^2}}{4p^2}(3sin^2(i) - 2) \qquad (7.3)$$

$$\dot{\omega} = \frac{3nR_\oplus^2 J_2}{4p^2}(4 - 5sin^2(i))$$

The groundtrack crosses the equator in some points that fix the groundtrack to the Earth at the equator. The two most important properties of the groundtrack are the revolutions to repeat, $k_{rev2rep}$ and, the days to repeat, $k_{day2rep}$. The spacing between two consecutive equator crossing points, known as groundtrack shift, is defined by how far the Earth rotates during the nodal period, relative to the ascending node. The angular spacing is:

$$\Delta\lambda_{rev} = (\omega_\oplus - \dot{\Omega})P_\Omega = \frac{2\pi R_\oplus k_{day2rep}}{k_{rev2rep}} \qquad (7.4)$$

The direction of the shift is westward. Perturbations, most notably J_2, cause the node to regress secularly to the west along the equator. The condition to obtain a repeated groundtrack after $k_{rev2rep}$ orbits is that the shift shall be equal to $k_{day2rep}$ times a complete rotation [104]:

$$\frac{\dot{\omega} + \dot{M}}{\omega_\oplus - \dot{\Omega}} = \frac{k_{rev2rep}}{k_{day2rep}} \qquad (7.5)$$

Equation 7.5 is an implicit equation in the semimajor axis, inclination and eccentricity. Once two of the previous are defined it can be solved for the remaining parameter. An example of a repeating groundtrack for an elliptic, inclined, 3 days and 10 orbits repeating orbit is given in Figure 7.1.

7.1.2   Sun-synchronous orbit

A Sun-synchronous orbit is a particular type of orbit that keeps the line of nodes fixed relative to the Sun [20]. If the rotation rate of the node is equal to the rotation of the Earth around the Sun ($\simeq 0.9856°/day$), we get a Sun-synchronous orbit. The natural perturbation caused by the Earth's oblateness is used to pull the orbit around in inertial space at a rate of 1 rotation per year. Approximately, a constant angle, with respect to the sun, can be maintained [109]. This type of orbit is particularly useful for observation purposes as it allows global coverage, at all latitudes, and it allows the satellite to see the same point on the Earth always with the same light condition. This is especially useful in the case of optical instrument, but it is not necessary for radars, as light effects can be adjusted with some post-processing. Moreover, as
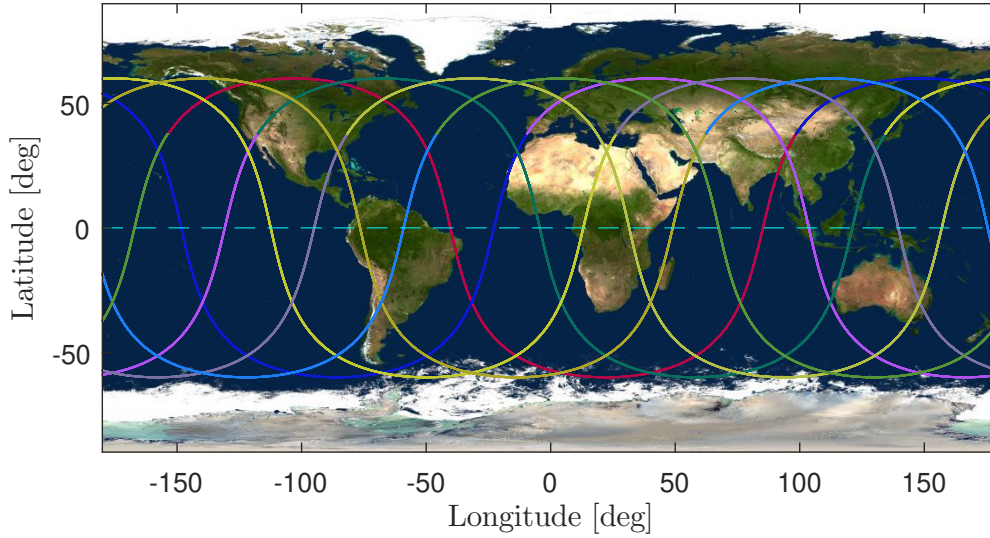
Figure 7.1: Repeating groundtrack orbit

the line of nodes remains roughly fixed with respect to the Sun's direction, solar panels are exposed to constant Sun radiation. The specific inclination of a Sun-synchronous orbit depends on the altitude and eccentricity of the satellite. In one sidereal year, 365.242190402 ephemeris days, the Earth completes a full revolution, 360°. By setting the line of nodes variation $\dot{\Omega}$, introduced in Eq. 7.5, equal to the Earth rotation around the Sun, one can find an expression in the inclination, altitude and eccentricity of the orbit. We can isolate the orbit eccentricity, and it yields to [20]:

$$i = acos\left(\frac{-2\dot{\Omega}_{SS}a^{7/2}(1-e^2)^2}{3\sqrt{\mu}J_2R_{\oplus}^2}\right) \tag{7.6}$$

7.1.3 Sun-synchronous repeated-ground track orbit

While flying on a Sun-synchronous orbit, the satellite repeats precisely its ground-track. The longitudinal shift of the satellite is due to Earth rotation to nodal regression [104]. The conditions to obtain a Sun-synchronous and repeat ground-track orbit can be condensed in a single equation [104]:

$$P_{\Omega}\left(1 - \frac{T_E}{T_y}\right) = \frac{k_{day2rep}}{k_{rev2rep}}T_E \tag{7.7}$$

This equation contains implicitly the altitude, the eccentricity and the inclination of the orbit. The expression for P_Ω is the one of Eq. 7.3. Eq. 7.7 shall be solved with the constrain on the inclination for a Sun-synchronous orbit of Eq. 7.6. Then, the system that needs to be solved is the following [104]:

$$
\begin{cases}
P_\Omega\big(1 - \frac{T_E}{T_y}\big) = \frac{k_{day2rep}}{k_{rev2rep}}T_E \\[2mm]
i = acos\Big(\frac{-2\dot{\Omega}_{Ss}a^{7/2}(1-e^2)^2}{3\sqrt{\mu}J_2R_\oplus^2}\Big) \\[2mm]
P_\Omega = \frac{2\pi}{\dot{M}+\dot{\omega}} = \frac{2\pi}{n+\dot{M_0}+\dot{\omega}}
\end{cases}
\tag{7.8}
$$

If we suppose circular orbits ($e = 0$), simply by tuning $k_{day2rep}$ and $k_{rev2rep}$, we get an equation in the semi major axis and inclination. It can be solved with a numerical solver, e.g. MATLAB *fsolve*.

7.2   Satellite constellations, state of the art

A constellation is a set of satellites distributed over space intended to work together to achieve common objectives [109]. We can not draw absolute rules for constellation design but there are some key issues that more often come up during trade-off. In the end, the constellation design is usually based on cost vs. performance. The key issues mentioned above are [109]:

- *coverage*: the principal performance parameter, strictly correlated with the mission requirements. It can be, for example, continuous or discontinuous. It determines the satellite attitude, its minimum elevation angle, its inclination and the constellation pattern

- *number of satellite*: it is the principal cost driver. The goal is to achieve the required coverage with the minimum number of satellites. However, sometimes fewer satellites does not mean a lower cost, it depends on several other parameters

- *launch options*: it represents a major cost driver and a high source of risk. It mainly depends on the number of satellites, their altitude and inclination. Nowadays, new launch options are available and some of them allow to strongly cut the launch cost.

- *environment*: vacuum, thermal, zero-g and radiation environment depend on the orbit and altitude and they mostly influence the satellite design and operations

- *orbit perturbations*: usually the atmospheric drag, Earth non-sphericity, SRP, Moon and Sun attraction. Perturbations depend on satellite orbit and perturbation together with constellation configuration influence the stationkeeping strategy

- *collision avoidance*: it is the largest threat as it may result to complete loss of the system. The entire system shall be designed in order to minimize the chances of collision

- *constellation build-up, replenishment, end-of-life*: it takes some time before the constellation reaches its final configuration so that it spends quite some time in a less-than-complete configuration and initially the performances are not at their best but they increase with time. One must take into account that the constellation may not be operative up to the time when a certain number of satellites are in orbit, however with degraded performances up to when all satellites are in orbit. One more issue is satellite failure, it influences the constellation operations. The decrease in performances due to one satellite failure shall be as little as possible. Usually, spare satellites are present in orbit, ready to replenish the broken ones. Finally, modern space regulations require planning an end-of-life strategy so that the satellite does not pollute the space environment becoming a debris or leading to a collision. The design shall plan the manoeuvres to bring the satellite to re-entry or to graveyard orbits

- *number of planes*: moving a satellite from one plane to another is extremely expensive. Usually, with fewer planes the constellation build-up is faster, the collision chances are lower and spacecraft failure implies lower constellation degradation. However, adding a plane usually increase the constellation performances

7.2.1 Walker-Delta constellation

A typical type of constellation is the Walker-Delta constellation [106]. It is characterised by a high symmetry. The constellation is made by N_{SC} satellites, then these N_{SC} satellites are evenly disposed in P orbital planes so that each plane is composed of S satellites. All the orbits are circular, at the same altitude and with the same inclination. For describing the Walker constellation we introduce the pattern unit PU, $1PU = 2\pi/N_{SC}$ $[rad]$. In a Walker constellation:

- on each plane, the S satellites are spaced at intervals of P patter units

- the P orbital planes are evenly spaced on the equator at intervals of S patter units

- when a satellite is at its ascending node, some satellite on a more easterly adjacent orbital plane has an argument of latitude of F patter units, where F is an integer assuming any value between 0 and $(P-1)$, $0 < F \le (P-1)$

In shorthand notation a Walker constellation is usually referred to as: $i : N_{SC}/P/F$. A typical example of Walker constellation is the GNSS Galileo, $56° : 24/3/1$ [37]. In this work we will consider just Walker-Delta constellations as they are simple to derive. However, the model we will define is not strictly dependent on the type of constellation and it can be adapted to any of them.

7.3 Orbital mechanics model

The most accurate physical model that we can exploit to describe the satellites orbits is an ephemeris model, but it would result in excessive complications. Other models available are the perturbed four, three or two body problem. In this work, the perturbed two-body problem was

selected as it is accurate enough to model the real system while it is mathematically simple and it does not require too much computing power. So that the orbits of the satellites that form the constellation have been described with a perturbed two-body problem. The perturbation that was considered is the J_2 effect due to the Earth non-sphericity. The J_2 effect has been considered as it is one of the two most important perturbations in LEO (as we will see in the following, low Earth orbits are the objects of this study) and because it allows defining repeating groundtrack orbits, strongly useful for coverage purposes. We will see that atmospheric drag has not been completely discarded but it was taken into account in another way. SRP and third body perturbations have been discarded as these are negligible with respect to the other two in LEO. The Earth has been modelled as a perfect sphere of radius 6378.16 km. Earth atmosphere is represented by an exponential model. The equations that describe the mathematical model of the satellite orbit are the following [20]:

$$\ddot{\mathbf{r}} + \frac{\mu}{r^3}\mathbf{r} + \mathbf{a}_{J_2} = 0$$

$$\mathbf{a}_{J_2} = \frac{3}{2}J_2\,\mu\,\frac{a^2}{r^4}\left[\frac{r_x}{r}\left(5\frac{r_z^2}{r^2}-1\right)\hat{\mathbf{i}} + \frac{r_y}{r}\left(5\frac{r_z^2}{r^2}-1\right)\hat{\mathbf{j}} + \frac{r_z}{r}\left(5\frac{z^2}{r^2}-3\right)\hat{\mathbf{k}}\right]$$

(7.9)

It can be written in the three components of a three-dimensional Cartesian reference frame as:

$$\begin{cases} \ddot{r}_x = -\frac{\mu}{r^3}r + a_{x-J_2} \\[2mm] \ddot{r}_y = -\frac{\mu}{r^3}r + a_{y-J_2} \\[2mm] \ddot{r}_z = -\frac{\mu}{r^3}r + a_{z-J_2} \\[2mm] a_{x-J_2} = \frac{3}{2}J_2\mu\frac{R_\oplus^2}{r^4}\frac{r_x}{r}\left(5\frac{z^2}{r^2}-1\right) \\[2mm] a_{y-J_2} = \frac{3}{2}J_2\mu\frac{R_\oplus^2}{r^4}\frac{r_y}{r}\left(5\frac{z^2}{r^2}-1\right) \\[2mm] a_{x-J_2} = \frac{3}{2}J_2\mu\frac{R_\oplus^2}{r^4}\frac{r_z}{r}\left(5\frac{z^2}{r^2}-3\right) \end{cases}$$

(7.10)

Then, once the position of the satellite is available it is possible to retrieve its longitude and latitude, for example one can exploit the method shown in [20].

7.4   Synthetic aperture radar model

The working principles of a synthetic aperture radar have been explained in Chapter 2. It is a very complex system and its corresponding physical model is equally complex. However, for the seek of simplicity and clearness, in this work the physical model has been synthesised with two blocks, one concerning the power demand required from the instrument and one concerning the image acquisition. The power block is useful to estimate the SAR power requirement that sizes the satellite batteries and solar arrays and define the maximum instrument acquisition time. While the image acquisition block allows the evaluation of the Earth coverage. We start the analysis with the image acquisition block. It is very easily represented by an electromagnetic

beam emitted by the SAR that intercepts the Earth surface. The scope of this block is to evaluate the portion of Earth surface imaged by the SAR starting from some physical input parameters. The ability of SAR to determine the distance between two illuminated objects is called range or slant. Mathematically, it is proportional to the speed of light and the inverse of the effective pulse-width [71]:

$$Range\ \ resolution = \frac{c}{2\beta} \tag{7.11}$$

as the range resolution gets finer, the pulse bandwidth and data rate grow accordingly. The radio frequency bandwidth of the system is determined by the variation in the frequency of the radar pulse driven by the transmitter [71]. Finally, the ground range or cross track resolution is geometrically related to the slant range resolution:

$$\delta_R = \frac{c}{2\beta\ sin\theta} \tag{7.12}$$

The direction orthogonal to the radar beam is called along track or cross range. Along this direction, the spatial resolution is determined by the Doppler bandwidth of the received signal. This means that, in principle, if phase-preserving processes are enforced, a SAR produces an image with an along-track spatial resolution largely independent from wavelength and target range. The theoretical along track resolution of a SAR is [71]:

$$\delta_{AT} = \frac{D_{AT}}{2} \tag{7.13}$$

The SAR antenna has its long axis in the flight direction, called azimuth direction, and its short axis along the range direction. The antenna transmits a pulse that travels to the target area illuminated and receives the reflected pulse. At each position the SAR system stores the phase histories of the responses and then it weights, phase shifts, and sum them to consider one single point target (resolution element) at a time while suppressing the others [71]. The processing system focus on each point target in turn. The image is then constructed by putting together all the targets responses. At any instant, thousands of pulses are summed for each resolution cell. Processing makes the power of a scatter, spread across many pulses, to concentrate into a single resolution element. At any pulse time, millions of resolution cells in the radar beam are illuminated. The radar pulses emitted illuminate the Earth surface over a large elliptical footprint that is made by millions of resolution cells. The imaging geometry is shown in Figure 7.2. The width of the beam that intercepts the Earth surface, called swath, is function of the diffraction-limited beam in the range direction and the illumination geometry [71]. The ground swath can be evaluated as [108]:

$$W_g = \frac{\lambda\,R}{D_R\,cos\theta} \tag{7.14}$$

where R represents the slant range from the antenna to the midpoint of swath. The illuminated surface can be described by means of the look angle θ. Modern SAR sensors are able to change the look angle, this is helpful as it allows to reduce or increase the size of the footprint and because some target properties can be investigated only within a small range of look angles. Reasonable look angles range between 15° and 70°. The SAR instrument can acquire images
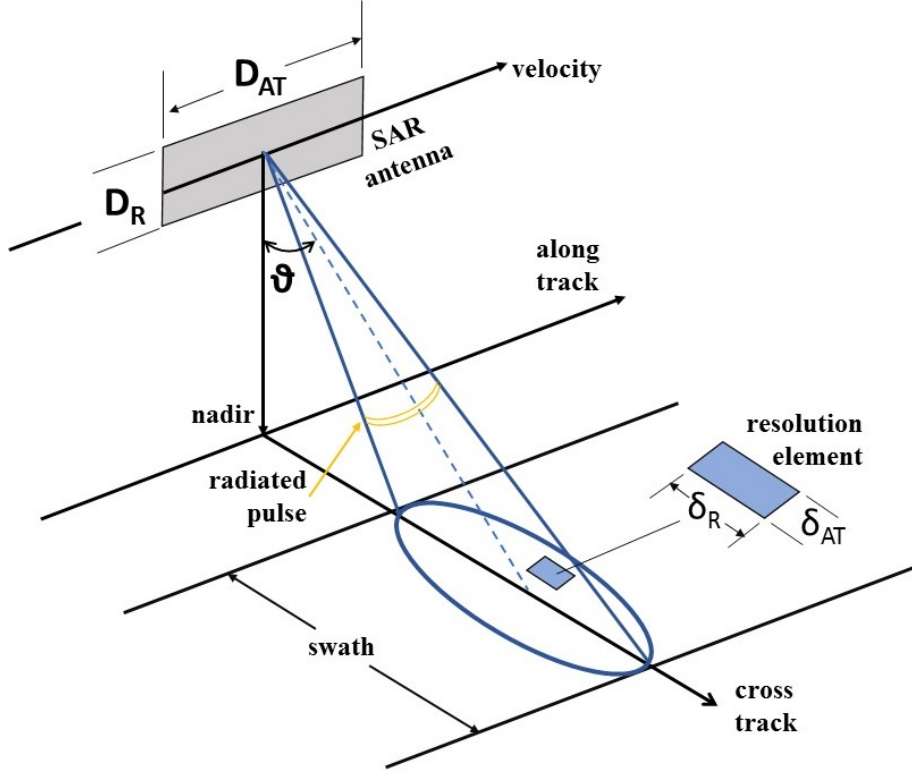
Figure 7.2: SAR imagery geometry. Adapted from [79]

in several modes as we have seen in Chapter 3, however, the equations and geometry that have been just introduced are valid for side-looking Strip-mode. This is the acquisition mode that has been considered for evaluation of SAR coverage because of its straightforwardness and wide applicability. Therefore, we have seen how the SAR sensor image the Earth surface, how to evaluate the images acquisition in order to calculate the coverage and implicitly we have seen what are the SAR physical parameters that enter the analysis and have been selected for calculation of the coverage.

The second block that forms the SAR physical model is the power block. In this sense, it is useful to evaluate the power transmitted by the SAR antenna that in turn is the input requirement for another sizing. The radar equation for a monostatic radar system is the following [13]:

$$P_r = \frac{P_t G^2 \lambda^2 \sigma}{(4\pi)^3 R^4} \tag{7.15}$$

We can assume that the radar performance is limited by noises, as the thermal noise. The average power of the noise is $k_B B T$. Usually, a specific SNR is required for a desired target detection performance. Then, we can write:

$$SNR = \frac{P_r}{F k_B B T} \tag{7.16}$$

It follows that:

$$SNR = \frac{P_t G^2 \lambda^2 \sigma}{(4\pi)^3 R^4 k_B T B F} \tag{7.17}$$

We introduce the number of elements that comprise the synthetic aperture n_{SA}:

$$n_{SA} = T_s f_R \tag{7.18}$$

where:

$$T_s = \frac{\lambda R}{2v\delta_{AT}} \tag{7.19}$$

so that n_{SA} becomes:

$$n_{SA} = \frac{f_R R \lambda}{2\delta_{AT} v} \tag{7.20}$$

and the SNR changes accordingly:

$$SNR = \frac{P_t G^2 \lambda^3 \sigma}{(4\pi)^3 R^3 k_B T B F 2 \delta_{AT} v} \tag{7.21}$$

The radar target cross section σ can be expressed as:

$$\sigma = \delta_{AT} \delta_R \sigma_0 \tag{7.22}$$

Finally, we introduce the relation for the average power as a function of the peak power:

$$\bar{P}_t = P_t \tau_i f_R \tag{7.23}$$

and we introduce atmospheric and system losses and thus the final form of the equation for the average power is [13]:

$$\bar{P}_t = \frac{2(4\pi)^3 R^3 k_B T F v SNR}{G^2 \lambda^3 \sigma_0 \delta_R} \tag{7.24}$$

where:

$$T = T_A + T_{TL/WG} + T_{LNA} = T_{mr}(1 - A_{mr}) + T_C A_C + T_{PHY}(1 - A_{PHY}) + (F - 1)T_0$$

$$G = \eta \frac{4\pi}{\lambda^2} A_{SAR} \tag{7.25}$$

From Equation 7.24 we can retrieve that the SNR is inversely proportional to the third power of range, independent of azimuth resolution, and it is function of the ground range resolution, inversely proportional to velocity and proportional to the third power of wavelength. Finally, increasing the range resolution requires higher transmitted power; this may be achieved by pulse compression technique [13].

7.5 Earth coverage with synthetic aperture radar

Earth coverage refers to the part of the Earth that a spacecraft instrument, in our case a synthetic aperture radar, can see at one instant or over a longer period [109]. In general, a vector from the spacecraft will be tangent to the surface of the Earth at a point called the geometric horizon [109]. The area inside the horizon is called the access area, it represents all points of the Earth's surface that the spacecraft can communicate with or look at. The direction
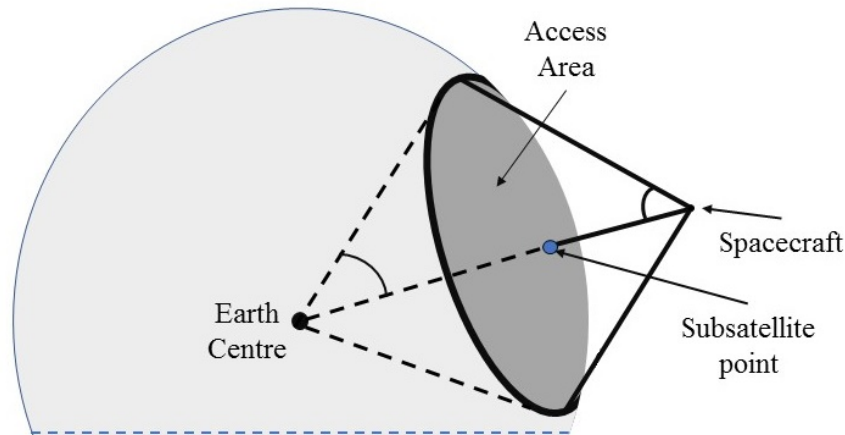
Figure 7.3: Geometry as viewed from the spacecraft. Adapted from [109]
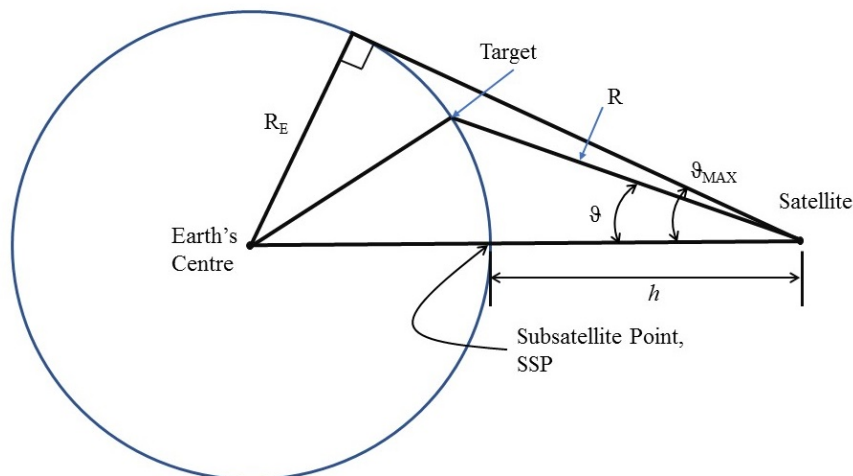
Figure 7.4: Satellite, target on Earth's surface, subsatellite point and access angles. Adapted from [109]

from the spacecraft to the centre of the Earth is called nadir, the opposite direction is called zenith. The vector from the spacecraft to the Earth's centre intersects the Earth's surface at a point called subsatellite point. This geometry is briefly shown in Figure 7.3 and Figure 7.4.

For precise work, we shall apply a correction for Earth oblateness. It has two distinct effects, first, the Earth appears slightly oblate, and second, the centre of the visible oblate Earth is displaced from the true geometric centre of the Earth [109]. However, in this work, for the seek of simplification we will consider the Earth as a perfect sphere.

The appearance of the Earth, as seen from space is not straightforward. Foreshortening influences the appearance of the Earth, especially at the edge of the Earth's disk. Near the horizon, any direction other than purely horizontal becomes nearly vertical. It means that all curves on the spacecraft centred celestial sphere, when projected onto the Earth, will intersect the horizon nearly perpendicular to it [109]. Moreover, all curves on the surface of the Earth near the

horizon will become nearly horizontal when seen from the spacecraft [109]. In general, circles on the spacecraft's celestial sphere will project onto the surface of the Earth as elongated in the vertical direction. For a more detailed description of the Earth appearance from space, please refer to [109]. The SAR field of view is rectangular, as seen from the spacecraft. The edge of any rectangular field of view from a spacecraft instrument projects onto the sky as a great circle arc and into space as a plane surface [109]. In general, the edges of a rectangular field of view from the spacecraft will intersect the surface of the Earth in a set of four intersecting small circles. However, the approximately rectangular shape is largely retained when the field of view is oriented toward nadir [109]. In LEO the satellite moves rapidly over the surface, and it is possible to define four parameters [109]:

- *footprint area*, the area that the instrument can see at any instant, we have already seen in the previous section how to define it for a SAR (Figure 7.2)

- *instantaneous access area*, all the area that the instrument could potentially see at any instant, this will be useful later in the calculation of the revisit time

- *area coverage rate*, the rate at which the instrument is accessing new land

- *area access rate*, the rate at which new land is coming into the satellite's access area

The coverage depends on several factors, such as the spacecraft control system, power, management system and mission operations. We have already seen how to compute the SAR footprint along with its analytic approximations. It is worth mentioning that a radar cannot work too close to the subsatellite point and it has an outer horizon and an inner horizon, defined by the maximum and minimum access angles. This geometry is shown in Figure 7.5. We have understood the basics of Earth coverage and we have seen how a SAR creates its footprint and how to compute it. We will now see in more details how to compute the coverage starting from the instrument footprint and compare it with the region of interest (as we have seen during the requirement definition, we are interested only in the Italian territory).

As a first simplification, the SAR beam elliptical footprint has been condensed in one single line, coinciding with the ellipse semi-major axis. In this way, the calculation of the footprint results much simpler while the coverage calculation does not lose accuracy. At a particular time interval t, the SAR footprint is defined by a line, on the left or on the right of the satellite subsatellite point. The position of the centre of this line is defined by the SAR access angle, while the edges of the line are separated by a distance equal to the SAR swath, Eq. 7.14. At this time interval, we imagine storing only the coordinates of the line edges (longitude and latitude). At the next time interval, $t + \Delta t$, a new line is defined. This is slightly shifted and inclined with respect to the previous one, due to the curvature of the satellite's ground track. We can again store only the coordinates of the borders of this second line. We can repeat this procedure for a certain time span t_{SAR} (we will see in the next section how this time span is computed) and we will obtain two series of points. This geometry is schematically shown in Figure 7.6. It is immediately visible how the series of discrete footprints generate a stripe, that coincides with the portion of the area acquired by the instrument. We now introduce a binary false matrix of $n \, x \, m$ elements. Let us call it BW. Each element can assume a value only equal to 0 or 1, however, initially, all elements are equal to 0. We assign an element (pixel)
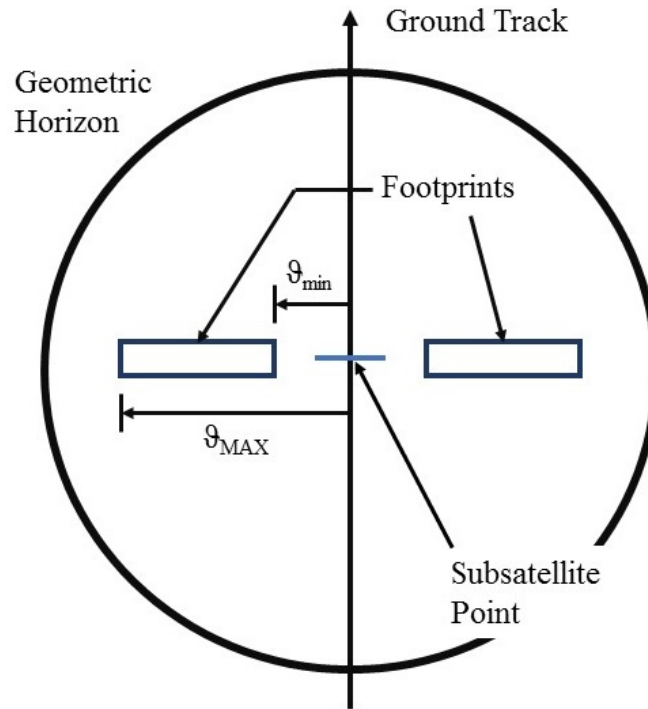
Figure 7.5: SAR access area, adapted from [109]

of the matrix BW to each of the points defined by the SAR footprints (Figure 7.6), the map between longitude-latitude coordinates of the points and matrix's element will be explained afterwards. The BW matrix is now made by many zeros and some ones, corresponding to the points defined by the SAR footprints. The ones are the borders of the SAR acquisition stripe, as the points were in the longitude-latitude domain. We can now generate the complete stripe and fill it with a simple algorithm (e.g. MATLAB's poly2mask function). The result is a series of contiguous ones whose shape resemble that of the stripe. This process is presented in Figure 7.7. In order to estimate the area covered with the single stripe created in a time interval t_{SAR}, we can compare the matrix B, which embeds the stripe, with another binary matrix, that represents the Italian territory. In this binary matrix, each 1 will correspond to a portion of the territory (the physical size of this portion depends on the rows and columns of the matrix), while a 0 corresponds physically to sea or to territory out of the Italian border. This binary matrix is shown in Figure 7.8. Therefore, we can compare the two binary matrices with the logical operator *and*, and produce a third matrix that represents the portion of Italian territory covered by the satellite. The size of the binary matrix representing the Italian territory depends on the SAR swath. If the swath is in the order of hundreds of km it would be pointless to use a number of rows and columns for which each entry corresponds to an area of a few km^2. As we will see later, the SAR considered in this work can produce a swath in the order of tens of km. In the worst case, the swath ranges between 18 and 20 km. The binary matrix selected has 1900 rows and 1540 columns, corresponding to 2,926,000 elements. The area it corresponds to,
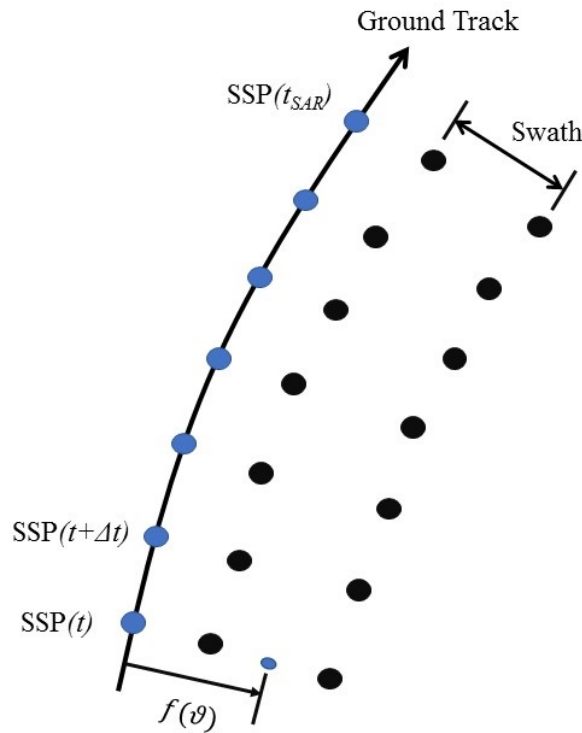
Figure 7.6: SAR coverage computation

measures about 1250 km (vertically) times 1100 km (horizontally), about 1,375,000 km^2. If we approximate that area with a 1900x1540 matrix, it means that each of the 2,926,000 elements corresponds to a square area of about 0.47 km^2; then a square with a 0.68 km side. It is clear that each element corresponds to an area much lower than the SAR swath, even in the worst case, where the element side is about 3.8% of the instrument swath. This leads to the definition of the error we can commit while computing the coverage. In the worst case of the minimum swath, when a pixel (element) from each side of the stripe is wrongly considered, the error is still confined within the 10% of the instrument swath. Increasing the swath, error decreases accordingly. Moreover, the MATLAB's function poly2mask used to build the SAR stripe from the edges of the footprints, employs an algorithm that ensures to avoid overestimation [75]. In order to explain how a point defined by its longitude and latitude is mapped into the binary matrix, we can use the following method. The dimensions of the real area represented by the binary matrix are known, along with the position and distance of two points, both in the binary matrix and in the longitude-latitude space. Then, we can retrieve the link between geographic position and matrix position from the two known points. We can apply this mapping to all the other points.

Longitude-latitude space   Binary matrix   Binary matrix
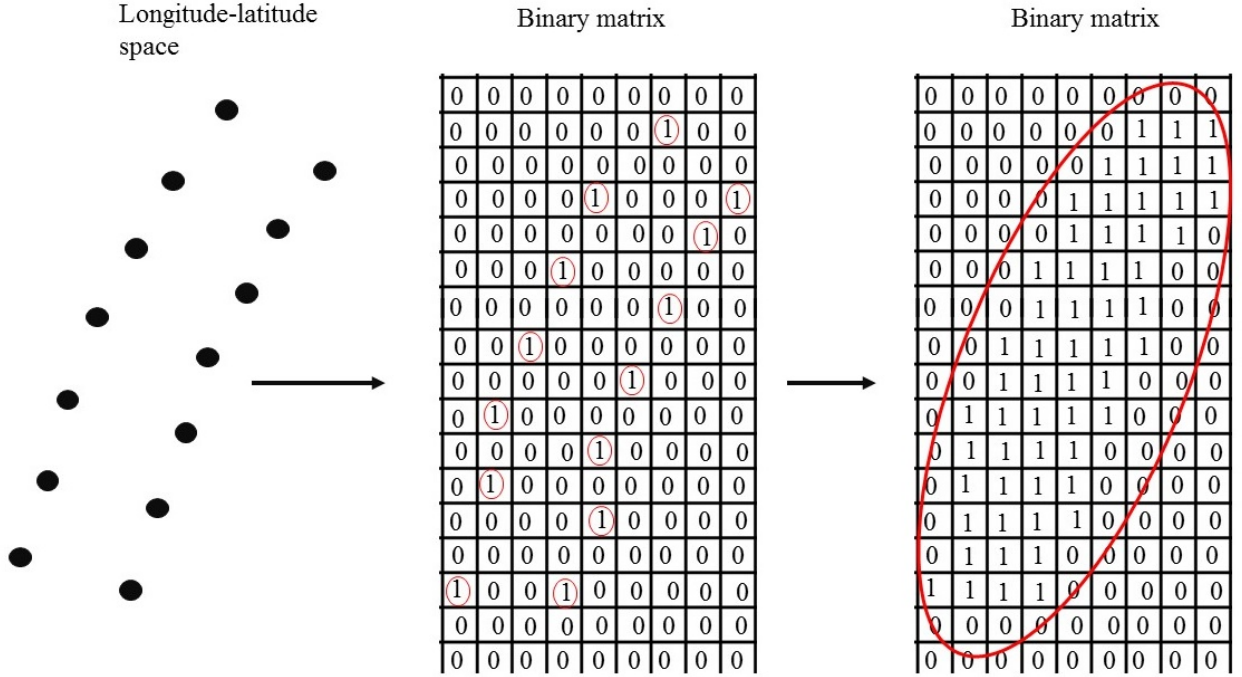
Figure 7.7: SAR stripe acquisition generation process. Note: this is just an illustrative sketch of the steps, it is not a real algorithm output

7.6   Power model

The aim of the power model is to define the maximum SAR acquisition time t_{SAR}. As we will see, the calculation is very sensitive to a series of parameters. Therefore, this is not to be considered as an exact estimation. A real power system is made by the solar arrays, a secondary battery (or even more than one), cables, a power control unit and a series of other elements. The physical model we employ is made only by a secondary battery and a power amplifier connected to the SAR instrument. The mathematical model describing this system will be exposed in the following. First of all, the model computes the target point distance (Figure 7.4), which depends on the satellite altitude and SAR access angle. Then, it computes the minimum SAR antenna area, given by [79]:

$$A_{SAR}^{min} = 4\frac{v\,\lambda\,tan(\theta)R}{c} \tag{7.26}$$

in case this area is higher than the antenna area (we will see later how the initial SAR antenna area is defined), a new antenna area is computed, maintaining the initial proportions. Then, the time that the satellite spends in eclipse is computed with a simple cylindrical shadow model:

$$\alpha_{ecl} = acos\Big(\frac{a}{R_\oplus}\Big)$$

$$t_{ecl} = 2\pi\sqrt{\frac{a^3}{\mu}}\,\frac{\pi - 2\alpha_{ecl}}{2\pi} \tag{7.27}$$

Figure 7.8: Binary matrix representing Italian territory

Then, the SAR average power request is computed through Eq. 7.24, 7.25 and 7.22. Since the SAR instrument makes use of a power amplifier, the power entering the power amplifier has been computed considering an efficiency of 0.45. We introduce the assumption that the payload power represents 60% of the total power budget [85]. We can adapt the power budget of [108] with the new payload power percentage. The power budget employed is shown in Table 7.1. Then, it was introduced an acquisition mode during an eclipse, when the operating subsystems would be: the payload, the power, the ADCS and the OBDH subsystems. It was assumed that each satellite carries a 40 Ah battery, that weighs about 5 kg. The size and weight of this battery are compatible with those of the satellite. In order to have an estimation of t_{SAR}, we can remove the capacity request from power, ADCS and OBDH subsystems. We considered a 90% depth-of-discharge, an electric line at 12 V, and an operative time from the previous three subsystems equal to the eclipse time. The remaining capacity is devoted to payload operations and we can simply retrieve the time required for discharging the remaining capacity of the battery that coincides with the SAR acquisition time t_{SAR}. However, for very low and very high (relatively) altitudes the power budget is no longer accurate, and the computation of t_{SAR} leads to very long or negative acquisition times. Both are infeasible. This is why a lower and an upper boundaries for t_{SAR} were defined. The lower boundary is equal to 1.5 minutes, a common acquisition time for small satellites flying on high altitudes [85]. While the upper boundary has been set to 5 minutes, a generic acquisition time for microsatellites [85].

Power Breakdown	
Subsystem	% of total power
Payload	60
Structure & Mechanism	1
Thermal Control	6
Power	6
TT&C	6
OBDH	5
ADCS	7
Propulsion	9
Total	100

Table 7.1: Power budget. Adapted from [108]

7.7 Mission analysis model

This section aims to put together the single models we have described so far and to explain how the algorithm developed computes the figures of merit of a constellation. The inputs of the algorithm are the following:

- Orbital parameters

    i number of satellites, N_{SC}

    ii number of planes, P

    iii phasing parameter, F

    iv number of orbits before ground track repeats, $k_{rev2rep}$

    v number of days before ground track repeats, $k_{day2rep}$

    vi altitude, a

    vii inclination, i

- SAR parameters

    i wavelength, λ

    ii minimum and maximum access angle, θ_{min} and θ_{MAX}

    iii working access angle, θ

    iv SAR antenna dimensions, D_R and D_{AT}

The SAR antenna dimension was defined through a statistical regression. The linear regression is based on the SAR antenna dimensions and SAR mass that belong to some of the satellites we have described in Chapter 3. The linear regression, produced, for our 200 kg microsatellite a SAR antenna dimension of 3.856 m^2. The regression is shown in Figure 7.9. The antenna
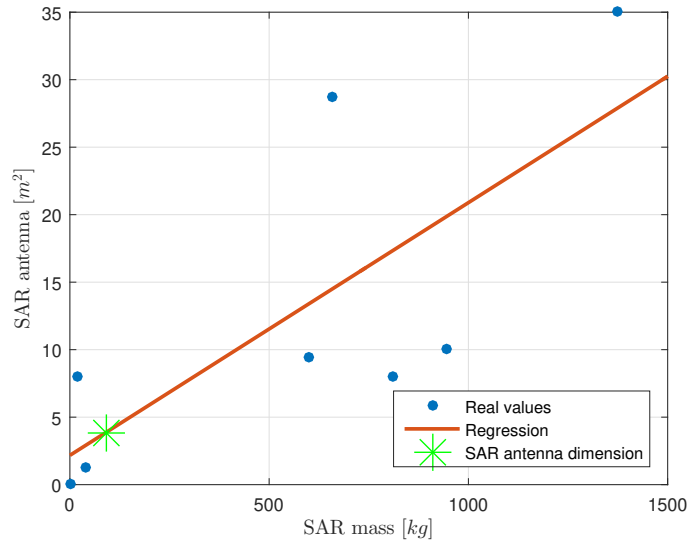
Figure 7.9: SAR antenna statistical regression

area has been distributed along the two dimensions so that the final antenna is 4.82 m long in the along track direction and 0.8 m long in the range direction. As explained in the power model section, in case these dimensions are not enough, due to satellite height and velocity, they are modified to the minimum values imposed by that particular case.

First of all the algorithm computes the SAR acquisition time t_{SAR} through the power model described in the previous section. Then it generates the constellation from the orbital parameters. It produces the six Keplerian elements for each of the satellite. Then, depending on the altitude and θ it computes the target distance (that is constant as the orbits are circular and then the altitude is constant), and the inner and outer horizon distance. Finally, it computes the SAR swath through Eq. 7.14. After this first part, it enters a loop on the planes and then a loop on the spacecraft per plane. Inside these loops, it computes the satellite orbit through the integration of Eq. 7.10 and from the Cartesian coordinates it computes the longitude and latitude coordinates of each subsatellite point. The integration is performed for one orbital period, and the discretization used is one point every 1.7 seconds. This has been selected as a trade-off between computational time and accuracy in SAR coverage stripe computation. Then, through vectors rotation, it computes the Cartesian position of the target point and the inner and outer horizon points on the right and on the left of the antenna (that depend on the minimum and maximum access angles, θ_{min} and θ_{MAX}). The Cartesian position allows the calculation of the longitude-latitude position of the previous points. Then, there is a first part devoted to revisit time calculation and a second one devoted to coverage calculation (these two part happen simultaneously). Let us start by seeing the revisit time part. Per each point of the inner and outer horizon, on the right and left side, the algorithm checks if at least one of these lays inside the area of interest defined in Table 6.1. If this is the case, the SAR is switched on, and the points are stored. Time instant after time instant, the points are stored for a maximum time equal to t_{SAR} or up until are of interest has been acquired (in any case for a time span lower than or equal to t_{SAR}). In this way, two stripes are built, one on the

left and one on the right of the antenna; as explained in Section 7.5. These two stripes, after being moved in the binary domain, are compared with the binary matrix representing Italy, exactly as we have seen in Section 7.5. Then, only the points of interest of the stripes (those that belong to the Italian territory as well) are stored, in order to keep track of the are acquired by the instrument. However, another information is stored: the time at which that area has been seen at. In such a way, the algorithm builds up a structure of the same dimensions of the binary Italian matrix, where it stores the acquisition time in each element. This process is repeated for $k_{rev2rep}$ times, in order to cover all the possible orbits of the satellite. In the end, the algorithm produces a matrix of elements, if an element is empty it means that the corresponding area has not been acquired. If the element is not empty, it contains the times when the corresponding area was acquired. These steps are repeated for all satellites per plane and for all planes (the two outer loops mentioned above), in order to cover the whole constellation. Finally, it is possible to evaluate the average revisit time (eventually the minimum and maximum as well), simply comparing the time spans between the acquisition of the same area and of all areas. At the same time, the algorithm computes the coverage as well. First of all, it checks if the position of the targets (that on the left side and that on the right side) lay inside a box slightly bigger than that of Table 6.1. If this is the case, it computes the coordinates of the border of the two footprints starting from the SAR swath. Then, these points are moved in the domain of the binary matrix. If at least one these points match the Italian territory, the SAR is switched on one single side, the one where the match was found. This is a difference from the revisit time calculation. The algorithm starts storing these points that belong on one side (without changing it). After a maximum time t_{SAR} (or after the region of interest has been flown), the algorithm creates the coverage stripe, as shown in Section 7.5. The process is repeated for $k_{rev2rep}$ orbits, for all satellites per plane and for all planes. At each time the coverage stripes are compared with a logical *or*, in order to keep track of total coverage. In the end, the total coverage is compared with the binary matrix representing the Italian territory, in order to get esteem of portion of territory covered by the instrument. The algorithm also computes the evolution of the coverage in time and the number of acquisitions per satellite. The logic that switches on the SAR is limited by some constraints. Let us suppose the SAR has acquired images for a time t_{SAR}, the maximum possible time. Then, before it can work again, it must wait for an interval of time equal to three-quarters of the orbit period. This allows simulating the recharging process of the battery. In the case the SAR acquires images for a time lower than t_{SAR}, and it switches off, it can still operate during the same orbit, but only for the remaining time before getting to t_{SAR}. In the coverage analysis, if the SAR antenna is looking at one side it has to keep looking at the same side for the whole operative time t_{SAR}. In the case the battery is not completely discharged and the SAR has been switched off after looking at one side, it can start acquiring images looking at the opposite side (if area of interest is present) for the remaining time before reaching t_{SAR}. However, before being able to switch side of looking the antenna must wait for a given period of time, in order to simulate the slew manoeuvre necessary to change the orientation. This time period has been set to 4 minutes, a typical order of magnitude of a slew manoeuvre that covers around 50°. If the SAR has been switched on for less than t_{SAR} and a time higher than three-quarters of the orbital period has passed by, then the SAR can operate again for a time equal to t_{SAR}. For the seek of clearness, the output of the mission analysis model are listed below:

- coverage, in terms of area of the Italian territory acquired

- evolution of coverage, how the coverage increases in time along with the time needed to reach the maximum coverage

- revisit time, average revisit time for each area, defined in the binary matrix, that composes the Italian territory and average revisit time for the whole Italian territory covered by the instrument

- number of acquisition per each satellite

A short flow chart of the model just explained is shown in Figure 7.10. While developing this
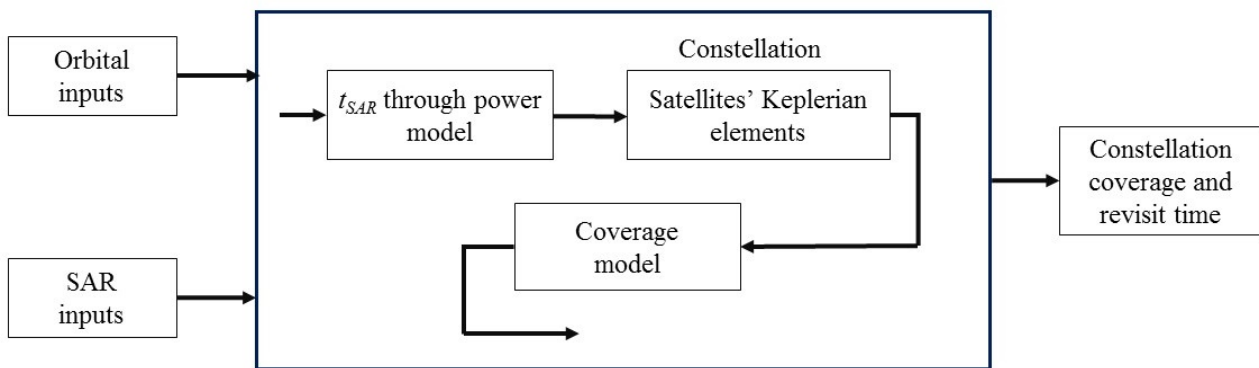
Figure 7.10: Mission analysis model logics

model, we put particular attention is some key points of a numerical simulation [109]:

1. spacing of grid points, this has been assessed considering the SAR swath dimensions together with the satellite velocity and the dimensions of the area of interests

2. gaps at the beginning and end of the simulation, this shall last long enough in order to avoid gaps recurring at the beginning and end of the simulation

3. step size, we chose a step size small enough relative to the dimensions of the coverage regions considering the satellite velocity as well

7.7.1 Model validation

Both the orbital mechanics model and the SAR model are based on strong theoretical backgrounds that are easily proven to be correct. The only model that requires validation is the mission analysis model. First of all, we have visually tested that the SAR acquisition process is coherent with the theoretical model implemented. This operation has been done for several cases, including some particular ones. Then, we have implicitly tested our model by comparing the results of the optimisation with some validated ones. This will be shown in Chapter 9. Comparison with other software of constellation calculus is complicated by the fact that different models are employed. Therefore, the number and type of the input parameters are different. Finally, a slightly different result is to be expected.

Chapter 8

Multi-objective optimisation for constellation design

In order to find a constellation (or more than one) that satisfies the requirements we have drawn, we decided to rely on a multi-objective genetic algorithm optimisation, as previously proposed by Huang et al. [62]. The optimisation has been divided into two parts. One, where only Sun-synchronous repeated-ground track orbits were considered, and one more general with repeated-ground track inclined orbits. Both of these two optimisations analyse Walker-Delta constellations in LEO.

8.1   Multi-objective genetic algorithm optimisation

The need to use an optimisation was forced by the large domain from which we can select a constellation. Exploring all the possible configurations would take too long and an optimisation is the best tool to find a good result in a reasonable time span. We just referred to a multi-objective optimisation because, as we will see later in this chapter, we defined several constellation properties, and we want to find a set of constellations. Within this set, theoretically made by the best constellations, each constellation will have a high score in at least one of the properties. Then, we will select the constellation that matches our criteria the most, between those that minimise the properties. This approach allows us to make a first selection between all the possibilities according to the properties we will define, and then we will choose the constellation that meets our requirements in a trade-off manner. A genetic algorithm is based on natural selection (biological evolution). This is particularly useful whenever the objective function is discontinuous, non-differentiable, stochastic or highly non-linear [77]. The genetic algorithm differs from a classical optimisation algorithm in the fact that it generates a population of points at each iteration where the best point in the population approaches an optimal solution. Moreover, it selects the next generation through random number generators, while a derivative-bases optimisation selects the next point by a deterministic computation [77]. The genetic algorithm begins by creating a random initial population (if none is provided by the user). Then, the algorithm exploits the individuals of the current population in order to determine that of the next generation. In order to generate the next population the algorithm follows few steps [76]:

  i assign a score to each individual of the current population by computing its fitness values (see next section)

 ii scales the raw fitness scores

iii select a set of individual according to their fitness scores, called parents

 iv select the individual with the lower fitness scores as elite to directly move to the next population

  v produce children trough parents by mutation (random changes to a single parent) or crossover (combining a pair of parents)

then, the algorithm stops when the stopping criteria are met (or when it matches the maximum number of generations selected by the user).

The objective function defined in this work and evaluated for each individual of the optimisation is structured like this:

  i input variables

 ii mission analysis model

iii cost functions computation

The optimisation variables are different for the two cases, and these will be discussed in specific sections.

8.2   Cost functions

The cost functions allow the evaluation of the constellation properties. The cost functions are the same for both the Sun-synchronous and the non-Sun-synchronous cases. They are calculated from the output parameters of the mission analysis model and from the optimisation variables. Cost functions are discussed in the following. Some of the cost functions are based on the work done by Huang et al. [62].

The first cost function J_1 aims at defining the coverage performance of the SAR constellation. Three geographic zones were defined. A first zone, from the northernmost Italian point, latitude N 47°2′31″ down to latitude N 44°30′16″, a second zone from the edge of the previous one down to latitude N 40°58′34″, and a third zone from the edge of the previous one down to latitude N 36°44′3". The first zone roughly comprises the following region: Valle d'Aosta, Trentino Alto Adige, Veneto, Friuli-Venezia Giulia, Lombardia, Piemonte and half of Emilia Romagna. On average, 36.7% of the total surface of these regions is devoted to agriculture. The second zone roughly comprises: half of Emilia Romagna, Toscana, Marche, Umbria, Lazio, Abruzzo, Liguria, Molise, and half of Puglia and Campania. On average, 43.6% of the total surface of these regions is devoted to agriculture. The third zone roughly comprises: half of Puglia and Campania, Basilicata, Calabria, Sardegna and Sicilia. On average, 49.7% of the total surface of these regions is devoted to agriculture. Then, we have defined 3 zones of interest along with a target coverage for each of these zones. The target coverage is equal to the percentage

Zone	Upper bound	Lower bound	% of cultivated area	Coverage target %
1	N 47°2′31″	N 44°30′16″	36.7%	56.7 %
2	N 44°30′16″	N 40°58′34″	43.6%	63.6 %
3	N 40°58′34″	N 36°44′3″	49.7%	69.7 %

Table 8.1: Coverage zones

of surface devoted to agriculture, increase by 20%. In this way, we can ensure to satisfy the coverage requirement of Table 6.1, because the formulation of the three zones and the 20% margin avoid the concentration of the coverage in a specific area with a lack of coverage in other areas of interest. Basically, this approach ensures that the coverage is well spread all over Italy, as the agricultural fields are. The three zones, their geographic borders and target coverage are listed in Table 8.1. The cost function J_1 (also called J_{cov}) is defined as:

$$J_1 = cov + \left(t_{cov} - 7\right) \tag{8.1}$$

where cov is defined as:

$$cov = \left(\sum_{i=1}^{3} cov_i - target_{cov,i} \right)(-1) \tag{8.2}$$

so that cov_i is the percentage of the total area of zone i covered with the instrument and $target_{cov,i}$ is the target value for coverage from the fifth column of Table 8.1. t_{cov} 7 in Eq. 8.1 is time (in days) required to get to the maximum coverage, and 7 days is the requirement for that parameter (see Table 6.1). The second cost function J_2 (or J_{rev}), relates with the revisit time:

$$J_2 = t_{rev} - t_{rev-req} \tag{8.3}$$

where $t_{rev-req}$ is the requirement for the revisit time stated in Table 6.1. The third cost function, J_3 (or J_{rob}), defines the robustness property of the constellation. This quantify the effect that derives from a one satellite failure. If a satellite fails, its contribution on the coverage and the revisit time is missing, and these two parameters degrade. This cost function has been defined as:

$$J_3 = \frac{N_{acqui,c}^{max}}{N_{acqui,c}^{TOT}} + \frac{N_{acqui,r}^{max}}{N_{acqui,r}^{TOT}} \tag{8.4}$$

where $N_{acqui,c}^{TOT}$ and $N_{acqui,r}^{TOT}$ are the total number of acquisition from all satellites for coverage and revisit respectively. While, $N_{acqui,c}^{max}$ and $N_{acqui,r}^{max}$ are the maximum number of acquisition between all satellites for coverage and revisit respectively. The higher the number of total acquisition for all satellites and the lower the number of maximum acquisitions for a satellite the better the robustness property will be. This means that the acquisition shall be distributed equally between all satellites and the number of acquisitions for a satellite shall be as low as possible. In this way, each satellite has a small contribution and therefore, its failure does not bring a huge decrease in constellation performances. In order to minimize this cost function, the number of satellites and planes shall be relatively high, and this is in contrast with the other cost functions (see below). Moreover, the robustness property benefit from large coverage overlaps. The fourth cost function, J_4 is a measure of the economic cost of at least part of the

constellation. In general, the satellite represents 25% of the total mission costs [108]. However, this percentage may increase for a constellation. It is clear that the total cost is proportional to the number of satellites. As the cost is an important factor to be kept low, this cost function is simply equal to the total number of satellites:

$$J_4 = N_{SC} \tag{8.5}$$

The remaining cost functions are based on the research done by Huang et al. in [62]. The fifth cost function assesses the collision probability of a constellation. A collision between satellite is a major issue that may lead to dangerous consequences to other operational spacecraft. In [62], the collision avoidance property was defined as the capability to avoid collision without performing manoeuvres. Two aspects are present, the collision opportunity [62]:

$$opp = \frac{\sqrt{\mu}}{\pi} \frac{N_{SC}(P-1)}{(h + R_\oplus)^{3/2}} \tag{8.6}$$

that refers to an incident in which two satellites may approach each other within a distance lower than the sum of the radii of these two satellites. The value of *opp* decreases by decreasing the number of satellites, planes and the constellation altitude. The constellation avoidance property increases with decreasing values of *opp*. The second aspect is the constellation miss distance Ψ. It is defined as the minimum value of miss distance ψ among all pair of satellites. The miss distance, ψ is the minimum angular separation between a pair of satellites [62]:

$$cos\psi = cos^2\alpha - sin^2\alpha \, cos\gamma \tag{8.7}$$

where

$$\alpha = \frac{\Delta u_{S/C}}{2} + tan^{-1}\Big[tan\Big(\frac{\Delta\Omega_{S/C}}{2}\Big)cosi\Big] \tag{8.8}$$
$$cos\gamma = cos^2 i + sin^2 i \, cos\Delta\Omega_{S/C}$$

The larger Ψ the better the collision avoidance property will be. The value of Ψ decreases with the number of satellites and orbital planes. The collision avoidance cost function (J_5 or J_{ca}) is defined as [62]:

$$J_5 = \frac{log\Big(\frac{\pi}{\sqrt{\mu}}opp\Big) - log\Big(\frac{\pi}{\sqrt{\mu}}opp_{lb}\Big)}{log\Big(\frac{\pi}{\sqrt{\mu}}opp_{up}\Big) - log\Big(\frac{\pi}{\sqrt{\mu}}opp_{lb}\Big)} + \frac{\frac{\pi}{2} - \Psi}{\frac{\pi}{2}} \tag{8.9}$$

where the subscripts *lb* and *up* represent the lower and upper bounds for *opp*:

$$opp_{lb} = \frac{\sqrt{\mu}}{\pi} \frac{N_{SC}(P-1)}{(h_{max} + R_\oplus)^{3/2}}, \quad opp_{ub} = \frac{\sqrt{\mu}}{\pi} \frac{N_{SC}(P-1)}{(h_{min} + R_\oplus)^{3/2}} \tag{8.10}$$

The sixth cost function is a measure of the launch cost. The launch property was defined as the constellation capability to be launched into orbit by an arbitrary launcher. It is assessed by two aspects, the cost related to orbit injection:

$$lch_h = Nh \tag{8.11}$$

it increases with the number of satellites and altitude. The lower its value the better the launch property will be. The second aspect is the payload capability, defined by orbit inclination:

$$lch_i = i - \phi_{site} \tag{8.12}$$

the lower the inclination (it must however be $\geq$ than ϕ_{site}), the lower the payload capability and the better the launch property. In the following, the value of ϕ_{site} has been set equal to 5°that is the latitude of the launch site in French Guiana. Finally, the launch cost function (J_6 or J_l) is defined as [62]:

$$J_6 = \frac{log\, lch_h - log(lch_h)_{lb}}{log(lch_h)_{ub} - log(lch_h)_{lb}} + \frac{i - \phi_{site}}{\frac{\pi}{2} - \phi_{site}} \tag{8.13}$$

where the subscripts lb and up represent the lower and upper bounds for lch:

$$(lch_h)_{lb} = min(N_{SC})\, h_{min}, \quad (lch_h)_{ub} = max(N_{SC})\, h_{max} \tag{8.14}$$

The sixth cost function measures the build-up capabilities of the constellation. Usually, it takes quite some time from the launch of the first satellite to the launch of the last satellite. This means that the constellation will spend a good portion of its life in a non-optimal operative condition. In the worst case, the first satellite may become non-operative before the launch of the last satellite. In [62], it was supposed that the orbital planes are built up one by one and there is no limit to the number of satellites by a single launch. Therefore, the number of orbital planes was used to evaluate the build-up period:

$$J_7 = P \tag{8.15}$$

the lower the number of planes, the better the build-up property will be. The next cost function, J_8 (or J_{sk}), relates to station keeping. The approach considered for station-keeping is relative station-keeping, that aims at maintaining the relative positions of all satellites with respect to each other. It was assessed with respect to the atmospheric drag effect. In this case, the satellites' altitude needs to be maintained as it decreases due to drag. Therefore, the station-keeping property was assessed by the cost of altitude maintenance. Supposing a 2-burn Hohmann transfer for altitude maintenance, the change in velocity is given by [62]:

$$\Delta v_{keep} = N_{SC} \left[\left(\sqrt{\frac{2\mu}{a_f} - \frac{2\mu}{a_n + a_f}} - \sqrt{\frac{\mu}{a_f}} \right) + \left(\sqrt{\frac{\mu}{a_n}} - \sqrt{\frac{2\mu}{a_n} - \frac{2\mu}{a_n + a_f}} \right) \right] \tag{8.16}$$

where a_n and a_f are the semi-major axis of the nominal orbit and of the final orbit after decay. a_f can be obtained by integration of the atmospheric drag equation:

$$(a_f - a_n) = -\frac{C_D\, A}{m}\, \rho \sqrt{\mu\, a}\, dt \tag{8.17}$$

where the atmospheric density ρ can be evaluated with an exponential model. This property can be improved by diminishing the number of satellites and increasing their altitude. The lower Δv_{keep} the better the station-keeping property will be. The relative cost function is [62]:

$$J_8 = log\, \Delta v_{keep} \tag{8.18}$$

The final cost function measures the EoL disposal of the constellation. A non-operational spacecraft must be removed from its orbit within 25 years from its end of life. Spacecraft in LEO shall be de-orbited to a disposal orbit that has a perigee low enough to allow quick re-entry under the drag effect. This property has been evaluated as the total change in velocity for all satellites [62]. De-orbiting can be achieved with a tangential burn, then, the total change in velocity is given by:

$$\Delta v_{EoL} = N_{SC} \left(\sqrt{\frac{\mu}{a_n}} - \sqrt{\frac{2\mu}{a_n} - \frac{2\mu}{a_n + r_p}} \right) \tag{8.19}$$

where the value of r_p was set to $250 \ km$ so that the drag effect will be enough to lower the apogee quickly and allow re-entry. The smaller Δv_{EoL} the better the EoL property. It can be reduced by reducing the number of satellites and their altitude. The relative cost function (J_9 or J_{EoL}) is given by:

$$J_9 = log \, \Delta v_{EoL} \tag{8.20}$$

All the nine cost functions shall be minimised in a trade-off way, as not all of them can be minimized at the same time. Minimising a certain cost function would mean increasing another one, depending on how they were defined. For the seek of clearness, the cost functions are reported here below:

$$\mathbf{J} = \begin{bmatrix} J_1, \ J_2, \ J_3, \ J_4, \ J_5, \ J_6, \ J_7, \ J_8, \ J_9 \end{bmatrix}^T \tag{8.21}$$

$$
\begin{aligned}
J_1 &= cov + \left(t_{cov} - 7 \right) \\
J_2 &= t_{rev} - 5 \\
J_3 &= \frac{cov}{N_{acqui,c}^{TOT}} N_{acqui,c}^{max} + \frac{24 t_{rev}}{N_{acqui,r}^{TOT}} N_{acqui,r}^{max} \\
J_4 &= N_{SC} \\
J_5 &= \frac{log\left(\frac{\pi}{\sqrt{\mu}} opp\right) - log\left(\frac{\pi}{\sqrt{\mu}} opp_{lb}\right)}{log\left(\frac{\pi}{\sqrt{\mu}} opp_{up}\right) - log\left(\frac{\pi}{\sqrt{\mu}} opp_{lb}\right)} + \frac{\frac{\pi}{2} - \Psi}{\frac{\pi}{2}} \\
J_6 &= \frac{log \, lch_h - log(lch_h)_{lb}}{log(lch_h)_{ub} - log(lch_h)_{lb}} + \frac{i - \phi_{site}}{\frac{\pi}{2} - \phi_{site}} \\
J_7 &= P \\
J_8 &= log \, \Delta v_{keep} \\
J_9 &= log \, \Delta v_{EoL}
\end{aligned}
\tag{8.22}
$$

8.3   Computational time and optimisation time

In general, the duration of the optimisation depends on the total number of individuals, that needs to be evaluated before reaching a stable solution, and on the time required for evaluating a single individual. Evaluating an individual means evaluating its score. In order to assess the score of an individual, the optimiser must compute the objective functions. We have seen in the previous chapter and in the sections above what is required to compute the cost functions. Basically, the optimiser shall run the mission analysis model and then compute

the cost functions. The procedure has to be repeated for all the individuals. Plus, at the end of a generation, the optimiser takes some time to retrieve the population of the next generation. However, the time required for designing a new population is much lower than the time required for evaluating an individual's score. Therefore, we can assume that the total time for the optimisation is proportional only to the total number of individuals. At each iteration, the computation of the mission analysis model represents a burden in terms of time. Its computational time depends strongly on the number of satellites because the algorithm shall compute the coverage and revisit for each satellite. These operations are computationally heavy. In order to estimate the time required for evaluating an individual's score, we have run 100 random iteration (random constellation and random altitude). The computer's system used for this test is an Intel(R) Pentium(R) CPU G4400 @ 3.30 GHz (2 cores) embedded with an 8 GB RAM. On this platform, on average an iteration took 87.5744 seconds. This means that in one day of computation, the computer can evaluate 986 individuals. This number is clearly too small, and running the optimisation on this platform would take too long. Therefore, we have decided to rely on a server machine. This machine was made available by the Department of Aerospace Science and Technology of Politecnico di Milano. The specifics of this server are listed in Table 8.2. The presence of 40 physical cores allow to evaluate the individuals of a same

Architecture	x86_64
CPU(s)	Physical 40 / Logical 80
Model Name	Intel(R) Xeon(R) CPU E5-4620 v4 @ 2.10 GHz

Table 8.2: Server specifics

generation in parallel, and then to decrease substantially the average individual computational time. Employing all 40 physical cores at a time reduced the average individual time to about 5.7 seconds. Finally, the running time for the simulations will be given in the following sections according to the case.

8.4 Sun-synchronous and repeated-ground track orbits

In this section, we will describe how we set the optimisation in the case of SSO and Repeated-ground Track Orbits. The Walker-Delta constellation is basically defined by the three indexes $N_{S/C}$, P, and F. We can assign a design variable to each of these parameters. We recall that $N_{S/C}$, P, and F must be integer numbers, P must be a divisor of $N_{S/C}$ and F must be higher than 0 and lower than or equal to $(P-1)$. As we have seen in the previous chapter, whenever we consider circular orbit and we fix a value for $k_{rev2rep}$ and $k_{day2rep}$ we get a system from 7.8 that can be solved for the inclination and semi-major axis of the orbit. Therefore, simply tuning all the possible combinations (within a reasonable range) of $k_{rev2rep}$ and $k_{day2rep}$, we can get all the possible orbits in the range of interest. $k_{day2rep}$ varies from 1 to 40 days, while $k_{rev2rep}$ varies from 1 to 623 orbits. With the mentioned values for $k_{rev2rep}$ and $k_{day2rep}$, and the condition for Sun-synchronous repeated-ground track orbits, there are 824 possible orbits between 400 km and 700 km of altitude. For the seek of clearness, these are not reported here. Again, each orbit is defined by a value of $k_{day2rep}$, a value of $k_{rev2rep}$, a semi-major axis and

an inclination. These four pieces of information could be stored in a matrix of 824 rows by 4 columns. This matrix can be sorted in ascending order of $k_{day2rep}$ and $k_{rev2rep}$. In order to be as much clear as possible, we report here only the first 10 orbits, listed in Table 8.3. As the

$k_{day2rep}$	$k_{rev2rep}$	Semi-major axis [km]	Inclination [deg]
1	15	6944.18	97.655
2	30	6944.18	97.655
2	31	6794.02	97.088
3	44	7049.01	98.070
3	45	6944.18	97.655
3	46	6843.17	97.270
4	59	7022.43	97.963
4	60	6944.18	97.655
4	61	6868.08	97.364
4	62	6794.02	97.088

Table 8.3: First ten Sun-synchronous repeated-ground track between 400 and 700 km altitude

row index increases so do $k_{day2rep}$ and $k_{rev2rep}$. Then, the row index of the matrix containing all the possible orbits was defined as the fourth design variables. As this number increases, the number of times the satellite crosses the equator, before repeating its orbit, increases as well. This index must of course be an integer. The design variables vector for the Sun-synchronous repeated-ground track case is given by:

$$\boldsymbol{x}_{SSORGT} = \begin{bmatrix} N_{S/C}, P, F, j_{SSORGT} \end{bmatrix}^T \tag{8.23}$$

The minimum number of satellites was set to 3, the minimum number of planes was clearly set to 2 and in turn, the minimum value that F can assume is 1. The index j_{SSORGT} can be at least 1. Then, the lower bound for these design variables is the following:

$$\boldsymbol{lb}_{SSORGT} = \begin{bmatrix} 3, 2, 1, 1 \end{bmatrix}^T \tag{8.24}$$

The upper bound for the number of satellites was set to 40. In general, a satellite that weighs around 200 kg (as the one we are considering in this work), costs about 100 $k€/kg$ [85], this means that producing 40 satellites leads to a cost of € 800M. This cost is already relatively high enough, and it can be set as the upper bound. In turn, the maximum number of planes is 40 and the maximum value for F is 39. The maximum for the index j_{SSORGT}, is equal to the total number of orbits we are considering, 824. Then, the upper bound for the design variables is the following:

$$\boldsymbol{ub}_{SSORGT} = \begin{bmatrix} 40, 40, 39, 824 \end{bmatrix}^T \tag{8.25}$$

These ranges lead to a total of 974792 possible constellation configurations. Exploring all these configurations would take more than 64 days with the available power of calculus. In a multi-objective genetic algorithm optimisation, it is possible to specify the total number of generations and the population of each generation. These two values shall be selected so

that the optimisation can get to the final result without computing unnecessary iterations. The minimum values of generations and population, that make the optimisation converge to a stable result, are the correct ones. Predicting these two values is a complex task, and running more than one optimisation is the simplest way to find them. We have to run multiple optimisations with an increasing number of generations and population and check from which values we get the same final result. If we run an optimisation with a number of generations x_1 and population x_2, and then we rerun with generations $x_3 > x_1$ and population $x_4 > x_2$ and we get the same result, it means that the values x_1 and x_2 are the correct ones (as we get the same result with a lower effort). We can rely on this approach as the random nature inside the genetic algorithm ensures that an insufficient number of iterations leads to different results. Unfortunately, in our work, we were limited by time and logistics matters. So that we have selected the number of generations and population in order to match our limitations and find a stable solution. We have run the simulation 5 times, with an increasing number of individuals and generations. Data about these simulations are given in Table 8.4. The results of the final simulation are

Population	Generations	Total number of individuals	Final population	Run time
500	60	30000	175	22
545	60	32700	191	30 †
550	60	33000	193	23
629	65	40885	221	25
633	75	47475	222	33

Table 8.4: Simulations details for Sun-synchronous repeated-ground track case. †: it took more time than the others as a lower number of cores was employed.

presented in the next chapter. We run multiple simulations to be sure that the optimisation got to a reliable solution. We can say that we found a solution as the evolution of the cost functions in the last simulations follow the same behaviour.

8.5 Repeated-ground track orbits

In this section, we will describe how we set the optimisation in the case of repeated-ground Track Orbits. The Walker-Delta constellation is again defined by three indexes and therefore we can assign a design variable to each of these parameters, exactly as we have done for the previous case. The same constraints on $N_{S/C}$, P, and F still apply. As it was explained in the previous chapter, a repeated-ground track (circular) orbit is defined by four parameter: $k_{day2rep}$, $k_{rev2rep}$, a and i. If we fix $k_{day2rep}$ and $k_{rev2rep}$, we can find multiple couples of a and i that satisfy Eq. 7.5. Therefore, $k_{day2rep}$, $k_{rev2rep}$ and i have been split in two design variables. All the possible combination, with $k_{day2rep}$ from 1 to 35 and $k_{rev2rep}$ from 1 to 500, have been stored in a 17500×2 matrix. The first column of the matrix contains the values of $k_{day2rep}$, while the second column contains the values of $k_{rev2rep}$. Then, the fourth design variables j_{RGT} is an index that defines the row of the matrix that contains the values of $k_{day2rep}$ and $k_{rev2rep}$. The fifth design variable is simply the inclination i. The design variables vector for the repeated-ground

track case is given by:

$$\boldsymbol{x}_{RGT} = \begin{bmatrix} N_{S/C}, \ P, \ F, \ k_{day2rep}, \ k_{rev2rep}, \ i \end{bmatrix}^T \tag{8.26}$$

The lower bound for each design variables is:

$$\boldsymbol{lb}_{RGT} = \begin{bmatrix} 3, \ 2, \ 1, \ 1, \ 1, \ 35 \end{bmatrix}^T \tag{8.27}$$

The lower bound on the inclination has been set to 35°as satellites on lower inclinations could not acquire images of the Italian territory. While the upper bound is:

$$\boldsymbol{ub}_{RGT} = \begin{bmatrix} 30, \ 30, \ 29, \ 35, \ 500, \ 90 \end{bmatrix}^T \tag{8.28}$$

In this case, the maximum number of satellites has been set to 30, in order to reduce the maximum number of combinations. The maximum number of planes and separation change accordingly. The design variable j_{RGT} can assume at most the value of 17500, as that is the number of rows in the relative matrix. The maximum value for the inclination is clearly 90°. In this case, there is one more constraint with respect to the previous case. Indeed, at the beginning of the cost function, the algorithm compute semi-major axis of the orbit a, given $k_{day2rep}$, $k_{rev2rep}$, and i. If a is lower than 450 km or higher than 650 km, that particular individual is not evaluated and all the cost functions are set to a very high number (10^5). The altitude range has been shortened with respect to the previous case where it was 400-700 km. This limitation was introduced in order to decrease the total number of combinations. The ranges mentioned for the design variables lead to a total of more than 62.5 billions possible constellation configurations (considering a discretisation of 0.01 on the inclination, that is the accuracy a launcher can grant on the orbit inclination). However, many of these constellations lay outside of the boundaries we have set, and therefore they are not evaluated. The optimisation computed a total of 240000 individuals through 200 generations. It lasted 4.83 days, with an average individual computational time of about 0.575 seconds (lower than the Sun-synchronous case as some individuals were not evaluated because they do not belong to the altitude range selected). The result of this optimisation is presented in the relative section of the next chapter.

Chapter 9

Optimisation results and discussion

In this chapter, we present the results of the optimisation simulations described in the previous chapter. We will analyse the results and through a trade-off analysis, we will select only a couple of constellations that are possible candidates for the mission. As for the optimisation, the results are differentiated in a Sun-synchronous case and a generally inclined case. The results are then compared with the research done by Huang et al. [62].

9.1 Sun-synchronous and repeated-ground track orbits

Figure 9.1 shows the Pareto-front solutions for the Sun-synchronous mission, each point representing an optimal constellation. The vertical axis indicates the altitude, the colour bar indicates the number of orbital planes and the horizontal axis of Figure 9.1a indicates the number of satellites. The second plot, 9.1b, contains one more information with respect to the first one, being the angular separation F along the second horizontal axis. The results are in line with what proposed by Huang et al. [62]. We can notice the presence of quite many individuals at the beginning of the number of satellites axis. This can be understood considering the fact that five out of nine of the cost function, Eq. 8.22, are minimised by decreasing the number of satellites. On the other hand, the cost functions on coverage and revisit time yield good result even with a low number of satellites, explaining again the higher initial concentration. On the other hand, the presence of individuals with a high number of satellites is explained by considering the cost functions about robustness, coverage and revisit time which decrease substantially by increasing the number of satellites. Most of the individuals have a relatively low number of orbital planes as decreasing P allows to decreasing most of the cost functions and good results in coverage and revisit time can be achieved even with few orbital planes. The individuals are quite fairly spread on the vertical axis, h, meaning that there is not a favourite altitude. However, the influence of altitude will be discussed in the following. We can nonetheless appreciate from Figure 9.1a the presence of some individuals at a fixed altitude of about 575 km. This altitude has been probably chosen multiple times as it produces a wide SAR swath and thus good results in coverage and revisit time while containing the cost functions of launch and station-keeping.
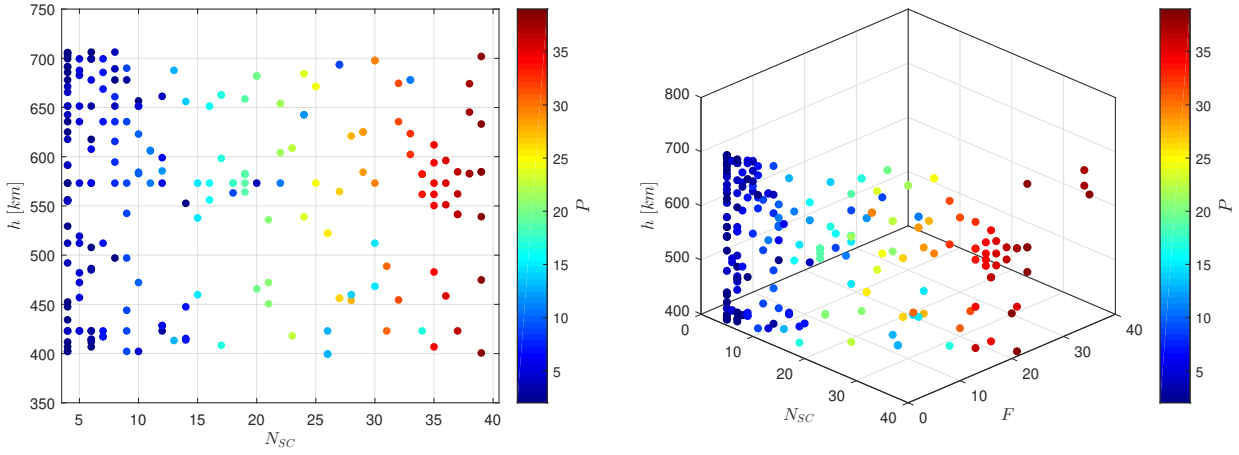
(a) Pareto-front for altitude, number of satellites (b) Pareto-front for altitude, number of satellites, and orbital planes orbital planes and angular separation

Figure 9.1: Pareto-front solutions for the Sun-synchronous case

9.1.1   Trade-off analysis

Basically, we start our trade-off analysis simply by removing all those constellations that do not respect the requirements in terms of coverage and revisit time that we have defined in Table 6.2. It means we neglect all the constellations with a revisit time higher than 5 days and that do not cover at least the percentage of area defined in Table 8.1. This operation reduced the initial 222 individuals down to 94 individuals. Figure 9.2 shows the relation between the revisit time of the solution and the optimisation variables. It appears clear that increasing the num-

(a) Revisit time versus number of satellites, alti- (b) Revisit time versus number of satellites and al- tude and number of orbital planes titude

Figure 9.2: Revisit time versus optimisation variables

ber of satellites diminishes the revisit time, as it is quite straightforward. However, a dramatic

decrease happens from about ten satellites on. We cannot highlight any dependence on the altitude as low revisit times are present both at high and low altitudes even for the same number of satellites. Finally, there are few constellations that have a large number of satellites but have not got a good revisit time. These may be present as they score a very result in other cost functions, such as robustness. Figure 9.3 shows four plots with straightforward constellation properties. In Figure 9.3a it is clear that the robustness property of the constellations increases

(a) Robustness versus number of satellites and number of orbital planes
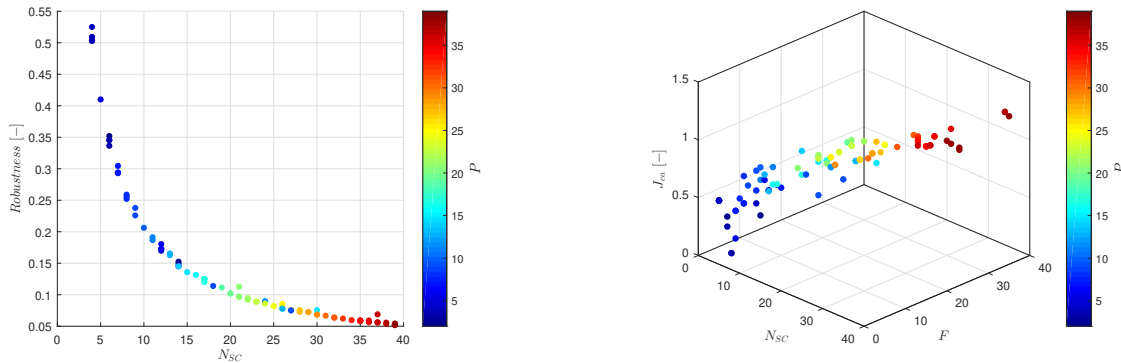
(b) J_{ca} versus number of satellites, angular separation F and number of orbital planes P
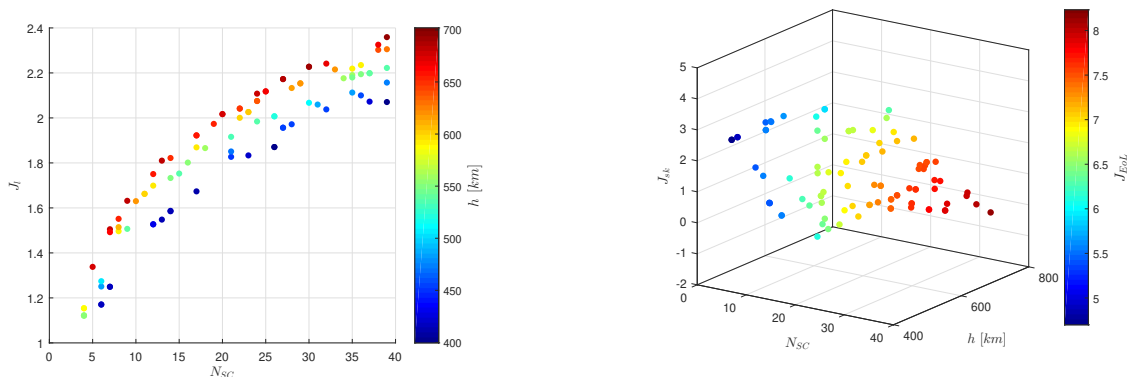
(c) J_l versus number of satellites and altitude

(d) J_{sk} versus J_{EoL}, number of satellites and altitude

Figure 9.3: Robustness, J_{ca}, J_l, J_{sk} and J_{EoL} versus optimisation variables, Sun-synchronous solutions

with the number of satellites, as demonstrated by Huang et al. [62]. Then, increasing the number of satellites improves the revisit time and robustness of the constellation. Figure 9.3b shows that the collision avoidance property of the constellations is minimised with a low number of satellites, orbital planes and small angular separation, as previously demonstrated by Huang et al. [62]. Then, we can already see the first trade-off between the robustness and collision avoidance properties, if one increases the other must decrease. Figure 9.3c shows clearly that the launch cost function can be reduced ether by decreasing the number of satellites either by decreasing the altitude. However, the strongest influence is given by the number of satellites. It is preferable to decrease the altitude, at a fixed number of satellites, in order to decrease the

launch cost function. This is again in accordance with Huang et al. [62]. Finally, Figure 9.3d shows that increasing the number of satellites increases both the station-keeping and end-of-life Δv, while high altitude leads to high end-of-life Δv and low station-keeping Δv. The opposite happens at low altitude. This is simply verified by considering that the atmospheric density decreases exponentially with the altitude and then also the relative station-keeping decreases; while the end-of-life burn becomes bigger with increasing altitude since the distance from the target altitude for re-entry is higher. This is confirmed by Huang et al. [62]. The relation between the Δv for station-keeping and end-of-life is shown in Figure 9.4a. It is quite difficult
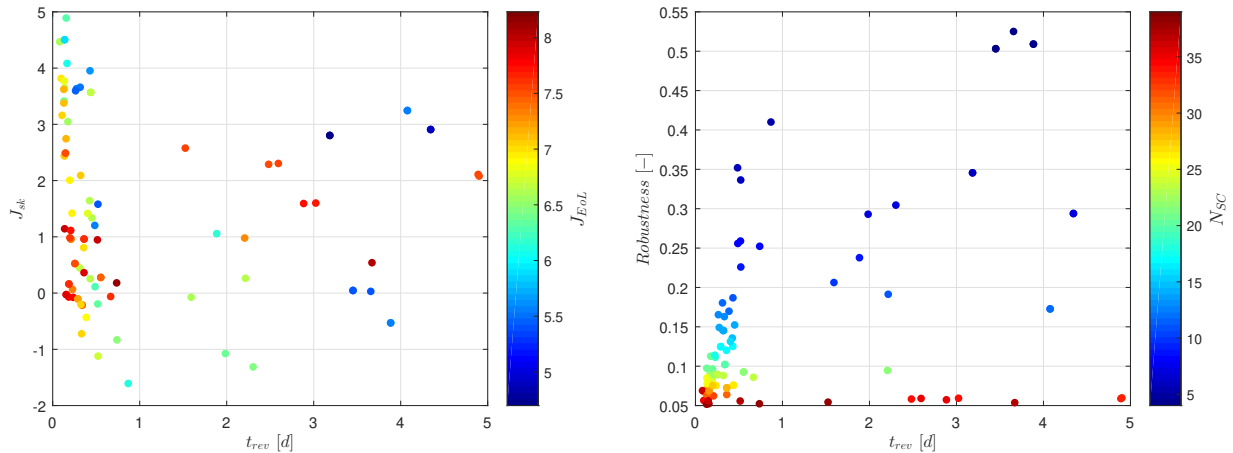
(a) Revisit time versus station-keeping and end-of-life cost functions

(b) Revisit time versus robustness and number of satellites

Figure 9.4: Revisit time versus station-keeping, end-of-life, robustness and number of satellites, Sun-synchronous solutions

to retrieve a relation between these three properties. Indeed, low revisit time are achievable with both low and high station-keeping Δv. However, as the Δv for station-keeping increases, the revisit time slightly decreases. This reflects the dependence of revisit time on the number of satellites. On the other hand, it appears that as the revisit time decreases so does the Δv for end-of-life. This would mean that there are solutions with a medium-high number of satellites at low altitude (see Figure 9.3) that ensure a very good revisit time. These solutions may be of interest as they minimise at least two cost functions, in particular the revisit time. Moreover, we know that as the revisit time decreases so does the robustness. Figure 9.4b confirms the relationship between robustness, revisit time and the number of satellites. It is interesting to observe the presence of light blue dots near the origin. those are solutions that have a medium number of satellites but, at the same time, they have a very good score in the revisit time and robustness. The plot of Figure 9.5a shows that low revisit times are obtained even with good collision avoidance, launch and manoeuvre properties. Low collision avoidance property, coming from a low number of satellites and orbital planes, leads to a low Δv for station-keeping and end-of-life and a low launch cost function; both due to a reduced number of satellites. As the launch cost function and the sum of station-keeping and end-of-life increase so does the collision avoidance property since the number of satellites is increasing as well. There are few blue dots

(a) J_{ca} versus J_l, $J_{sk}+J_{EoL}$ and revisit time

(b) Robustness versus J_l, $J_{sk}+J_{EoL}$ and number of satellites
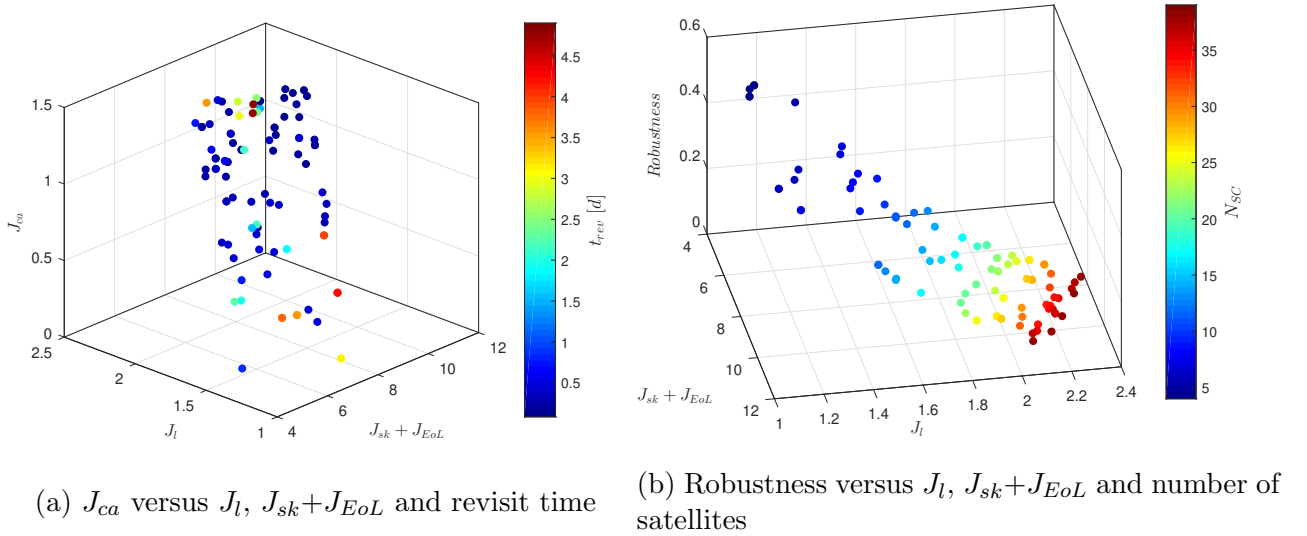
Figure 9.5: Relation between cost functions and optimisation variables, Sun-synchronous case

with very low J_l, $J_{sk} + J_{EoL}$ and J_{ca} cost functions. These are solutions with a medium-high number of satellites (low revisit time), at low altitude (good launch property and manoeuvring property) and a low number of planes (low collision avoidance cost function). These solutions are particularly interesting as they minimize four cost functions at the same time. These are the same constellations we have appreciated in Figure 9.4a, where they had good revisit time and low end-of-life Δv. Figure 9.5b confirms that good robustness comes at the price of high launch cost and manoeuvring cost ($J_{sk} + J_{EoL}$). However, if we fix J_l and the robustness values we find that few solutions are available, where some have lower values of $J_{sk} + J_{EoL}$ even if they have the same number of satellites. This is clearly due to the different altitude.

We now move on to the next step of our trade-off analysis, in order to find the final constellations that are possible candidates for our mission. We have selected two ranges of altitude that are of particular interest for our research. One lies between 450 and 500 km and the other lies between 550 and 600 km. This restriction leads to a final number of 25 constellations. These, along with their cost functions are shown in Table 9.1. The colour of the cells represents the score of the constellation, red means a bad score while green means a good score. The information about coverage is missing as all these constellations respect the coverage requirement. We will try to select a maximum of four constellations between these 25. During the selection, we first gave particular attention to the number of satellites, the number of orbital planes and the revisit time. Then, all the other cost functions. In the 450-500 km range there is a constellation that has 6 satellites in three orbital planes at 485 km of altitude (9th row of Table 9.1). Other than having a low number of satellites and planes it also has good collision avoidance, launch, station-keeping and end-of-life properties. Its revisit time is about 12 hours, therefore a good value respecting the requirements. Nonetheless, it has poor robustness properties, due to the lower number of satellites. Figure 9.7 and Figure 9.6 show the constellation along with some properties. Looking at Figure 9.7a we can notice that the constellation actually reaches the

N_{SC}	P	F	i [deg]	h [km]	t_{cov} [d]	t_{rev} [h]	J_{rob}	J_{ca}	J_l	J_{sk}	J_{EoL}	t_{SAR} [min]	$k_{day2rep}$	$k_{rev2rep}$
21	21	10	97.19	450.6	31.9	3.13	0.10	-0.79	-0.43	3.41	6.39	5.00	32	493
28	28	15	97.20	454.0	37.9	3.29	0.07	-0.82	-0.33	3.64	6.71	5.00	38	585
32	32	20	97.20	454.5	27.9	3.24	0.06	-0.78	-0.29	3.77	6.85	5.00	28	431
27	27	12	97.21	456.2	30.9	10.49	0.08	-0.72	-0.34	3.57	6.70	5.00	31	477
36	36	25	97.22	458.5	28.9	2.30	0.06	-0.74	-0.25	3.82	7.01	5.00	29	446
21	21	3	97.27	472.2	2.9	4.19	0.11	-0.86	-0.41	3.05	6.58	5.00	3	46
39	39	21	97.28	474.8	36.9	3.06	0.05	-0.69	-0.22	3.62	7.22	5.00	37	567
35	35	18	97.31	482.9	36.9	3.08	0.06	-0.74	-0.25	3.38	7.18	5.00	37	566
6	3	1	97.32	485.0	30.6	12.48	0.34	-1.29	-0.80	1.58	5.43	5.00	31	474
31	31	10	97.33	488.7	17.9	2.60	0.07	-0.74	-0.28	3.16	7.10	5.00	18	275
35	35	20	97.57	550.4	26.9	59.57	0.06	-0.68	-0.21	2.29	7.58	4.99	27	407
36	36	21	97.57	551.2	27.9	62.24	0.06	-0.74	-0.20	2.30	7.61	4.93	28	422
14	2	1	97.58	552.7	13.0	10.81	0.15	-1.47	-0.50	1.34	6.67	4.82	15	226
4	4	1	97.59	555.1	16.7	82.84	0.50	-1.49	-0.89	0.05	5.43	4.64	17	256
4	4	1	97.59	556.1	17.7	87.74	0.53	-1.49	-0.89	0.03	5.44	4.57	18	271
16	16	2	97.59	556.1	17.9	9.65	0.13	-0.84	-0.45	1.42	6.82	4.57	18	271
35	35	20	97.61	561.8	26.9	117.37	0.06	-0.68	-0.20	2.11	7.63	4.16	27	406
34	34	19	97.61	561.8	26.9	117.64	0.06	-0.76	-0.21	2.08	7.60	4.16	27	406
18	9	8	97.62	563.2	28.4	5.34	0.11	-1.03	-0.41	1.42	6.98	4.05	31	466
4	4	1	97.73	591.4	16.7	93.23	0.51	-1.49	-0.87	-0.53	5.59	2.27	17	254
35	35	20	97.74	593.8	29.9	72.57	0.06	-0.67	-0.19	1.60	7.77	2.14	30	448
8	8	6	97.74	594.6	25.8	11.68	0.26	-1.07	-0.65	0.11	6.30	2.10	29	433
36	36	21	97.74	596.1	26.9	69.23	0.06	-0.74	-0.18	1.59	7.81	2.01	27	403
17	17	8	97.75	598.3	36.9	8.55	0.12	-0.81	-0.41	0.81	7.07	1.89	37	552
12	6	4	97.76	599.0	35.8	7.46	0.18	-1.23	-0.52	0.45	6.72	1.85	36	537

Table 9.1: Constellations between 450 and 500 km and 550 and 600 km, Sun-synchronous case
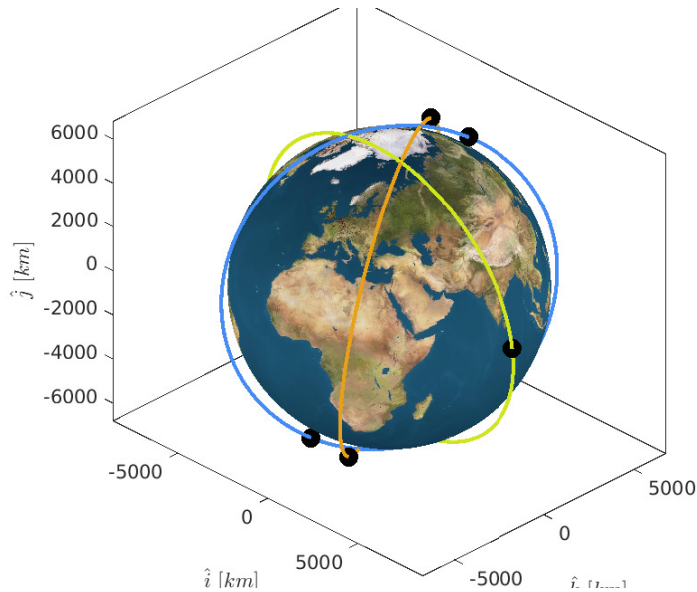
Figure 9.6: Orbits and satellites initial configuration for the 6 satellites constellation, Sun-synchronous case
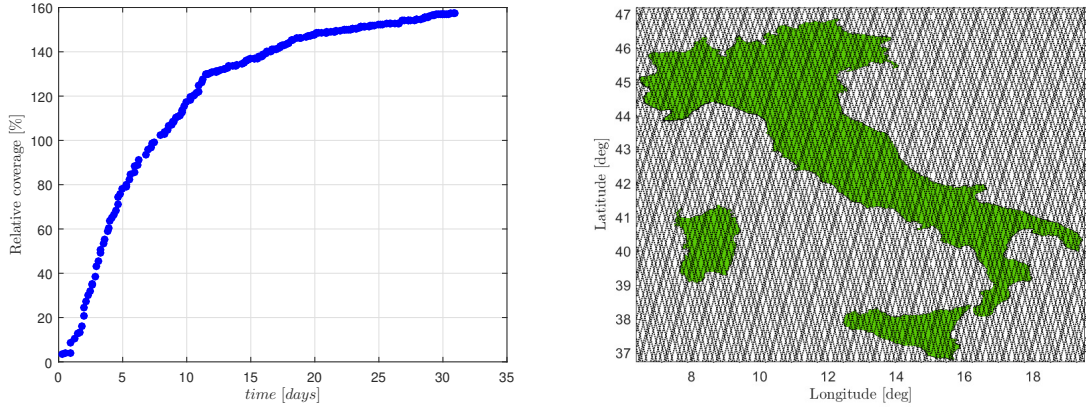
(a) Coverage evolution in time with respect to the coverage requirement

(b) Satellites ground tracks points within the Italian territory
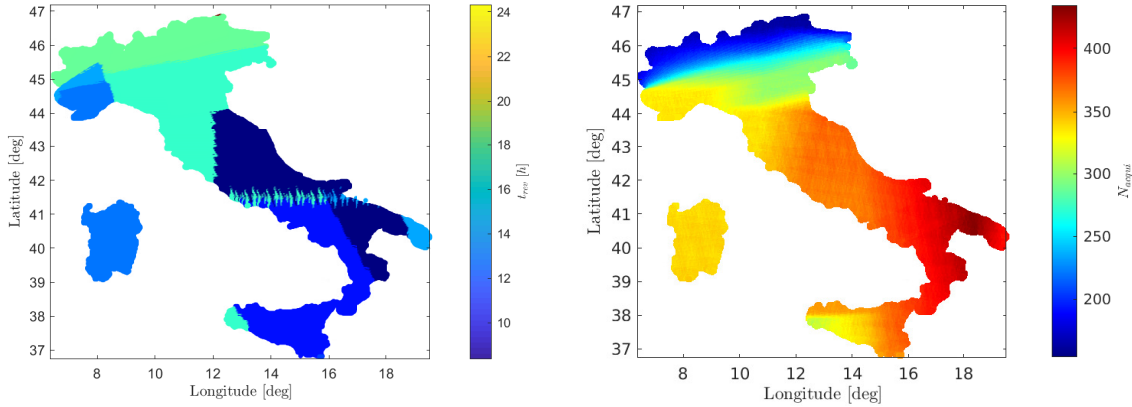
(c) Constellation revisit time within the Italian territory

(d) Number of acquisition per geographic area in the specific time span $k_{day2rep} = 31$ days

Figure 9.7: Possible constellation with 6 satellites in Sun-synchronous orbits

complete coverage of the area requested by the requirement in less than 10 days and it can cover even more area than that requested. Finally, Figure 9.7d shows through a colour bar how many acquisitions of the same geographic area the constellation can grant. These degrade moving south as the revisit time, shown in Figure 9.7c. Although this constellation has an average revisit time of about 12 hours, it can go down even to 30 hours in some regions (see Figure 9.7c). Moving to the region between 550 and 600 km, at the 13th row of Table 9.1, there is a constellation with 14 satellites distributed over two orbital planes. The number of satellites is slightly higher than the previous constellation, however, the very low number of orbital planes is profitable, especially for the build-up property of the constellation. This constellation grants an average revisit time of about 10 hours. It has a very high collision avoidance property, again due to the low number of orbital planes. It has also relatively good launch and station-keeping properties. On the other side, the end-of-life property is average, due to the fact that it flies on a height of 552.7 km. As the previous constellation, the robustness property has a relatively poor score, however, we have to accept this fact if we privilege the number of satellites. This
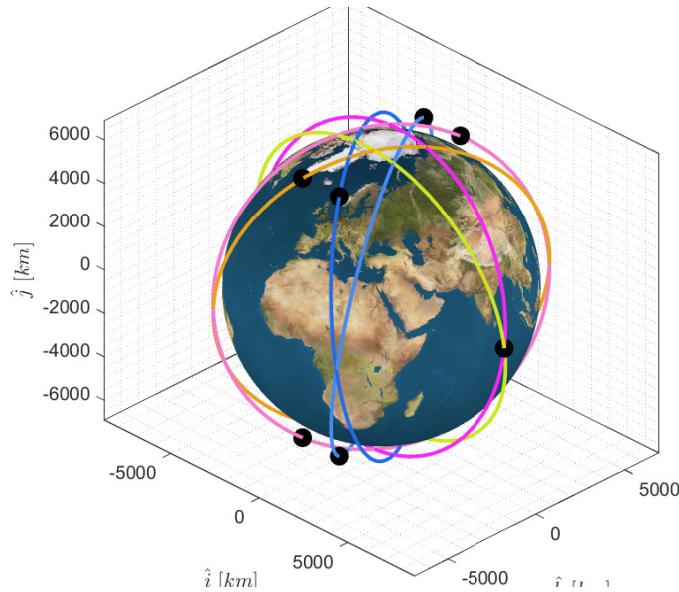
Figure 9.8: Orbits and satellites initial configuration for the 12 satellites constellation, Sun-synchronous case

constellation actually reaches the complete coverage of the area requested by the requirement in less than 5 days and it can cover even more area than that requested. Its average and maximum number of acquisitions is higher than the previous constellation, although the lower time span, mostly due to the higher number of satellites. In this case, the southern regions are the most covered. This constellation has a very uniform revisit time from north to south, with a maximum difference of less than 2 hours. Another possible constellation has 12 satellites in 6 orbital planes at 599 km altitude (last row of Table 9.1. This constellation is not too different from the one with 14 satellites. It has a better average revisit time, a little bit more than 7 hours, due to the higher number of orbital planes and the higher altitude. These two values lead to slightly worse collision avoidance property. However, this constellation has good station-keeping property (due to the high altitude) and, launch, end-of-life and robustness property comparable to the previous constellation of 14 satellites. With respect to the first constellation of 6 satellites, this one has better revisit time and a better end-of-life and robustness properties. This constellation with 12 satellites is shown in Figure 9.9 and Figure 9.8. This constellation reaches the target coverage in about 6 days, Figure 9.9a. In this case, the number of acquisitions in relation to the time span is comparable with the previous one. The revisit time is some southern region can go down even to less than 4 hours, Figure 9.9c. However, the absolute difference in revisit time is slightly higher than the previous constellation. There is also one last constellation of particular interest. It has only 4 satellites in 4 orbital planes at 555 km of altitude. The low number of satellites allows for very high collision avoidance, launch, station-keeping and end-of-life properties, better than any other constellations we have seen so far. However, this comes with poor robustness and the poorest revisit time, more than 80 hours on average. This constellation has a 4 days gap in the coverage, then in the worst case, it reaches the coverage goal in about 10 days. The revisit time is some are is quite poor because of the lower number of satellites. This is also reflected in the number of acquisitions. This
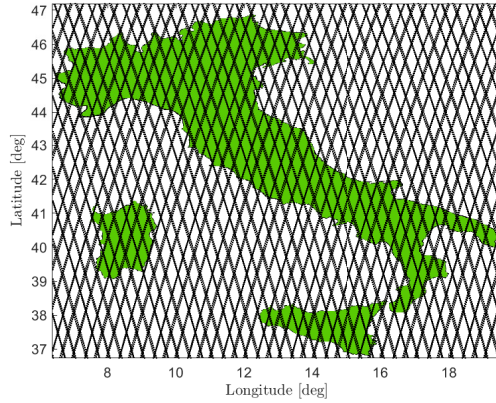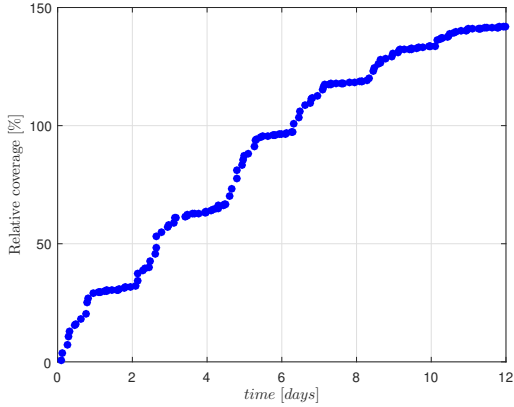
(a) Coverage evolution in time with respect to the coverage requirement

(b) Satellites ground tracks points within the Italian territory
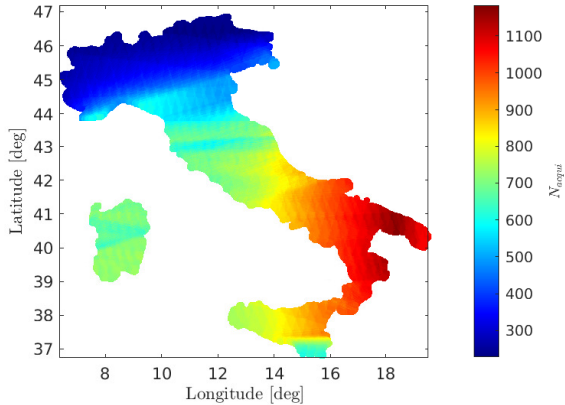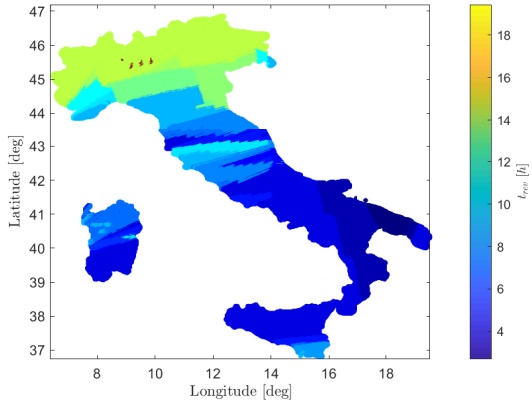
(c) Constellation revisit time within the Italian territory

(d) Number of acquisition per geographic area in the specific time span $k_{day2rep} = 36$ days

Figure 9.9: Possible constellation with 12 satellites in Sun-synchronous orbits

clarifies the fact that a lower number of satellites worsens the properties of the constellation. Finally, we have found two constellations with few satellites, one of which has even a relatively good revisit time. These two are preferable if the first driver becomes to keep the number of satellites as low as possible. On the other side, there are two more constellations with a higher number of satellites but one of them has a very low number of orbital planes, while the other has a very good revisit time with a lower number of satellites. If we want a constellation with the lowest number of satellites that has however a good revisit time, we should probably choose the one with 6 satellites at 485 km (Figure 9.7). On the other side, if we want a constellation with a better revisit time with a relatively low number of orbital planes, we should choose the one with 12 satellites at 599 km (Figure 9.9).

9.2   Repeated-ground track orbits

Figure 9.10 shows the Pareto-front solutions for the generally inclined mission, each point representing an optimal constellation. The vertical axis indicates the altitude, the colour bar indicates the number of orbital planes and the horizontal axes indicate the number of satellites and their inclination. The results are compliant with what found by Huang et al. [62]. There
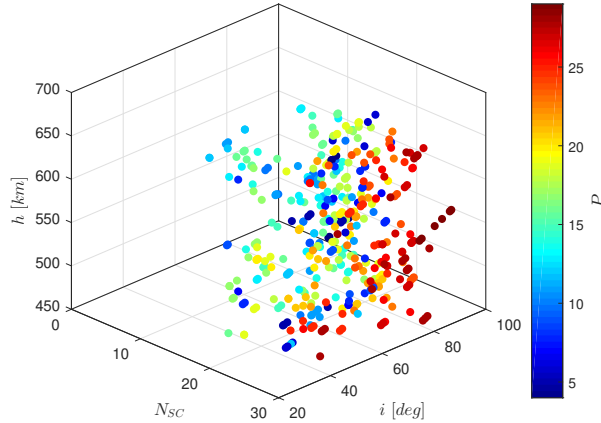
Figure 9.10: Pareto-front solutions for the generally inclined case

are 420 final individuals. This time the solutions are present from 10 satellites on, and, the concentration is higher after 15 satellites. Moreover, in terms of inclination, the higher concentration starts at 60°. For what concerns the altitude, we can not retrieve any particular behaviour, as the solutions are fairly distributed along the vertical axis.

9.2.1   Trade-off analysis

We immediately start by removing all the solutions that do not respect the coverage and revisit time requirements (exactly as we have done for the Sun-synchronous case). This operation reduces the number of solutions to 268. Figure 9.11a and Figure 9.11b show the dependence of the revisit time from the design variables. While, Figure 9.11c and Figure 9.11d show some properties of the constellations versus the design variables. Most of the solutions have a very good revisit time (Figure 9.11a) that increases sharply after 10 satellites (Figure 9.11b). There are interesting solutions with high number of satellites that have a low number of orbital planes with a very low revisit time (blue and light-blue dots in Figure 9.11b). Individuals with a high score in the revisit time are found at both low and high inclinations, we should prefer those at low inclinations as the launch cost is lower. Figure 9.11c show a property that has already been underlined in the Sun-synchronous case. Increasing the number of satellites increases the robustness of the constellation, while decreases the collision avoidance property. Figure 9.11d clearly shows that robustness and launch properties cannot be minimised at the same time, as if one increases the other decreases. This property has already been underlined in [62]. Figure 9.12 shows some of the most interesting constellation properties versus the optimisation variables, in particular the inclination that is the new variable with respect to the Sun-synchronous case.
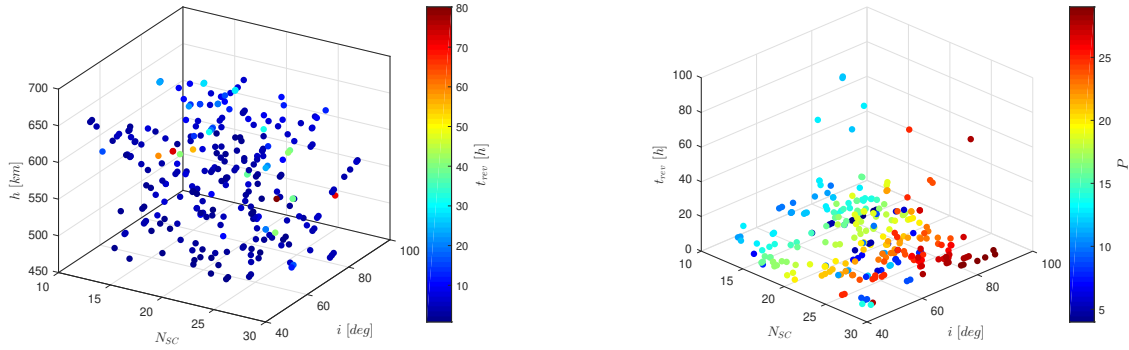
(a) Revisit time versus number of satellites, altitude and inclination

(b) Revisit time versus number of satellites, inclination and number of orbital planes
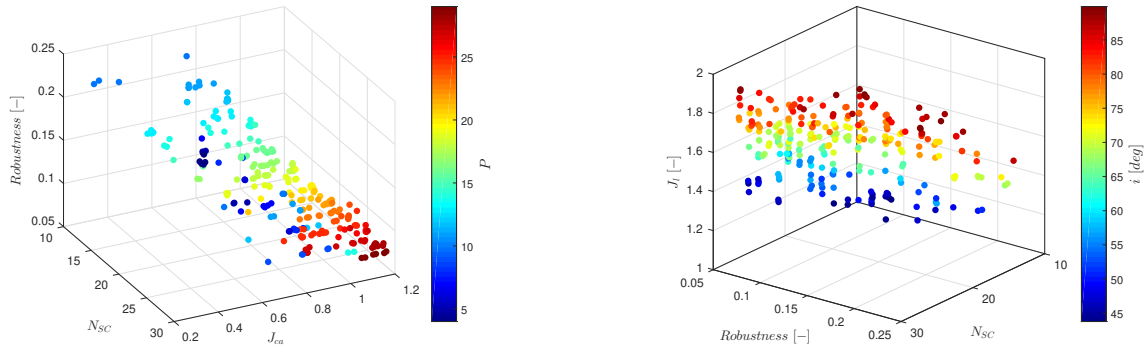
(c) J_{ca} and robustness versus number of satellites and orbital planes

(d) J_l and robustness versus number of satellites and inclination

Figure 9.11: Revisit time, robustness, J_{ca} and J_l, versus optimisation variables, generally inclined solutions

Figure 9.12a confirm that the inclination has no influence on the station-keeping and end-of-life properties. The behaviour of these two properties follow what described in [62]. There are few light-blue dots in the middle of the surface. These are good solutions as they do not have high station-keeping and end-of-life cost functions and the inclination is not too high as well. By looking at Figure 9.12b, we understand that the solutions we have previously underlined, fly at an altitude of about 550 km. In Figure 9.12c there are some interesting solutions near the origin. These individuals have good collision avoidance, station-keeping and end-of-life properties, due to the lower number of satellites. Moreover, these solutions have relatively low inclinations meaning that their launch property is good as well. Exactly as we have done in the Sun-synchronous case, we will proceed considering the two altitude ranges, one between 450 and 500 km and one between 550 and 600 km. Then, we will select at least one constellation per range. The solutions that lay in the two altitude ranges are 135. These are shown in Table 9.2 along with their cost functions scores.
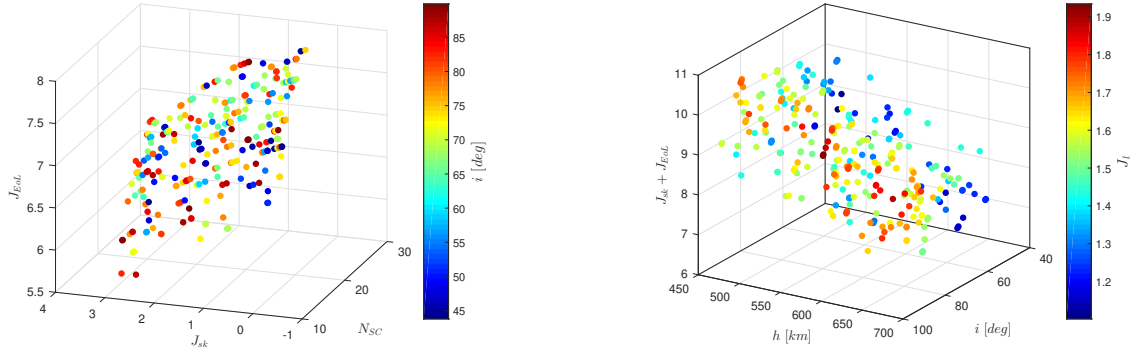
(a) J_{sk} and J_{EoL} versus number of satellites and inclination

(b) Sum of J_{sk} and J_{EoL} and, J_l versus altitude and inclination
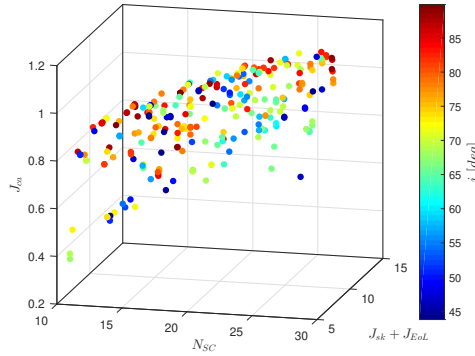
(c) J_{ca} and sum of J_{sk} and J_{EoL} versus number of satellites and inclination

Figure 9.12: Solutions properties versus optimisation variables, generally inclined solutions

N_{SC}	P	F	i [deg]	h [km]	t_{cov}	t_{rev} [h]	J_{rob}	J_{ca}	J_l	J_{sk}	J_{EoL}	t_{SAR}	†	‡
23	23	9	82.56	451.4	21.8	4.90	0.09	1.10	1.68	3.49	6.49	5.00	22	337
14	14	8	89.42	451.5	13.9	4.62	0.15	0.94	1.57	2.99	6.00	5.00	14	215
11	11	8	82.69	451.6	21.2	6.55	0.19	0.86	1.40	2.75	5.76	5.00	22	337
14	14	8	89.73	452.1	13.9	4.60	0.15	0.94	1.58	2.98	6.00	5.00	14	215
18	9	6	79.48	452.8	26.7	10.91	0.11	0.82	1.55	3.22	6.26	5.00	27	413
20	20	9	71.27	453.4	23.7	2.69	0.10	1.08	1.49	3.32	6.37	5.00	24	366
28	28	14	81.05	454.3	19.9	4.68	0.08	1.16	1.74	3.64	6.72	5.00	20	306
28	28	14	81.94	455.8	19.9	4.65	0.08	1.16	1.75	3.61	6.73	5.00	20	306
26	26	12	81.49	456.8	16.9	4.81	0.08	1.04	1.72	3.52	6.67	5.00	17	260
21	21	3	80.26	457.3	27.8	3.65	0.11	0.96	1.62	3.30	6.46	5.00	28	428
28	28	14	82.82	457.3	19.9	4.65	0.08	1.17	1.76	3.59	6.74	5.00	20	306
21	21	16	73.91	457.6	7.9	3.08	0.10	1.06	1.55	3.29	6.46	5.00	8	122
22	22	13	83.04	457.7	19.8	3.03	0.10	1.11	1.67	3.34	6.51	5.00	20	306
26	26	10	71.82	457.9	20.8	5.87	0.08	1.17	1.60	3.50	6.68	5.00	21	320

N_{SC}	P	F	$i\ [deg]$	$h\ [km]$	t_{cov}	$t_{rev}\ [h]$	J_{rob}	J_{ca}	J_l	J_{sk}	J_{EoL}	t_{SAR}	†	‡
21	21	16	74.38	458.4	6.9	2.80	0.10	1.06	1.55	3.28	6.47	5.00	8	122
14	14	2	77.32	460.4	26.7	4.32	0.15	0.83	1.44	2.84	6.08	5.00	27	412
18	18	15	64.59	461.3	20.8	3.32	0.11	1.04	1.38	3.08	6.34	5.00	21	319
20	5	3	65.65	462.3	25.6	3.46	0.10	0.78	1.44	3.17	6.45	5.00	26	395
27	27	12	67.51	462.8	19.8	12.33	0.08	0.87	1.57	3.46	6.76	5.00	20	304
25	25	12	57.01	463.0	19.1	2.88	0.08	1.14	1.42	3.38	6.68	5.00	20	303
22	11	5	53.60	463.6	29.5	1.45	0.09	0.84	1.33	3.24	6.56	5.00	30	454
14	14	11	86.67	463.8	9.9	5.61	0.15	0.95	1.55	2.78	6.11	5.00	10	153
14	14	11	86.76	464.0	9.9	5.57	0.15	0.95	1.55	2.78	6.11	5.00	10	153
27	27	12	68.41	464.6	19.8	16.73	0.08	0.89	1.58	3.43	6.77	5.00	20	304
25	25	12	57.90	464.6	19.1	3.09	0.08	1.15	1.43	3.35	6.70	5.00	20	303
12	12	11	71.21	465.4	18.8	4.41	0.17	0.89	1.31	2.60	5.97	5.00	19	289
23	23	6	67.84	465.7	25.7	3.95	0.09	1.08	1.52	3.25	6.62	5.00	26	395
12	12	11	71.66	466.1	18.8	4.59	0.17	0.89	1.32	2.59	5.97	5.00	19	289
20	10	6	55.10	466.5	22.7	1.76	0.10	0.95	1.31	3.09	6.49	5.00	23	348
12	12	11	72.18	466.9	18.8	4.42	0.17	0.89	1.33	2.58	5.98	5.00	19	289
24	12	9	66.58	467.0	21.7	2.42	0.09	0.69	1.52	3.27	6.67	5.00	22	334
18	18	8	66.16	468.0	16.8	2.51	0.11	0.91	1.41	2.96	6.40	5.00	17	258
22	11	6	57.21	468.4	29.6	1.69	0.09	0.97	1.38	3.16	6.60	5.00	30	454
10	10	8	86.87	468.5	20.8	5.88	0.22	0.76	1.43	2.37	5.81	5.00	21	321
18	18	14	78.20	470.5	12.8	4.04	0.12	0.95	1.55	2.92	6.42	5.00	13	198
20	20	4	85.71	471.4	24.8	7.85	0.10	1.04	1.68	3.01	6.53	5.00	26	397
20	20	4	86.60	472.9	24.8	7.78	0.10	1.03	1.69	2.99	6.54	5.00	26	397
17	17	4	63.93	473.4	26.6	3.18	0.12	0.95	1.36	2.82	6.38	5.00	27	409
22	22	7	80.02	474.5	21.8	20.16	0.09	1.11	1.65	3.06	6.65	5.00	22	335
16	16	9	78.51	477.1	18.8	9.35	0.13	1.00	1.52	2.69	6.35	5.00	19	289
25	25	11	45.97	480.3	18.9	1.34	0.08	0.91	1.30	3.09	6.82	5.00	20	301
19	19	15	87.84	480.8	11.9	3.95	0.11	0.98	1.69	2.80	6.55	5.00	12	183
15	15	10	84.53	481.0	12.9	4.37	0.14	0.92	1.57	2.56	6.32	5.00	13	198
16	8	7	44.28	481.1	23.6	1.65	0.13	0.75	1.12	2.63	6.38	5.00	24	361
13	13	10	56.87	481.1	10.8	4.60	0.16	0.82	1.19	2.42	6.17	5.00	11	166
25	25	9	57.98	481.3	20.0	4.35	0.08	0.98	1.44	3.07	6.83	5.00	21	317
25	25	11	46.86	481.4	18.9	1.22	0.08	0.90	1.31	3.07	6.83	5.00	20	301
24	24	13	88.21	481.4	15.9	3.09	0.10	1.14	1.78	3.03	6.79	5.00	16	244
13	13	10	57.32	481.7	10.8	4.90	0.16	0.82	1.19	2.41	6.18	5.00	11	166
21	21	16	53.49	482.7	13.8	1.45	0.10	1.00	1.33	2.87	6.67	5.00	14	211
14	7	5	47.06	483.6	22.6	1.81	0.15	0.73	1.10	2.45	6.27	5.00	23	346
22	22	8	75.81	483.8	22.8	4.65	0.09	1.08	1.61	2.90	6.72	5.00	23	349
26	26	14	71.24	483.9	19.8	2.56	0.08	1.13	1.62	3.07	6.89	5.00	20	303
21	21	12	50.62	484.1	17.0	1.13	0.10	1.01	1.29	2.85	6.68	5.00	18	271
18	18	15	50.16	484.4	18.7	1.48	0.11	1.04	1.23	2.69	6.52	5.00	19	286
22	22	14	53.80	484.6	14.1	1.22	0.09	1.09	1.35	2.89	6.73	5.00	15	226

N_{SC}	P	F	i [deg]	h [km]	t_{cov}	t_{rev} [h]	J_{rob}	J_{ca}	J_l	J_{sk}	J_{EoL}	t_{SAR}	†	‡
24	8	6	63.19	486.1	28.6	1.83	0.08	0.91	1.49	2.95	6.82	5.00	29	438
24	8	7	69.26	487.2	30.6	2.27	0.08	0.94	1.57	2.93	6.83	5.00	31	469
19	19	14	83.11	487.9	9.9	6.56	0.12	1.03	1.64	2.68	6.60	5.00	10	152
24	24	10	71.80	488.9	21.8	5.02	0.08	1.09	1.60	2.90	6.84	5.00	22	333
13	13	10	76.11	489.2	18.8	7.38	0.16	0.89	1.42	2.28	6.23	5.00	19	288
21	21	9	54.50	491.5	20.0	2.10	0.10	0.76	1.35	2.72	6.73	5.00	21	316
27	27	13	77.57	493.9	19.8	4.38	0.08	1.12	1.71	2.93	7.00	5.00	20	303
18	18	9	71.41	494.1	16.8	2.70	0.11	1.04	1.49	2.53	6.59	5.00	17	257
14	14	11	78.67	494.6	12.8	5.17	0.15	0.95	1.48	2.27	6.34	5.00	13	197
27	27	13	78.46	495.4	19.8	4.75	0.07	1.14	1.72	2.91	7.01	5.00	20	303
23	23	13	86.62	497.5	15.8	2.56	0.09	1.09	1.76	2.71	6.86	5.00	16	243
25	25	10	69.63	499.5	21.7	41.46	0.08	0.96	1.59	2.76	6.96	5.00	22	332
12	12	10	81.75	499.6	12.9	6.65	0.18	0.71	1.46	2.03	6.22	5.00	13	197
17	17	8	45.47	550.4	27.8	1.82	0.12	0.92	1.20	1.57	6.86	4.99	29	430
18	18	8	73.63	551.2	17.8	3.40	0.12	0.88	1.56	1.61	6.92	4.93	18	269
17	17	8	46.36	551.4	27.8	1.80	0.12	0.92	1.21	1.55	6.86	4.91	29	430
15	15	8	57.37	553.3	21.7	1.95	0.14	0.72	1.30	1.40	6.75	4.77	22	327
20	5	3	70.69	553.4	25.6	3.83	0.10	0.72	1.56	1.68	7.03	4.76	26	388
29	29	13	77.05	554.4	19.8	5.34	0.07	1.07	1.78	2.04	7.41	4.69	20	299
20	5	3	71.47	554.4	25.6	3.87	0.10	0.72	1.57	1.67	7.04	4.69	26	388
27	27	12	68.12	555.3	20.8	39.09	0.08	0.88	1.64	1.95	7.34	4.62	21	313
11	11	10	69.44	556.0	10.8	4.11	0.19	0.74	1.33	1.04	6.45	4.58	11	164
29	29	13	77.93	556.2	19.8	5.21	0.07	1.09	1.79	2.01	7.42	4.55	20	299
11	11	10	69.64	556.3	10.8	4.17	0.19	0.74	1.33	1.04	6.45	4.55	11	164
11	11	10	69.78	556.5	10.8	4.21	0.19	0.74	1.33	1.04	6.45	4.54	11	164
13	13	11	73.19	557.2	12.8	59.23	0.16	0.52	1.43	1.19	6.62	4.48	13	194
21	21	5	65.75	558.2	25.7	5.80	0.10	0.96	1.53	1.65	7.11	4.41	26	387
24	8	3	76.85	559.1	30.7	2.60	0.08	0.93	1.71	1.77	7.24	4.35	31	463
20	20	7	75.82	559.6	27.7	4.44	0.10	1.08	1.63	1.58	7.06	4.31	28	418
24	8	3	77.54	560.2	30.1	2.54	0.08	0.93	1.71	1.76	7.25	4.27	31	463
18	18	11	78.31	562.1	14.8	3.14	0.11	1.04	1.62	1.44	6.97	4.14	15	224
23	23	9	66.62	564.3	22.7	6.96	0.09	0.94	1.57	1.65	7.23	3.98	23	342
29	29	12	82.94	564.3	19.9	3.91	0.07	1.13	1.85	1.88	7.46	3.98	20	299
16	16	2	79.50	564.7	28.8	7.67	0.13	0.88	1.59	1.28	6.86	3.95	29	433
22	22	7	71.05	566.1	25.7	38.10	0.09	1.11	1.61	1.58	7.19	3.86	26	387
20	20	15	54.69	566.2	15.8	1.53	0.10	1.08	1.38	1.48	7.09	3.85	16	237
20	20	15	54.95	566.5	15.8	1.47	0.10	1.08	1.39	1.47	7.10	3.83	16	237
22	22	7	71.38	566.6	25.7	38.25	0.09	1.11	1.61	1.57	7.19	3.82	26	387
24	6	4	61.80	566.8	24.6	2.41	0.08	0.87	1.53	1.65	7.28	3.81	25	371
21	7	4	63.71	567.5	25.6	2.26	0.10	0.73	1.51	1.51	7.15	3.76	26	386
16	16	2	67.27	567.6	28.6	8.14	0.13	0.97	1.45	1.23	6.88	3.75	29	431
29	29	12	85.78	568.9	18.9	4.01	0.07	1.18	1.89	1.81	7.48	3.66	20	299

N_{SC}	P	F	i [deg]	h [km]	t_{cov}	t_{rev} [h]	J_{rob}	J_{ca}	J_l	J_{sk}	J_{EoL}	t_{SAR}	†	‡
15	15	10	64.86	569.2	12.8	3.74	0.14	0.82	1.40	1.14	6.82	3.65	13	193
24	12	3	66.15	569.2	26.7	2.32	0.08	1.00	1.59	1.61	7.29	3.65	27	401
19	19	13	81.10	569.7	12.8	2.97	0.11	0.88	1.68	1.37	7.06	3.61	13	194
27	9	7	48.11	572.2	25.6	0.99	0.08	0.97	1.42	1.68	7.42	3.45	26	384
21	21	10	51.82	572.3	22.0	1.28	0.10	1.05	1.37	1.43	7.17	3.44	23	340
27	9	7	49.00	573.2	25.6	0.86	0.08	0.97	1.43	1.67	7.43	3.38	26	384
29	29	13	88.78	573.9	15.9	6.15	0.07	1.14	1.93	1.73	7.50	3.34	20	299
21	7	4	83.75	574.0	25.7	3.09	0.10	0.84	1.75	1.40	7.18	3.33	26	388
13	13	5	76.57	574.6	25.7	5.34	0.16	0.76	1.48	0.92	6.70	3.29	26	387
21	7	5	74.64	574.6	23.7	3.15	0.10	0.87	1.64	1.39	7.18	3.29	24	357
29	29	12	89.36	574.8	15.9	3.37	0.07	1.19	1.93	1.71	7.50	3.28	20	299
14	14	11	86.26	576.4	13.9	6.32	0.15	0.95	1.63	0.96	6.78	3.18	14	209
18	18	16	78.63	576.5	17.8	3.73	0.12	0.78	1.63	1.21	7.03	3.17	18	268
22	22	6	78.79	576.8	26.8	5.83	0.10	1.10	1.71	1.41	7.24	3.15	27	402
20	20	10	88.96	578.1	15.9	3.46	0.10	1.07	1.79	1.29	7.15	3.07	16	239
11	11	5	78.13	578.5	24.7	7.63	0.19	0.77	1.44	0.69	6.55	3.05	25	372
14	14	11	87.28	581.8	10.9	6.49	0.15	0.95	1.64	0.88	6.80	2.84	12	179
18	18	12	75.63	581.8	20.8	3.79	0.12	0.88	1.60	1.13	7.06	2.84	21	312
22	22	6	75.89	582.2	27.7	6.19	0.10	1.05	1.68	1.32	7.26	2.82	28	416
10	10	8	68.20	582.9	21.7	5.50	0.21	0.34	1.29	0.52	6.47	2.77	22	326
24	24	9	80.84	584.4	23.8	41.73	0.09	1.14	1.77	1.37	7.35	2.68	24	357
10	10	8	69.21	584.4	21.7	5.63	0.21	0.36	1.31	0.50	6.48	2.68	22	326
16	16	4	78.59	584.9	28.8	4.95	0.13	0.99	1.59	0.96	6.95	2.65	29	431
24	24	9	81.73	585.8	23.8	39.63	0.09	1.14	1.78	1.35	7.36	2.60	24	357
16	16	4	73.75	586.5	23.8	4.42	0.13	0.92	1.54	0.93	6.96	2.56	24	356
21	7	2	62.00	587.0	26.6	2.49	0.10	0.83	1.50	1.20	7.23	2.53	27	399
23	23	6	70.86	590.2	25.7	4.29	0.09	1.04	1.64	1.24	7.34	2.34	26	385
22	11	7	69.65	590.9	29.7	2.88	0.10	0.94	1.61	1.18	7.29	2.30	30	444
21	7	2	65.19	591.5	26.6	2.99	0.10	0.85	1.54	1.13	7.25	2.27	27	399
16	8	6	73.83	592.5	26.6	4.38	0.13	0.86	1.54	0.84	6.98	2.21	27	400
23	23	12	55.93	593.3	14.1	1.96	0.09	1.09	1.47	1.19	7.35	2.16	15	221
25	25	7	60.34	593.4	22.7	2.06	0.08	0.90	1.55	1.27	7.43	2.16	24	354
25	25	7	61.18	594.8	22.7	2.45	0.09	0.91	1.56	1.25	7.44	2.08	24	354
28	28	11	48.10	596.1	22.0	1.49	0.07	1.20	1.45	1.34	7.56	2.01	23	338
25	25	10	65.02	596.3	20.7	24.11	0.08	1.01	1.61	1.23	7.44	2.00	21	310
25	25	10	65.92	597.6	20.7	21.16	0.08	1.00	1.62	1.20	7.45	1.93	21	310
17	17	8	48.16	598.1	27.8	2.91	0.12	0.93	1.27	0.81	7.07	1.90	29	426

Table 9.2: Generally inclined constellations between 450-500 km and 550-600 km. † = $k_{day2rep}$; ‡ = $k_{rev2rep}$. t_{cov} in days and t_{SAR} in minutes

During the trade-off, we will favour first the constellation with a low number of satellites, orbital planes, a low inclination and a good revisit time. Between 450 and 500 km, there are

a good number of solutions with a low number of satellites and a good revisit time. However, there is one in particular that appears to be a very good compromise. It is a constellation with 14 satellites over 7 orbital planes at 483 km altitude with an inclination of 47.06°(row 51 of Table 9.2). Despite the low inclination, this constellation has a very low revisit time, about 2 hours. The low inclination and the relatively small number of satellites and orbital planes produce good launch and collision avoidance properties. Station-keeping and end-of-life properties are good as well, due to the relatively high altitude, considering we are analysing the 450-500 range, and the low number of satellites. The only property that is not good is clearly the robustness. This constellation is shown in Figure 9.13 and Figure 9.14.   This constellation reaches the
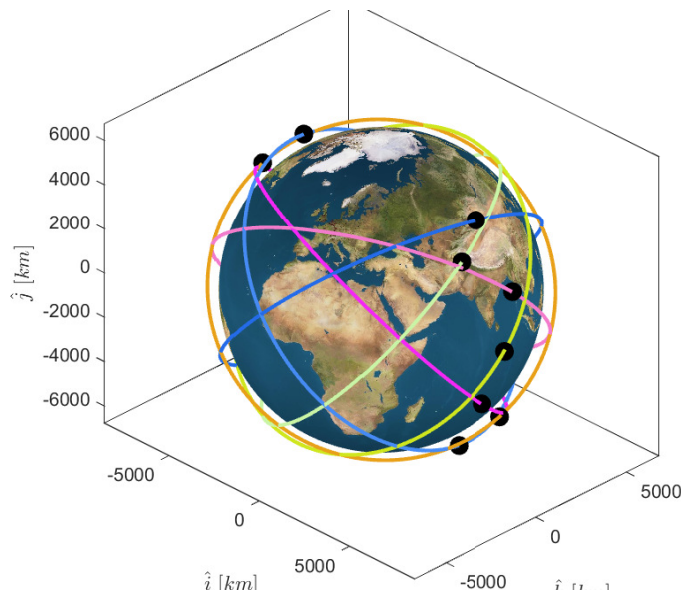
Figure 9.13: Orbits and satellites initial configuration for the 14 satellites constellation

coverage requirement in less than 5 days (Figure 9.14a). Moreover, it has a very uniform revisit time (Figure 9.14c). The number of acquisitions is relatively high, in particular in the central regions of Italy (Figure 9.14d). There are other interesting constellations, but all of them have either more satellites or more orbital planes than the one we have chosen. Therefore, we can suppose we have chosen the best constellation according to our requirements. We now move to the next range of altitude, between 550 and 600 km. There is a constellation with 10 satellites over 10 orbital planes at 68.2°of inclination and 582.9 km of altitude. This constellation has a revisit time of 5 hours and a half. Despite the low robustness, due to the relatively low number of satellites, it scores pretty well in all the other cost functions. Indeed, this constellation has very good collision avoidance and launch property, because of the low number of satellites and inclinations. For the same reason, it has also very good station-keeping and end-of-life properties. On the other side, it has 10 orbital planes, meaning that the build-up process might be a little bit slow. This constellation is shown in Figure 9.15 and Figure 9.16.   This constellation reaches the coverage requirements in about 5 days (Figure 9.16a). As the previous constellation, this one has a very uniform revisit time over the Italian territory (Figure 9.16c). Finally, it concentrates more acquisition over the southern regions (Figure 9.16d). There are also some other interesting constellations. One with 16 satellites over 8 planes at 73.83° and 592.5 km
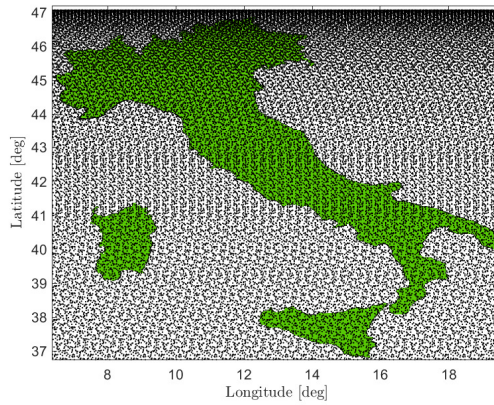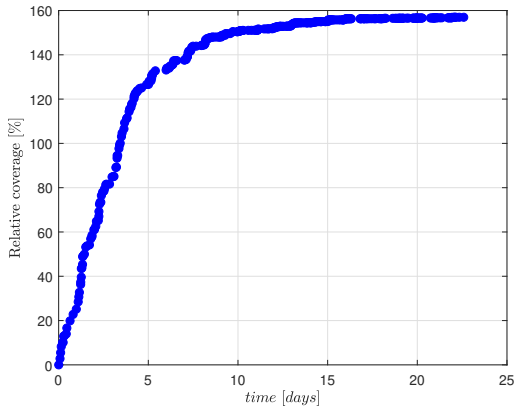
(a) Coverage evolution in time with respect to the coverage requirement

(b) Satellites ground tracks points within the Italian territory
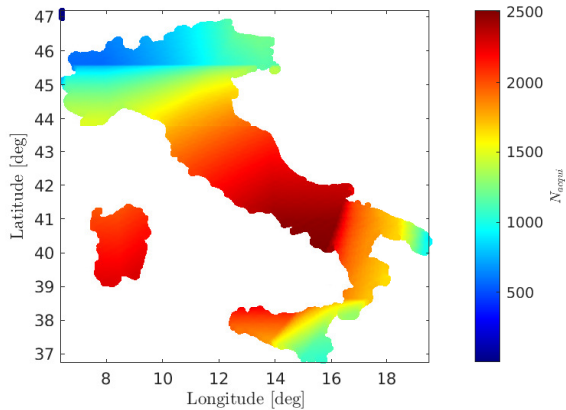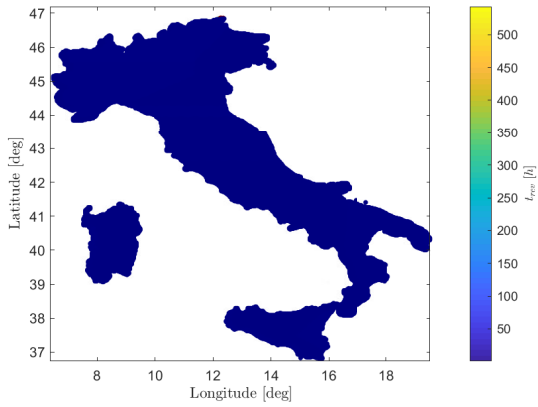
(c) Constellation revisit time within the Italian territory

(d) Number of acquisition per geographic area in the specific time span $k_{day2rep} = 23$ days

Figure 9.14: Possible constellation with 14 satellites

that has good revisit time (about 4.4 hours) and good launch, station-keeping and end-of-life properties. On the other side, it has a relatively high number of satellites and orbital planes and poor robustness and collision avoidance properties. One last possible constellation with a very good revisit time (about 3.8 hours), robustness, collision avoidance and build-up properties, has 20 satellites over 5 planes at 70.69° and 553.4 km. Finally, for the generally inclined case, we have found some interesting constellations. In particular, one with 14 satellites at 483 km altitude and 47.06° that has a very good revisit time and good launch, collision avoidance and build-up properties. In addition, one other constellation with 10 satellites at 587 km and 62° that scores very well in all the properties but robustness and build-up.
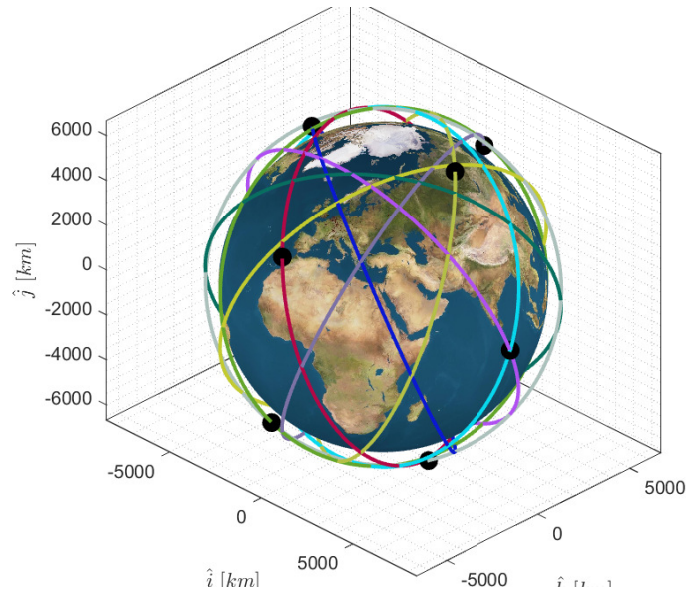
Figure 9.15: Orbits and satellites initial configuration for the 10 satellites constellation

9.3   Final constellations design

For the seek of clearness the four possible constellations we have found, where two of them are in Sun-synchronous orbits, are listed together with their main characteristics in Table 9.3. The performances of these constellations, in relation with the requirements of Table 6.2, are briefly shown in Table 9.4. Finally, the flowchart of Figure 9.17 recalls the process we have followed to find the four final constellations.

#1 (SSO)	Constellation Walker Delta	N_{SC} 6	P 3	P 1	i [deg] 97.32	h [km] 485.0	m_{SC} [kg] 200	J_{rob} 0.34	J_{ca} 0.33
	J_l 1.25	Δv [m/s] 490.1	m_{SAR} [kg] 90	A_{SAR} [m²] 3.856	θ_{min} [deg] 20	θ_{MAX} [deg] 60	t_{SAR} [min] 5	W_g [km] 22.9	Band X
#2 (SSO)	Constellation Walker Delta	N_{SC} 12	P 6	P 4	i [deg] 97.76	h [km] 599.0	m_{SC} [kg] 200	J_{rob} 0.18	J_{ca} 0.78
	J_l 1.70	Δv [m/s] 913.6	m_{SAR} [kg] 90	A_{SAR} [m²] 3.856	θ_{min} [deg] 20	θ_{MAX} [deg] 60	t_{SAR} [min] 1.85	W_g [km] 28.4	Band X
#3	Constellation Walker Delta	N_{SC} 14	P 7	P 5	i [deg] 47.06	h [km] 483.6	m_{SC} [kg] 200	J_{rob} 0.15	J_{ca} 0.73
	J_l 1.10	Δv [m/s] 1152	m_{SAR} [kg] 90	A_{SAR} [m²] 3.856	θ_{min} [deg] 20	θ_{MAX} [deg] 60	t_{SAR} [min] 5	W_g [km] 22.8	Band X
#4	Constellation Walker Delta	N_{SC} 10	P 10	P 8	i [deg] 68.20	h [km] 582.9	m_{SC} [kg] 200	J_{rob} 0.21	J_{ca} 0.34
	J_l 1.29	Δv [m/s] 738.4	m_{SAR} [kg] 90	A_{SAR} [m²] 3.856	θ_{min} [deg] 20	θ_{MAX} [deg] 60	t_{SAR} [min] 2.77	W_g [km] 27.6	Band X

Table 9.3: Final 4 constellations design along with main characteristics

	Coverage requirement	Spatial resolution [m]	t_{rev} average [h]	t_{rev} min [h]	t_{rev} max [days]	t_{cov} [days]
#1 (SSO)	Satisfied (157%)	3 x 3	12.49	8.4	1.01	8.9
#2 (SSO)	Satisfied (142%)	3 x 3	7.46	7.5	0.810	3.4
#3	Satisfied (157%)	3 x 3	1.81	0.83	22.5	19
#4	Satisfied (150%)	3 x 3	5.5	3.8	10.9	4.4

Table 9.4: Final 4 constellations main performances in relation with the use case requirements
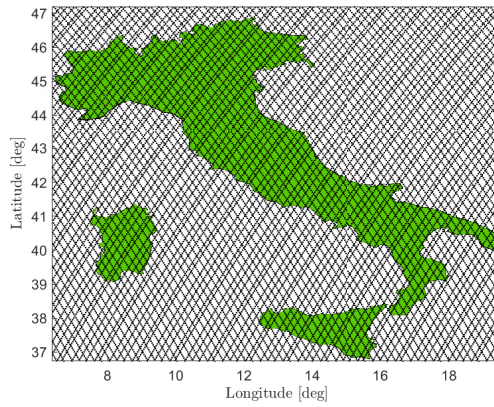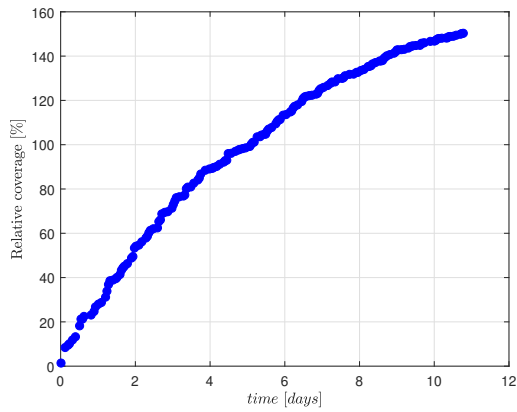
(a) Coverage evolution in time with respect to the coverage requirement

(b) Satellites ground tracks points within the Italian territory
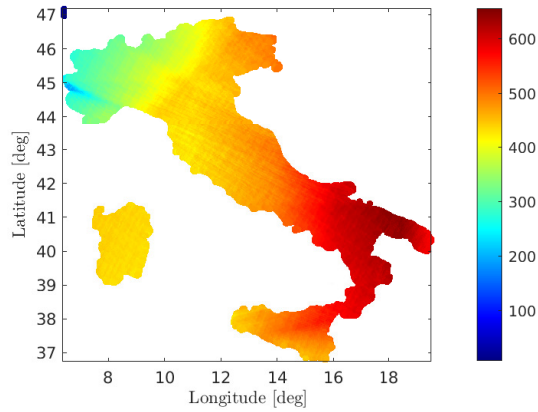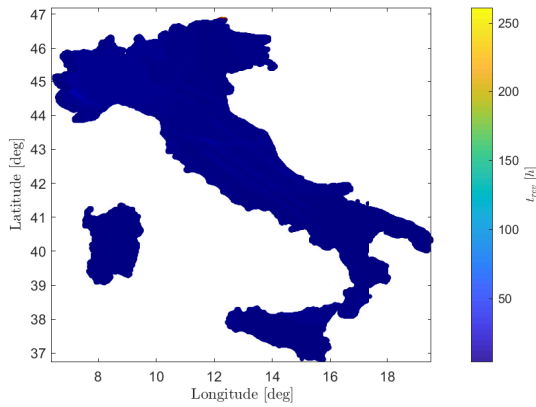
(c) Constellation revisit time within the Italian territory

(d) Number of acquisition per geographic area in the specific time span $k_{day2rep} = 22$ days

Figure 9.16: Possible constellation with 10 satellites
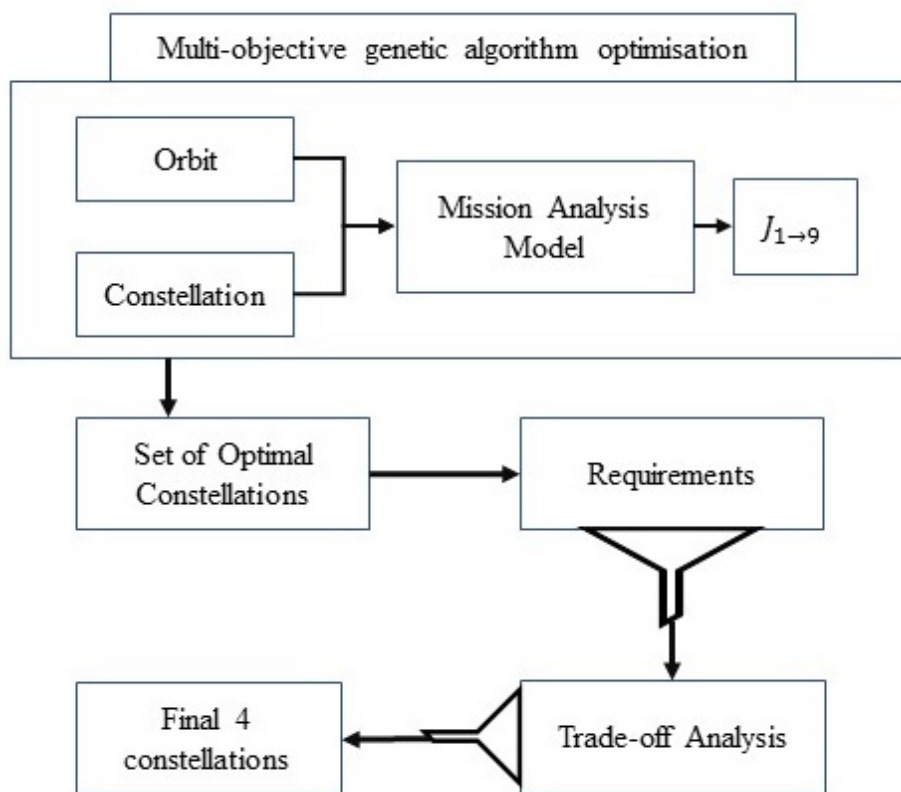
Figure 9.17: Schematic representation of the logical process used for the constellations design

Chapter 10

Economic, environmental and social profitability

10.1 General advantages

According to the Joint Research Centre [111], the first reason for precision agriculture adoption is its economic benefits. Moreover, the application of information technologies into PA methods optimises production efficiency, increase quality and minimise environmental impact and risk. It is stated that precision agriculture is seen as a way to help meet the measures defined in environmental legislation, as it reduces environmental degradation. Zarco et al. [111] sustain that the main cost types associated with PA are: information costs, cost involving data processing and learning costs. While, the potential benefits focus on: crop yield improvements, optimisation of inputs and improvement of the management and quality of the work. It was also underlined that when the field size is small or the farmer does not own the technology, specialist contractors may be suitable for the use of equipment among different farmers. The yield monitoring has been the first concept that gave rise to precision agriculture, thanks to its economic and environmental potential. The efficiency of VRT applications varies depending upon the crop, the geographic area, the field size and type of agriculture. However, its economic advantage ranges between 10 to 25 €/ha [111]. PA may also lead to changes in the mix of preventive and curative pesticide use, saving inputs and preserving the environment. Variable rate spraying by sensor controlled technology reduced insecticide use by 13% with an annual cost savings of 7.2 €/ha due to inputs reduction and 5 €/ha in machine cost [111]. Automatic guidance system offer several straightforward benefits, such as, profitability, work simplification and enabling working at any hour. The economic benefits of guiding systems is very variable (from 2 up to 45 €/ha), it consists in the reduction of overlapping (reduction of inputs) and higher yield. Schrijver et al. [94], described all the environmental advantages from precision agriculture. The most important are: reduction of carbon footprint, reduction of soil erosion, reduction of water and fertilizers outflow, water pollution prevention, reduction of excessive chemicals introduction into soil, reduction of emissions into air, reduction of water waste, reduction of plant protection products thanks to maps, improved nitrogen use. The reader can find additional confirmations of the advantages from precision agriculture at: [80], [57], [53], [89], [42], [11].

10.2   Italian case study

The need for a national constellation of satellites that provide free of charge data for agriculture is underlined by the fact that many farmers do not trust precision agriculture as they think it is not cost effective and initial set-up costs are too high [111]. As measured by the Italian Mipaaf in 2015 only 1% of the UAA was processed with precision agriculture technologies [8]. At that time the goal was to reach 10% by 2020. At the present that value has not been reached yet, however, is it was forecasted that 10% would be matched by the end of 2022. As it is not available the information about which level of precision agriculture is exploited by the farmers that represent that 10%, we make the safe assumption that those farmers are already using the highest level available and therefore no more improvements can be brought to their fields. In order to be more accurate, a survey, targeting all the farmers that make use of precision agriculture, about the technologies they are using, shall be conducted. Therefore, we are going to completely neglect the presence of that 10% of UAA on the forthcoming calculations. As the UAA was 12777044 ha in 2017, we subtract its 10% and we obtain 11499340 ha.

As a first very rough calculation we can simply take the total Italian UAA, 12777044 ha and multiply by a factor that represents an average profit from the employment of precision agriculture technologies. Frascarelli in [52] considers three different levels of precision agriculture, a basic plus strip-till level, an intermediate level and an advanced level. Considering constant yield those three levels brought a reduction in costs between 60 and 80 €/ha in the case of corn with respect to the case of traditional agriculture. Therefore, if we use the strong hypothesis that those values can be applied for any type of field size and any type of crop we just need to multiply the cost reduction for the total area harvested. It yields 689960400 € with 60 €/ha cost reduction and 919947200 € with 80 €/ha cost reduction. We stress again the fact that these values are obtained with the hypothesis of no yield increment and equal advantages for any field and crop types. So, we can appreciate that the two values are quite different from each other, this means that a more accurate approach shall be used, taking into account the different crop types, field sizes and PA technologies as much as possible.

We can start considering the differentiation of farms exposed in Chapter 4, this is again presented in Table 10.1 with some more useful details. For this first calculation, we take out the family business as one may agree that, that type of farm might not be immediately driven to choose precision agriculture technologies since profit is not their first goal. Then, we completely disregard the last column of Table 10.1. Furthermore, we remove 10% of UAA as stated before. As it is reasonable to assume that bigger sizes farms are the first to adopt new technologies and approaches, the 10% of the total UAA has been removed in the three classes 5-19.99, 20-99.99 and over 100 according to their relative incidence on the total UAA. The result is summarized in Table 10.2. Then, we consider the division of crop types in arable land, woody and shrub crops, permanent forage,-permanent grassland and pasture; as given in Chapter 4. We subtract the UAA employed by the family business and the 10% already processed with PA technologies from the three types of crops according to their relative abundance and finally obtain the three values shown in Table 10.3. Moreover, we can distribute the three crops types among the five UAA classes according to their relative incidence, as shown in Table 10.4. Chiodini in [14] summarizes the results obtained from the adoption of three different levels of precision agriculture: assisted driving, automatic driving and automatic driving plus yield map and site-specific

UAA Classes	Agricultural Enterprises				Enterprises with agricultural secondary activity				Agricultural enterprises active on occasion			
	Units	UAA	Units %	UAA %	Units	UAA	Units %	UAA %	Units	UAA	Units %	UAA %
Up to 0.99	57473	18249	13,9%	0,2%	25161	11501,1	29,1%	1,5%	144182	73947	26,2%	2,6%
1–4.99	106344	295754	25,7%	3,5%	36947	87845,1	42,7%	11,5%	274658	667493	49,9%	23,2%
5–19.99	145135	1544017	35,1%	18,5%	17469	170169	20,2%	22,2%	108789	995370	19,8%	34,6%
20–99.99	90282	3786450	21,8%	45,4%	5967	241387	6,9%	31,6%	20991	789487	3,8%	27,4%
100 and more	14102	2693128	3,4%	32,3%	1011	254116	1,2%	33,2%	1855	353737	0,3%	12,3%
Total	413336	8337598			86555	765018			550475	2880035		

UAA Classes	Family business (self-consumption)				Total			
	Units	UAA	Units %	UAA %	Units	UAA	Units %	UAA %
Up to 0.99	272806	123193	58,6%	15,5%	499622	226890	33,0%	1,8%
1–4.99	169701	334697	36,4%	42,1%	587650	1385789	38,8%	10,8%
5–19.99	19823	172066	4,3%	21,7%	291216	2881622	19,2%	22,6%
20–99.99	3182	117287	0,7%	14,8%	120422	4934611	7,9%	38,6%
100 and more	257	47151	0,1%	5,9%	17225	3348132	1,1%	26,2%
Total	465769	794393			1516135	12777044		

Table 10.1: Farms differentiation according to their size and economic type. Source: ISTAT. The table has been slitted in two parts just for reason of space

UAA Classes	UAA	Average UAA
Up to 0.99	103697.1	0.46
1–4.99	1051092.1	2.51
5–19.99	2283655	9.98
20–99.99	4391423	41.09
100 and more	2875080	194.54
Total	10704947	

Table 10.2: UAA and average UAA per classes of UAA. Source: ISTAT

	Arable land	Woody and shrub crops	Permanet forage-permanet grassland and pasture	Total
UAA	7150908	2292112	3334021	12777041
Relative UAA	55.97%	17.94%	26.09%	
Minus family business UAA	6886110	2027314	3069223	11982648
Minus 10%	6375029	1516233	2813682	10704947

Table 10.3: UAA per types of crops. Source: ISTAT

UAA Classes	Arable lands	Woody and shrub crops	Permanent forage-permanent grassland and pasture
Up to 0.99	58036	18603	27059
1–4.99	588263	188559	274270
5–19.99	1278090	409672	595893
20–99.99	2457741	787791	1145891
100 and more	1609092	515769	750219

Table 10.4: UAA per types of crops and UAA classes

Farm/Crop	Rice	Corn	Alfalfa
Small Farm	70	60	15
Big Farm	60	59	13

Table 10.5: Economic advantage €/ha from assisted driving. Source: [14]

treatments in the case of rice, corn, and alfalfa and, differentiating between small, big, regular, irregular filed and between small and big farm. For a detailed description of the analysis, please refer to [14]. The results for costs reduction and feasibility are listed in Tables 10.5, 10.6, 10.7 and 10.8.   In this first calculation, the data from the tables referring to [14] have been used as follow:

- UAA up to 0.99 has been considered as small farm with small and irregular field exploiting only automatic driving systems (values from Table 10.6)

- UAA in 1-4.99 has been considered as small farm with small and regular field exploiting only automatic driving systems (values from Table 10.6)

- UAA in 5-19.99 has been considered as big farm with big and irregular fields and divided into two parts, one exploiting only automatic driving (values from Table 10.6) and one

Farm/Crop	Field Size	Rice	Corn	Alfalfa
Small Farm	Small and Irregular	187	188	56
	Small and Regular	120	103	50
	Big and Irregular	135	122	51
	Big and Regular	98	74	48
Big Farm	Small and Irregular	183	183	49
	Small and Regular	96	98	43
	Big and Irregular	110	117	44
	Big and Regular	73	69	41

Table 10.6: Economic advantage €/ha from automatic driving. Source: [14]

Farm/Crop	Field Size	Rice	Corn	Alfalfa
Small Farm	Big and Irregular	162	195	60
	Big and Regular	126	148	56
Big Farm	Big and Irregular	187	190	52
	Big and Regular	149	143	49

Table 10.7: Economic advantage €/ha from automatic driving and yield maps. Source: [14]

Technology/Crop	Investment	Field	Farm Size [ha]		
			Rice	Corn	Alfalfa
Level 1	2000-4000	-	<10	10-20	20-30
Level 2	20k-40k	Smalland Irregular	20-30	20-40	50-100
		Small and Regular	20-40	20-60	75-100
		Big and Irregular	20-40	30-60	75-100
		Big and Regular	30-60	40-70	100-200
Level 3	30k-50k	Big and Irregular	30-40	30-40	75-100
		Big and Regular	30-50	30-60	75-100

Table 10.8: Field size limits for precision agriculture adoption. Level 1 refers to Table 10.5, Level 2 refers to Table 10.6 and Level 3 refers to Table 10.7. Source: [14]

  automatic driving and yield map (values from Table 10.7)

- UAA from 20 has been considered as big farm with big and regular fields exploiting automatic driving and yield map (values from Table 10.7)

Then, a cost reduction averaged between rice and corn was attributed to arable lands and the cost reduction for alfalfa was attributed to permanent forage-permanent grassland and pasture. A suitable value for woody and shrub crops is missing. Therefore, it has been used the value of 30 €/ha as suggested in [100] as an average economic advantage due to precision farming. This value is quite low compared with the others, but it allows us to remain on the safe side and do not overestimate the final profit. Finally, simply multiplying the field size for the cost reduction we can obtain the total cost reduction for this first approach. It is equal to about €1,057,500,000. This means that under the assumptions that were made (see above), adopting precision agriculture technologies would lead to a notional cost reduction of more than 1 billion Euro. However, this number relies on a few assumptions that can be relaxed while obtaining higher accuracy. This is the scope of the following calculations.
As a step forward we can consider the family businesses that have been neglected in the previous calculation. It is reasonable to assume that this type of farmers can adopt precision agriculture. They would not need to buy new tractors or special equipment since they might just pay the service providers, that owns the suitable machinery, for processing their crops. Ideally, the farmer freely downloads the data collected by the satellites, then she or he provides them to the company paid for fertilizing the fields by means of precision agriculture technologies.

UAA Classes	Agricultural Enterprises	Enterprises with agricultural secondary activity	Agricultural enterprises active on occasion	Family business (self-consumption)
Up to 0.99	50% small farm and 50% big farm, both with small and irregular field. Level 2 only	50% small farm and 50% big farm, both with small and irregular field. Level 2 only	50% small farm and 50% big farm, both with small and irregular field. Level 2 only	Small farm with small and irregular field. Level 2 only
1–4.99	50% small farm and 50% big farm, both with small and regular field. Level 2 only	50% small farm and 50% big farm, both with small and regular field. Level 2 only	50% small farm and 50% big farm, both with small and regular field. Level 2 only	Small farm with small and regular field. Level 2 only
5–19.99	50% small farm and 50% big farm, both with big and irregular filed. 50% level 2 and 50% level 3	50% small farm and 50% big farm, both with big and irregular filed. 50% level 2 and 50% level 3	50% small farm and 50% big farm, both with big and irregular filed. 50% level 2 and 50% level 3	Small farm with big and irregular field. 50% level 2 and 50% level 3
20–99.99	50% small farm and 50% big farm, both with big and regular filed. 50% level 2 and 50% level 3	50% small farm and 50% big farm, both with big and regular filed. 50% level 2 and 50% level 3	50% small farm and 50% big farm, both with big and regular filed. 50% level 2 and 50% level 3	Small farm with big and regular field. 50% level 2 and 50% level 3
100 and more	50% small farm and 50% big farm, both with big and regular filed. 50% level 2 and 50% level 3	50% small farm and 50% big farm, both with big and regular filed. 50% level 2 and 50% level 3	50% small farm and 50% big farm, both with big and regular filed. 50% level 2 and 50% level 3	Small farm with big and regular field. 50% level 2 and 50% level 3

Table 10.9: Distribution of economic advantages onto the UAA classes. For Levels definition see Table 10.8

UAA Classes	Agricultural Enterprises			Enterprises with agricultural secondary activity			Agricultural enterprises active on occasion			Family business (self-consumption)		
	Crop class 1	Crop class 2	Crop class 3	Crop class 1	Crop class 2	Crop class 3	Crop class 1	Crop class 2	Crop class 3	Crop class 1	Crop class 2	Crop class 3
Up to 0.99	Level 1	30	-	Level 1	30	-	Level 1	30	-	Level 1	30	-
	50% small farm and 50% big farm											
1–4.99	Level 1	30	-	Level 1	30	-	Level 1	30	-	Level 1	30	-
	50% small farm and 50% big farm											
5–19.99	Level 1	30	-	Level 1	30	-	Level 1	30	-	Level 1	30	-
	50% small farm and 50% big farm											
20–99.99	Level 2 and 3	30	Level 2 and 3	Level 2 and 3	30	Level 2 and 3	Level 2 and 3	30	Level 2 and 3	Level 2 and 3	30	Level 2 and 3
	Big and regular field. 50% level 2 and 50% level 3											
100 and more	Level 2 and 3	30	Level 2 and 3	Level 2 and 3	30	Level 2 and 3	Level 2 and 3	30	Level 2 and 3	Level 2 and 3	30	Level 2 and 3
	Big and regular field. 50% level 2 and 50% level 3											

Table 10.10: Distribution of economic advantages onto the UAA classes, third level of accuracy. For Levels definition see Table 10.8

Relying on the same assumption from the previous calculation but adding the fields owned by family businesses lead to a total cost reduction of about €1,134,000,000. It is slightly higher than the value found before as in terms of total UAA family businesses represent only the 6.22%.

As a third attempt to be more accurate we keep considering the family business and we apply a differentiation between UAA classes and the four types of enterprises stated in Table 10.1 while employing the costs reductions given by [14]. In order to be as much clear as possible the way the data from Tables 10.6 and 10.7 have been distributed is shown in Table 10.9. This approach leads to an economic advantage of about €1,012,900,000, slightly lower to the one of the previous calculation due to the better differentiation employed. We can repeat the same calculation excluding the family business category but this does not change too much the result that decreases to about 950 M€. As a last attempt to seek for the maximum possible accuracy we can introduce the data of Table 10.8 as well, meaning we consider the fact that a level of technology becomes profitable only after a certain field size. As before, the cost reduction theory applied is summarized in Table 10.10. Up to 20 ha only assisted driving can be used. From 20 ha on the fields are assumed to be big and regular in size and a joint between automatic driving and automatic driving plus yield map has been assumed. This subdivision leads to a cost reduction of about €775,237,000. The value is lower than the previous calculations as a

result of the assumption made and of the field size restriction in the application of technologies. If we instead suppose to assign each farm type and field type cost reduction belonging to level 2 and 3 to any UAA classes after 20 ha the total cost reduction increases to about €892,800,000. Just for clearness, the previous number was obtained using all the cost reductions from Table 10.6 and Table 10.7 averaged, in the case of arable crops and permanent forage-permanent grassland and pasture, irrespective of the farm business type. This might be a real case, as a big field may still be divided into several small fields with different crops. For woody and shrub crops the value of 30 €/ha was assumed, as explained above.

We can appreciate that the numbers obtained are very sensitive to the assumptions made. We can roughly estimate that the total cost reduction obtained by employing precision agriculture in Italy would be around 1 B€ per year, as shown in the previous calculations. However, it is not wrong to assume that this value may be actually even higher as we have made some conservative assumptions and luck some data. These key point that would lead to a higher final result are:

- constant yield was assumed, but in most cases, precision agriculture technologies lead to increasing yield and therefore a higher income

- the quality increase was neglected: even if the harvest does not increase the product quality is nonetheless higher thanks to precision agriculture processes; it is quite difficult to estimate the economic benefit brought by a higher quality as it is afflicted by many parameters but it stands that a higher quality comes with higher product price

- economic profit for each crop type (or at least the most common) lacks: we have assumed an average value between rice and corn for arable lands and an average generic value for woody and shrub crops but this leads to inaccuracies especially from the low value used for woody and shrub crops. Detailed tests for economic advantages brought by precision agriculture in most of the crop types should be carried out

- calculations rely on the limited farms' differentiation of Table 10.1 in 4 different business types and 5 UAA classes meanwhile information about fields shape is missing. A detailed farm differentiation with more UAA classes and considering the field shapes should be carried out

- restrictions, based on field size, in precision agriculture profitable adoption were considered, however, this limit shall be better assessed in order to understand that, even for small farms, is not profitable to adopt those technologies, in light of the fact that they might just rent the machinery without actually buying them

- data of profitability of precision agriculture from different sources may diverge quite a lot, this is reasonable considering the fact that it is quite impossible to define a unique revenue increase since it depends on too many variables. However, a list of profits for the most common crops and the different technologies used in precision agriculture would be useful

We have seen that at the time being it is not possible to draw an accurate economic advantage from the national adoption of precision agriculture, however, we have tried to estimate its order of magnitude in a reasonable manner. A tool that allows the farmer to compute her or his

revenue increase is available at *https://tool.pamcoba.eu/*, it is defined for a couple of crop types and it allows to select the level of precision agriculture technology from a suitable list.

As the attempts we have done in calculating the economic profit are quite influenced by the assumptions on the basis, we can try to compute the economic profit in specific cases where accurate data are available. We can analyse the input reduction brought by precision agriculture. In 2019 4345403 tonnes of fertilizer were distributed in the Italian fields. According to [98], precision agriculture can reduce the input amount by around 10%. This would save more than 400000 tons of fertilizer per year. Others [58] calculated the fertilizer reduction to be around 20%, with a cost reduction of 40 €/ha. This produces a cost reduction of more than 300 M€ considering the total area harvested, however, this value is overestimated as different crops require different amounts of fertilization. Wheat, on average, requires between 50 and 180 kg/ha of fertilizer. 3077543 ha are devoted to wheat cultivation in Italy, assuming average fertilization of 115 kg/ha and the reduction introduced from PA technologies of [98] leads to a total saving of about 39 tons per year. Fertilizers on average cost 1.04 €/kg, then, in the case of wheat, the saving would be equal to more than 41 M€ per year. The same approach can be exploited for plant protection products. In 2018, around 114395 tons of plant protection products have been used. The benefit forecasted by [98] leads to a reduction of more than 11000 tons per year. On average wheat requires around 0.5 kg/ha of plant protection products, while grapevine requires much more, about 25 kg/ha. In Italy, 793941 ha are devoted to wheat and 729835 ha for grapevine. These value combined with an input reduction of 10% from precision agriculture lead to a total saving of 40 tons of products per year in the case of wheat and 1824 tons per year in the case of grapevine. A similar method could be employed for water consumption. Every year, between 50 and 60 Bm^3 of water are consumed in Italy. A percentage between 60 and 70% of this total amount is devoted to agriculture and livestock. According to the last ISTAT report on water consumption [69], the 20.3% of the UAA was irrigated in 2015, about 2.5 Mha. This value may change year by year according to weather conditions. Approximately, 11.6 Bm^3 of water are used for agriculture [68]. According to [12] and [111] reductions from 20 up to 25% are achievable with precision agriculture in water consumption, with an average cost saving of 44 €/ha depending on water and electricity costs. This implies that the water reduction would be in the order of billions of m^3 and the cost reduction in the order of tens of millions. We can examine the specific example of industrial crops, rice and sugar beet. Industrial crops require 500 to 1000 litres of water per square metre. These crops cover 461865 ha of surface. With a 10% specific water reduction from PA suggested by [98], we can estimate a cut of about 36 Mm^3 for industrial crops water consumption. Rice requires 2300 l/kg and 1475512 tons were produced in 2018. In this case, the water-saving would be more than 300 Mm^3. Finally, sugar beet requires 175 l/kg, and 2201016 tons were produced in 2018. Precision agriculture would bring a water reduction of 38 m^3 for sugar beet production. It is clear that decreasing the usage of fertilizers, plant protection products and water does not carry with it only a cost reduction for farmers. The biggest benefit is the one brought to the environment which everyone can benefit from. Lower chemicals for crops production would decrease their amount in soil and aquifers and especially in the harvest. In turn, the food would be healthier and the soil would have higher regenerative capabilities, ensuring constant production in the long run. It is quite hard to estimate these secondary effects but their tremendous impact on everyone's life is more than clear.

Corn - PA level	Level 1	Level 2	Level 3	Level 4	Level 5
Increase in net income	125	295	396	134	298

Table 10.11: Level 1: Automatic guiding system, section control technique and VRT. Level 2: Minimum processing technique with automatic guiding system and section control technique. Level 3: Minimum processing technique with automatic guiding system, section control technique and VRT. Level 4: Strip tillage with automatic guiding system and section control technique. Level 5: Strip tillage with automatic guiding system and section control technique and VRT. All values in €/ha. Source:[90]

Wheat - PA level	Level 1	Level 2	Level 3
Increase in net income	34	66	253

Table 10.12: Level 1: Automatic guiding system and section control technique. Level 2: Automatic guiding system, section control technique and VRT. Level 3: Minimum processing technique with automatic guiding system, section control technique and VRT. All values in €/ha. Source: [90]

As the last step, we will try to estimate the economic benefits brought by precision agriculture in the case of three particular crops: rice, wheat and corn. For these calculations, we rely on an approach similar to the one used previously. In 2018 217195 hectares were cultivated with rice. The steps we are going to follow are: we neglect a 10% already processed with PA, consider the five UAA classes of Table 10.1, the cost reductions from three levels of precision agriculture given by [14] in Table 10.5, 10.6, 10.7 and the profitability threshold of Table 10.8. Then, averaging all the cost reduction for the five classes and taking into account the field size limits leads to a total cost cut for rice production of about 26.65 M€. This is not a perfect calculation as we lack some data, as stated above, but we can be quite sure that the order of magnitude is correct as all the possible cases have been taken into account equally. Moreover, it has to be stressed that the parameters used do not consider a plausible increase in the production and the resulting profit. Regarding corn, the approach is exactly the same. Corn covers 591206 hectares. For this crop, the economic advantage was calculated to be more than 57 M€. However, we can rely also on other available data. Kverneland group in [90] experimented with different levels of technology on a number of fields. Their results, in terms of increasing net income, are presented in Table 10.11 along with the technologies employed. By means of these new data, distributing them equally among the UAA classes, we can estimate the economic profitability for corn of about 124 M€ (still considering the field size thresholds), more than twice than before. The Kverneland group repeated the same tests for wheat, their results are shown in Table 10.12. In Italy, 1821725 ha are cultivated with wheat. Following the same steps as for corn, with the cost reductions from [98] we can estimate a profitability of about 144 M€; while with those from [90] we estimate 148 M€ of profitability. In this case, the two values are much closer than for corn. Concluding, we have tried to estimate the economic advantage that

can be obtained by introducing precision agriculture technologies in Italian agriculture. At the moment, these procedures are still not diffused. However, their benefits are getting more and more clear to everyone. It was not possible to draw the exact advantage for national agriculture as we lack specific data. Anyhow, we calculated its order of magnitude to be slightly lower than 1 B€ per year. Obviously, the earnings are much higher than the investments in most of the cases, especially considering the onset of new companies that offer precision agriculture services even for small farms. More specific calculations, for input reductions and specific crops, demonstrated the advantages and we can rely much more on them since exact test cases were employed. Moreover, strict assumptions were made, so that we can be sure that the values obtained are not an overestimation of the real ones. This information allow us to underline the need for accurate data, coming from different sources (e.g. satellites), that feed the system, as they are at the basis of the technologies exploited in precision agriculture.

Chapter 11

Conclusions and future developments

At the beginning of this work, we have seen the main role that agriculture plays in society. At the same time, we also stressed that agriculture needs to improve its production while decreasing its environmental footprint. We have presented precision agriculture as a possible solution as it leads to an increase of production and quality, a decrease of inputs (especially chemical) and, in general, a better and more sustainable management of the agricultural field and the crop. The importance of precision agriculture and its diffusion has been underlined by the EU in its Green Deal programme (especially in the context of the *From Farm to Fork* project) and by the Italian government with the document *Guidelines for the development of precision agriculture in Italy*. At this point, we have introduced the Synthetic Aperture Radar. This instrument produces valuable information that is used for decision making in the precision agriculture process. We have then deepened the powerful of SAR in agriculture applications, which is complementary with optical sensors. However, a SAR can operate any time and in any weather condition, granting the continuity of data, which cannot be garanteed by an optical sensor. The SAR is particularly suitable for being carried on a LEO satellite, that benefits from its high altitude (with respect to a plane or an UAV), its lack of continuous human piloting and its high recursive passages. We have then identified a constellation of SAR microsatellites as the object to be pursued, to design a system with high performance and a contained cost that may also be complementary to the constellations or single satellites that are already flying. Before moving to the actual design of the constellation, we have defined the requirements for the relative mission. This process was based on the analysis of the actual user needs, being Italian agriculture, and the actual offer of SAR products from other constellations (commercial and civilian). We have put particular attention to the technological limits of the current civilian satellites (such as Sentinel-1), and the economic limits of the current commercial constellations. The requirements were drawn to overcome these limitations and put the average Italian farmer (but even the smaller ones) in a position that she/he can access high quality and affordable SAR products. The affordability limits, of satellites' images for precision agriculture, has been already underlined in previous research ([100]) and it is one of the reasons that push for a constellation that produces images accessible to everyone. The requirements we have defined are reflected in the final constellation design. As a further step, and a central part of this work, we have implemented a model to simulate the operations of a SAR constellation and evaluate its performances. This model is based on two main blocks, an orbital and a SAR one. The

orbital block simply propagates the orbits of all the satellites of the constellation. The SAR block simulates the acquisition of the instrument in the Italian territory. The model outputs the coverage and the revisit time of the constellation. Its advantages it that we can control each input parameter and, at will, we can simply increase its accuracy. Then, still looking for the constellation that best fits our requirements, we have employed the multi-objective genetic algorithm optimisation. This method allowed us to reach a good solution in a relatively short time and analyse the constellation under several points of view, without going trhough all the possible constellation configurations. We have built an objective function that takes two sets of parameters, orbital and SAR parameters. This objective function makes use of the constellation model we have built and assess different properties of the constellation, defined according to another scientific research [62]. In the end, we had to choose between a set of possible solutions that resulted from the optimisation. Through a trade-off analysis, based on the properties of each constellation, we chose few possible constellations that respect the requirements we imposed and had a good evaluation of the properties we decided to prioritised, such as revisit time and the total number of satellites. We came up with few solutions for a Sun-synchronous constellation and a generally inclined constellation. Therefore, we had first defined the requirements based on the real use case and then we found some possible constellations trough an optimisation based on a mission analysis model that we tailored exactly for a LEO constellation of microsatellites with Synthetic Aperture Radar. This first analysis and design of a LEO constellation for the observation of the Italian territory (in this work applied to agriculture with precision farming as final user requirements) may become particularly useful in the forthcoming future. The Italian government may decide to start a similar programme of a constellation for observation, in optical and microwaves ranges, of the Italian territory due to its vast range of applications of national interest. In the end, we have tried to estimate the economic, social and environmental benefits that precision agriculture, based on satellite data, could bring. Our estimation, even if based on some approximations, underlined the profitability of this approach to agriculture, even for small farmers. However, an extremely accurate calculation appears very complicated, due to the lack of information and the huge variety of test cases. Favouring the spread and adoption of precision agriculture appears to be the best way to have an accurate measure of its economic and environmental advantaged for most of the cases.

Each of the four pillars of this work (requirements definition, the model for constellation analysis, results from optimisation and trade-off analysis and, the profitability of precision agriculture) are an initial analysis that can be deepened in the future. Requirements concerning other areas could be defined and in particular requirements concerning the particular features of the SAR and the accuracy of its products. The mission analysis model appears to be accurate enough for the objective of this work, however, it can easily be improved by taking into account other orbital perturbations for a more accurate propagation of the satellites orbits. The SAR model and the simulation of its acquisitions are based on a theoretical model that neglects some effects and technical features. Including them in the model would increase for sure the accuracy and allow to exploit all the capabilities of the instrument. However, it is a complex task that requires a broad knowledge of the instrument itself. More accurate validation of the model may lead to the definition of its parts that need to be improved first. The model has been built so that it can simply be adapted to other types of constellations. Then, a broaden

analysis would take into account not only the Walker-Delta constellation, but other configuration as well. According to the mission scenario, one may think to add optical sensors as well, and configure a mixed (optical and SAR) constellation. The optimisation could be improved as well. In particular, we relied on the general multi-objective genetic algorithm functions provided by MATLAB. One could define its functions that generate the next generation, though mutation and crossover, specifically tailored for the satellite constellation case. This might, at least, speed up the convergence process of the optimisation. Instead, we can assume that the objective function is accurate enough, as it is based on a specific research done at a higher level. Finally, we have already stressed out that the calculation of the profitability of precision agriculture needs more research that asses the advantages for several types of crops and test cases.

Appendix

Parameter	Acronym	Meaning	Band frequency
Leaf Area Index	LAI	Relates to the amount of light that can be intercepted by plants. It is used to predict photosynthetic primary production, evapotranspiration and for crop growth	X, L, C
Fraction of absorbed photo-synthetically active radiation	fAPAR	Relates to the primary productivity of photosynthesis, can also be used as an indicator of the state and evolution of the vegetation cover	visible
Normalized difference vegetation index	NDVI	Provides a measurement of crop health, recognizes crop health issues	red + nir
Soil Moisture	mv	Relates to plant growth and it is a primary factor in farm productivity	L, C, X
Plant Height	-	It is associated with growth form, position of the species in the vertical light gradient of the vegetation, competitive vigour, reproductive size, whole-plant fecundity, potential lifespan	C, L, S
Leaf relative Water Content	RWC	It is a measure of plant water status in terms of the physiological consequence of cellular water deficit	X, C, L
Stem Diameter	-	Correlates with the amount of wood in the stem of the tree, its total biomass or biomass of its parts or its competitive position in the forest	-
Row Orientation	-	Relates to the amount of light that can be intercepted by plants suppressing the growth of weed	L
Row Spacing	-	Relates to crop yield, weed growth, soil conditions, light interception and practical applications	X
Lodging	-	It is the collapse of the stalk of a plant or the entire plant, caused by high plant populations, high nitrogen fertilization, external factors	X
Surface Roughness	-	It is utilised in sediment and nutrient transport models, and surface water flow. Used in estimation of near-surface soil moisture and vegetation biomass	L, C, Ku

Crop growth rate	-	Relates with plant light absorption, water content, temperature and nutrient content. It can be used to predict crop yield	X, L, C
Fraction of vegetation cover	FVC	Quantifies the spatial extent of the vegetation, it is independent from the illumination direction and it is sensitive to the vegetation amount	red + nir
Canopy vigor	-	It is used to predict crop yield and to understand crop water need	red + nir
Vegetation Drought index	VDI	Quantifies drought severity, plant stress and relates to soil condition	infrared
Canopy chlorophyll content index	CCCI	It is a robust canopy nutrition control measure that enhances the process of precise fertilizer application	red + nir
Red-edge chlorophyll index	CIRedEdge	Prediction of chlorophyll amount in the plant	red + nir
Crop water stress index	CWSI	Usefull to monitoring and quantifying water stress as well as for irrigation scheduling	C, red + nir
Enhanced Vegetation Index	EVI	Sensitive to plant canopy differences like leaf area index, canopy structure, and plant phenology and stress	red + nir
Green Chlorophyll Index	GCI	It is used to estimate the content of leaf chlorophyll in plants, it reflects the physiological state of vegetation	visible
Nitrogen nutrition index	NNI	It is used for accurately diagnosing the in-season crop N status, estimation of grain yield, grain amylose and protein contents, crop N requirement, photosynthesis capacity, crop N partition, and N use	red + red-edge
Red-edge difference vegetation index	REDVI	It is affected by chlorophyll content, it is a slight alteration to the traditional NDVI and is adopted for use with high spectral resolution reflectance	red-edge
Red-edge inflection point	REIP	Relates to the level of nitrogen supply	red-edge
Ratio vegetation index	RVI	It is used for green biomass estimations and monitoring, it is very sensitive to vegetation and has a good correlation with plant biomass	red + nir
Soil-adjusted vegetation index	SAVI	It is used to correct NDVI for the influence of soil brightness in areas where vegetative cover is low	red + nir
Transformed chlorophyll absorption reflection index	TCARI	Indicates the relative abundance of chlorophyll, it is affected by the underlying soil reflecance, particularly in vegetation with a low LAI	visible

Wide Dynamic Range Vegetation Index	WDRVI	It enables a robust characterization of crop physiological and phenological characteristics	red + nir
Atmospherically Resistant Vegetation Index	ARVI	It is presently shown to have a dynamic range similar to NDVI's, but is on average less sensitive to atmospheric effects	visible + nir
Cellulose Absorption Index	CAI	Describes the average depth of the cellulose absorption feature, it is useful for quantifying plant litter cover	nir

Table 1: List of SAR and optical parameters for agriculture

Approximate net irrigation depths [mm]	Shallow rooting crops	Medium rooting crops	Deep rooting crops
Shallow and/or sandy soil	15	30	40
Loamy soil	20	40	60
Clayey soil	30	50	70
	vegetables, carrots, cucumber, onions	beans, beets, peas, soybeans, sugarbeet, tobacco, tomatoes	alfalfa, barley, cotton, grapes, maize, olives, sugarcane, wheat

Table 2: Approximate net irrigation depth for different crops and soils. Source: FAO

Italy	January	February	March	April	May	June
[mm] of rainfall	1165	1028.4	1171.9	1441.5	1303.9	1074.1
[mm/d] of rainfall	37.58	36.73	37.80	48.05	42.06	35.80
	July	August	September	October	November	December
[mm] of rainfall	823.2	987.2	1545.4	1809.8	1947	1579
[mm/d] of rainfall	26.55	31.85	51.51	58.38	64.90	50.94

Table 3: Average monthly and daily rainfall in Italy. Source: ISTAT

Crop	Crop water need (min) [mm/growing period]	Crop water need (max) [mm/growing period]	Crop water need (max) [mm/growing period]	Total growing period (min) [days]	Total growing period (max) [days]	Toral growing period (average) [days]	Growing period
Alfalfa	800	1600	1600	100	365	232.5	mar-oct
Barley/Oats/Wheat	450	650	650	120	150	135	nov-jul
Bean	300	500	500	95	110	102.5	may-aug
Cabbage	350	500	500	120	140	130	may-sep
Citrus	900	1200	1200	240	365	302.5	feb-nov
Cotton	700	1300	1300	180	195	187.5	apr-oct
Maize	500	800	800	125	180	152.5	apr-aug
Melon	400	600	600	120	160	140	apr-sep
Onion	350	550	550	150	210	180	mar-sep
Pea	350	500	500	90	100	95	apr-aug
Pepper	600	900	900	120	210	165	may-oct
Potato	500	700	700	105	145	125	feb-jun
Rice (paddy)	450	700	700	90	150	120	apr-sep
Sorghum/Millet	450	650	650	120	130	125	apr-aug
Soybean	450	700	700	135	150	142.5	apr-aug
Sugarbeet	550	750	750	160	230	195	oct-apr
Sunflower	600	1000	1000	125	130	127.5	apr-aug
Tomato	400	800	800	135	180	157.5	feb-jul

Table 4: List of crops and their irrigation needs. Source: FAO

	January	February	March	April	May	June	July	August	September	October	November	December	Average	Total
Piemonte	47.3	41.2	54.3	96.2	106.1	71.4	52.1	68.6	88.2	97.5	91.6	54.8	72.44	869.3
Valle d'Aosta	38.9	35.5	50.5	94.6	112.9	75.8	59.1	70.9	78.5	86	70.8	41.8	67.94	815.3
Lombardia	50.2	43.6	57.1	85.8	98.7	80.6	64.6	79.1	94.4	102	92.7	63.3	76,00	912.1
Veneto	45.4	41.2	57	81	90.6	92.9	73.6	86.2	92.9	99	86.8	66.2	76.06	912.8
Trentino Alto Adige	30.5	28.6	42.1	62.1	87.5	94.8	95.5	95.1	91.5	90.3	69.4	46.8	69.51	834.2
Friuli Venezia Giulia	55.5	50.9	73.7	94.5	103.4	104.8	88.7	104.2	120.7	115.5	108	84.5	92.03	1104.4
Liguria	61.6	49.2	57.4	95.8	78.3	53.3	33.8	49.2	95.4	116.7	112.1	80.5	73.6	883.3
Emilia Romagna	50.8	47.3	58.8	77.3	66.9	62.8	42.7	58.5	83.5	98.2	93.5	72.2	67.7	812.5
Toscana	57.3	53.9	58.1	73.5	62.7	51.6	32.8	47.2	89.7	108.3	112.3	84.5	69.32	831.9
Umbria	56	55.8	61.6	75.2	66.6	54.6	33.1	45	82.1	93.7	107.8	86	68.12	817.5
Marche	51.8	52.1	62.8	71.2	60.5	60.9	41.3	52	79.8	88	97.6	85.5	66.95	803.5
Lazio	71.7	68.7	67.6	78.8	59.2	42.5	28	36.6	77.1	104.1	128.7	100.8	71.98	863.8
Abruzzo	63.4	58.4	63.8	67	53	50.1	35.3	40.7	68.1	84.8	109.7	91.4	65.47	785.7
Molise	67.9	58.2	60.4	62.5	46.9	39.7	31.1	32.3	62.4	75.4	108	89.5	61.19	734.3
Campania	76.9	66.1	68.9	68.9	45.6	34.5	29	27.4	69.4	85	116.2	99.1	65.58	787
Basilicata	66.7	57.5	58.1	57.1	38.2	31.7	26.9	27.9	58	78.2	85.1	83.6	55.75	669
Calabria	88.8	75.1	75.7	56.8	37.7	20.1	19.8	22.3	62.8	88.9	108.9	111.4	64.02	768.3
Puglia	55.3	50	53.3	48.5	34	28	23.8	24.2	55.2	67.7	79.5	75.6	49.59	595.1
Sicilia	76.7	49.7	50.4	43.6	23.5	8.8	6.4	12.1	52.4	71.2	85.6	93.7	47.84	574.1
Sardegna	52.3	45.4	40.3	51.1	31.6	15.2	5.6	7.7	43.3	59.3	82.7	67.8	41.86	502.3
ITALY	1165	1028.4	1171.9	1441.5	1303.9	1074.1	823.2	987.2	1545.4	1809.8	1947	1579	1323.03	15876.4

Table 5: Average rainfall per month per region. All values in mm. Source: Mipaaf [51]

2018	Total surface [ha]	Total production [100 kg]	ton/ha	€/ton	Number of farms	UAA [ha]	Average UAA [ha]	Average revenue [€]	Average costs (70%) [€]
Piemonte									
Cereals	349724	26103569	7.46	222.85	25844	380245	14.71	24,473.6	17,131
Common wheat	77580	3375907	4.35	200.50	14857	86859	5.85	5,100.81	
Durum wheat	2613	85058	3.26	217.68	556	8186	14.72	10,432.5	
Rye	330	12208	3.70	210.00	92	184	2.00	1,553.75	
Barley	19730	927695	4.70	197.39	5362	16045	2.99	2,777.26	
Oats	554	15591	2.81	166.58	289	566	1.96	918.13	
Corn	134812	13684970	10.15	185.50	17851	146644	8.21	15,468.9	
Rice	110520	7848670	7.10	382.33	1948	115943	59.52	161,602	
Valle d'Aosta									
Cereals	1435	181000	12.61	282.49	244		0.15	539.60	377.7
Common wheat	32	1920	6.00	282.49	12	3	0.25	423.73	
Durum wheat	6	230	3.83	200.50	12	2	0.17	128.10	
Rye	6	230	3.83	210.00	12	1	0.08	67.08	
Barley	150	33000	22.00	550.00	208	22	0.11	1,279.81	
Oats	470	48600	10.34	166.58					
Corn	470	29000	6.17	185.50					
Rice	301	68020	22.60	382.33					
Liguria									
Cereals	51343	5764023	11.23	194.46	637	665	1.04	2,279.11	1,595.37
Common wheat	163	4430	2.72	200.50	165	264	1.60	871.87	
Barley	91	1837	2.02	197.39	60	176	2.93	1,168.84	
Corn	50406	5717229	11.34	185.50	298	72	0.24	508.35	

139

Lombardia

Cereals	334020	28772336	8.61	222.85	22271	401707	18.04	34,625.2	24,237
Common wheat	58761	3205559	5.46	200.50	9018	65965	7.31	8,000.78	
Durum wheat	17459	903960	5.18	217.68	3365	28336	8.42	9,490.78	
Rye	296	10369	3.50	210.00	92	343	3.73	2,742.65	
Barley	22448	1210093	5.39	197.39	3522	22435	6.37	6,778.02	
Oats	240	8559	3.57	166.58	107	911	8.51	5,057.89	
Corn	138642	17080029	12.32	185.50	15154	171070	11.29	25,797.9	
Rice	92862	6137517	6.61	382.33	2096	98823	47.15	119,140	

Veneto

	132883	8413645	6.33	222.85	40790	311854	7.65	10,787.8	7,551
Cereals	95018	6123640	6.44	200.50	17792	94869	5.33	6,889.98	
Common wheat	16169	974305	6.03	217.68	3249	22678	6.98	9,155.57	
Durum wheat	62	2635	4.25	210.00	18	243	13.50	12,048.7	
Rye	16857	1006521	5.97	197.39	3980	40261	10.12	11,922.5	
Barley	184	8124	4.42	166.58	13	19	1.46	1,074.94	
Oats	1329	112570	8.47	185.50	27857	141995	5.10	8,009.04	
Corn	3248	184946	5.69	382.33	206	6518	31.64	68,883.3	
Rice	3339	180843	5.42						

Friuli-Venezia Giulia

Cereals	159600	15686101	9.83	193.53	10327	83149	8.05	15,314.8	10,720
Common wheat	13030	595246	4.57	200.50	2215	13038	5.89	5,391.43	
Durum wheat	397	19156	4.83	217.68	2215	13038	5.89	6,182.59	
Barley	6170	293227	4.75	197.39	2173	8861	4.08	3,825.31	
Oats	21	885	4.21	166.58	27	145	5.37	3,770.08	
Corn	136955	14558694	10.63	185.50	8854	57430	6.49	12,790.5	

	Trentino Alto Adige								
Cereals	586	25525	4.36	196.28	770	595	0.77	660.63	462.44
Common wheat	67	2680	4.00	200.50	178	153	0.86	689.36	
Durum wheat	7	210	3.00	217.68	43	15	0.35	227.80	
Rye	60	2400	4.00	210.00	112	105	0.94	787.50	
Barley	76	2740	3.61	197.39	66	39	0.59	420.52	
Oats	16	510	3.19	166.58	39	15	0.38	204.22	
Corn	305	15325	5.02	185.50	383	262	0.68	637.60	

	Emilia-Romagna								
Cereals	319260	22149262	6.94	222.85	31939	382203	11.97	18,501.5	12,951
Common wheat	137000	8560105	6.25	200.50	19719	142180	7.21	9,032.89	
Durum wheat	72124	4126632	5.72	217.68	9631	95264	9.89	12,319.4	
Rye	324	11508	3.55	210.00	112	335	2.99	2,231.01	
Barley	21287	1077925	5.06	197.39	4963	20459	4.12	4,120.40	
Oats	336	11306	3.36	166.58	301	1028	3.42	1,914.34	
Corn	57170	5879240	10.28	185.50	8684	75073	8.64	16,491.5	
Rice	6325	339133	5.36	382.33	217	7082	32.64	66,902.7	

	Toscana								
Cereals	156174	5469318	3.50	222.85	13007	165244	12.70	9,915.03	6,940
Common wheat	30638	1069425	3.49	200.50	3727	26134	7.01	4,907.39	
Durum wheat	66413	2117155	3.19	217.68	6360	79968	12.57	8,725.24	
Rye	152	3162	2.08	210.00	15	494	32.93	14,387.1	
Barley	22540	612871	2.72	197.39	3621	17868	4.93	2,648.43	
Oats	14849	381729	2.57	166.58	1944	15604	8.03	3,437.32	
Corn	11463	956897	8.35	185.50	2461	9543	3.88	6,004.60	
Rice	204	10239	5.02	382.33	8	389	48.63	93,309.3	

	Umbria								
Cereals	88940	4739545	5.33	197.65	13237	92944	7.02	7,395.45	5,177
Common wheat	27300	1433200	5.25	200.50	6548	31688	4.84	5,093.83	
Durum wheat	24200	1086000	4.49	225.92	2885	24846	8.61	8,731.32	
Rye	120	4500	3.75	210.00	87	84	0.97	760.34	
Barley	19200	912000	4.75	197.39	6217	20254	3.26	3,054.56	
Oats	1620	51340	3.17	166.58	1042	2769	2.66	1,402.87	
Corn	12000	1070000	8.92	185.50	2700	6792	2.52	4,160.83	

	Marche								
Cereals	152203	6589805	4.33	195.18	23580	185171	7.85	6,636.05	4,645
Common wheat	13946	686691	4.92	200.50	2105	7618	3.62	3,572.85	
Durum wheat	109850	4587977	4.18	225.92	16688	136591	8.18	7,723.14	
Barley	16564	732461	4.42	197.39	9000	22942	2.55	2,225.02	
Oats	816	23742	2.91	166.58	364	2067	5.68	2,752.26	
Corn	5394	370057	6.86	185.50	1871	4068	2.17	2,767.00	

	Lazio								
Cereals	84096	3925790	4.67	197.65	15748	110596	7.02	6,479.76	4,536
Common wheat	13480	566600	4.20	200.50	5601	14263	2.55	2,146.08	
Durum wheat	39500	1379000	3.49	225.92	4820	51642	10.71	8,450.41	
Rye	207	5730	2.77	210.00	544	1073	1.97	1,146.58	
Barley	15180	581150	3.83	197.39	5912	18855	3.19	2,410.09	
Oats	1780	48600	2.73	166.58	2051	6305	3.07	1,398.17	
Corn	13240	1322900	9.99	185.50	3758	9567	2.55	4,718.48	

	Abruzzo								
Cereals	89914	3528806	3.92	197.65	15566	69469	4.46	3,461.85	2,423

Common wheat	22605	863020	3.82	200.50	5918	14939	2.52	1,932.31
Durum wheat	34345	1197740	3.49	225.92	6779	32277	4.76	3,751.30
Rye	195	5900	3.03	210.00	3	376	125.33	79,634.8
Barley	20375	714750	3.51	197.39	7205	16051	2.23	1,542.59
Oats	3593	69100	1.92	166.58	1009	1831	1.81	581.35
Corn	7681	634296	8.26	185.50	1845	3396	1.84	2,819.61

Molise								
Cereals	68520	2393320	3.49	197.65	15609	92653	5.94	4,097.90	2,868
Common wheat	3600	134600	3.74	200.50	1626	6249	3.84	2,881.02
Durum wheat	60000	2070000	3.45	225.92	12330	60765	4.93	3,841.18
Rye	20	420	2.10	210.00	102	1937	18.99	8,374.68
Barley	1650	68700	4.16	197.39	4179	10420	2.49	2,049.24
Oats	1450	38000	2.62	166.58	4069	9933	2.44	1,065.69
Corn	1500	70000	4.67	185.50	492	987	2.01	1,736.61

Campania								
Cereals	111405	4314519	3.87	197.65	30141	104424	3.46	2,651.94	1,856
Common wheat	17078	599462	3.51	200.50	10485	17137	1.63	1,150.28
Durum wheat	56499	1869168	3.31	225.92	14243	44981	3.16	2,360.42
Rye	85	2300	2.71	210.00	13	5	0.38	218.55
Barley	13154	469429	3.57	197.39	10106	13288	1.31	926.23
Oats	10266	328745	3.20	166.58	10636	18623	1.75	934.01
Corn	13888	1031490	7.43	185.50	5852	7957	1.36	1,873.33

Puglia								
Cereals	415321	11538550	2.78	195.18	51279	436747	8.52	4,618.37	3,232
Common wheat	15300	365000	2.39	200.50	1551	10102	6.51	3,115.38
Durum wheat	345500	9901000	2.87	225.92	44645	348026	7.80	5,046.90

Barley	22700	544700	2.40	197.39	6157	28623	4.65	2,201.93	
Oats	24850	536400	2.16	166.58	7840	32423	4.14	1,487.04	
Corn	840	66800	7.95	185.50	53	177	3.34	4,926.50	

Basilicata									
	159945	4337605	2.71	197.65	23481	204364	8.70	4,665.09	3,265
Cereals	6998	183586	2.62	200.50	3192	9851	3.09	1,623.29	
Common wheat	115707	3307247	2.86	225.92	18217	140877	7.73	4,993.73	
Durum wheat	278	5456	1.96	210.00	112	79	0.71	290.71	
Rye	17310	411991	2.38	197.39	6548	25742	3.93	1,846.93	
Barley	17200	333192	1.94	166.58	5794	24469	4.22	1,362.78	
Oats	825	38792	4.70	185.50	714	894	1.25	1,092.12	

Calabria									
Cereals	64613	1868633	2.89	224.03	22570	77619	3.44	2,228.18	1,559
Common wheat	10269	302511	2.95	200.50	5013	8817	1.76	1,038.84	
Durum wheat	23916	666371	2.79	225.92	8669	28266	3.26	2,052.47	
Rye	1354	39050	2.88	210.00	85	368	4.33	2,622.11	
Barley	7805	209820	2.69	197.39	6190	15938	2.57	1,366.29	
Oats	12817	308528	2.41	166.58	5713	14465	2.53	1,015.28	
Corn	4259	197240	4.63	185.50	987	3571	3.62	3,108.16	
Rice	629	27249	4.33	382.33	6	676	112.67	186,609	

Sicilia									
Cereals	289057	8035539	2.78	195.18	45755	301460	6.59	3,574.81	2,502
Common wheat	400	10100	2.53	200.50	402	2324	5.78	2,926.75	
Durum wheat	273025	7591250	2.78	225.92	41513	254005	6.12	3,843.47	
Barley	5055	134870	2.67	197.39	5666	23684	4.18	2,201.39	
Barley	5500	132400	2.41	166.58	2933	11543	3.94	1,578.17	
Oats	188	14500	7.71	185.50	20	36	1.80	2,575.29	

	Sardegna								
Cereals	51165	1396658	2.73	226.37	12300	132674	10.79	6,665.25	4,666
Common wheat	85	2373	2.79	200.50	92	1023	11.12	6,224.16	
Durum wheat	20684	581608	2.81	225.92	6045	44318	7.33	4,657.30	
Barley	14289	309382	2.17	197.39	5682	35243	6.20	2,650.88	
Barley	11361	182334	1.60	166.58	5198	36594	7.04	1,882.12	
Oats	1504	115653	7.69	185.50	181	2094	11.57	16,502.5	
Rice	3238	205218	6.34	382.33	95	5721	60.22	145,923	

Table 6: Cereal production and revenue per region

Bibliography

[1]   European Global Navigation Satellite Systems Agency. *Report on agriculture user needs and requirements - Outcome of the European GNSS' user consultation platform.* 2019. URL: https://www.gsc-europa.eu/sites/default/files/sites/all/files/Report_on_User_Needs_and_Requirements_Agriculture.pdf.

[2]   European Space Agency. *TalkingFields - Demonstration Project on Services for Precision Farming.* 2014. URL: http://esa-sen4cap.org/ (visited on 05/25/2020).

[3]   European Space Agency. *FruitLook - Services to Improve Water Use Efficiency of Vineyards and Deciduous Fruit orchards in South Africa.* 2020. URL: https://business.esa.int/projects/fruitlook (visited on 05/25/2020).

[4]   AGI. *System Tool Kit (STK).* URL: https://www.agi.com/products/stk (visited on 04/05/2021).

[5]   Agrocares. *What is the difference between precision, digital and smart farming?* 2017. URL: https://www.eugenius-asso.eu/about1.html# (visited on 05/25/2020).

[6]   Mangimi & Alimenti. *Grano, Russia e Ucraina verso una stretta delle esportazioni?* 2020. URL: https://mangimiealimenti.it/articoli/3031-grano-russia-e-ucraina-verso-una-stretta-delle-esportazioni (visited on 05/20/2020).

[7]   Clement Atzberger. "Advances in remote sensing of agriculture: Context description, existing operational monitoring systems and major information needs". In: *Remote sensing* 5.2 (2013), pp. 949–981.

[8]   G Blasi et al. "Linee guida per lo sviluppo dell'agricoltura di precisione in Italia". In: *Rome, ITALY* (2017).

[9]   Dan G Blumberg. "High resolution X-band SAR imagery for precise agriculture and crop monitoring". In: *Proc. 3rd Int. Workshop Sci. Appl. SAR Polarimetry Polarimetric Interferometry.* 2007.

[10]   L Busetto et al. *USING SATELLITE MAPS TO SUPPORT VARIABLE RATE FERTILISATION.* 2016. URL: http://www.nereus-regions.eu/copernicus4regions/user-%20stories-sheets/ (visited on 12/28/2020).

[11]   Tacy Callies. *Advantages Of Precision Agriculture.* 2008. URL: https://www.growingproduce.com/citrus/advantages-of-precision-agriculture/ (visited on 03/25/2021).

[12]   Micaela Cappellini. "Allarme siccitÃ in Italia: mai cosÃ¬ poca acqua negli ultimi sessant'anni". In: *Il Sole 24 Ore, Economia* (2020).

[13]   Yee Kit Chan and Voon Chet Koo. "An introduction to synthetic aperture radar (SAR)".
        In: *Progress In Electromagnetics Research* 2 (2008), pp. 27–60.

[14]   Gabriele Chiodini. *Cerealicoltura tra agricoltura di precisione e digitale*. URL: `https:
        //www.cesarweb.com/wp-content/uploads/2018/03/3_Agricoltura-precisione_
        Chiodini.compressed.pdf` (visited on 03/25/2021).

[15]   COLDIRETTI. *Clima, in Italia solo il 7 dei gas serra viene dall'agricoltura*. 2020. URL:
        `https://www.coldiretti.it/ambiente-e-sviluppo-%20sostenibile/clima-
        in-italia-solo-il-7-dei-gas-serra-viene-%20dallagricoltura` (visited on
        12/18/2020).

[16]   European Commission. *EU Green Deal: benefits for farmers*. 2020. URL: `file:///C:
        /Users/vittorio/AppData/Local/Temp/factsheet_benefits_farmers_en.pdf.pdf`
        (visited on 03/14/2020).

[17]   European Commission. "Farm to fork strategy: for a fair, healthy and environmentally-
        friendly food system". In: *DG SANTE/Unit "Food information and composition, food
        waste"* (2020).

[18]   European Commission. *The aommon agricultural policy at a glance*. 2020. URL: `https://
        ec.europa.eu/info/food-farming-fisheries/key-policies/common-agricultural-
        policy/cap-glance_en` (visited on 03/18/2021).

[19]   Centro di ricerca Politiche e Bioeconomia CREA. *L AGRICOLTURA ITALIANA CONTA
        2019*. 2020. URL: `https://www.crea.gov.it/documents/68457/0/ITACONTA_2019%
        20_def_WEB+%281%29.pdf/897ebbdf-e266-6b0e-7ca5-%200e74cf348b41?t=
        1579706396164`.

[20]   Howard D Curtis. *Orbital mechanics for engineering students*. Butterworth-Heinemann,
        2013.

[21]   M Davidson et al. *Copernicus L-band SAR Mission Requirements Document*. 2019.

[22]   Group on Eath Observation. *GEO Home FAQ*. 2020. URL: `https://www.earthobservations.
        org/index.php` (visited on 06/10/2020).

[23]   EO4AGRI. *EO4AGRI ABout the project*. 2020. URL: `https://eo4agri.eu/node/3`
        (visited on 03/18/2021).

[24]   ESA. *Capella X-SAR (Synthetic Aperture Radar) Constellation*. 2020. URL: `https:
        //directory.eoportal.org/web/eoportal/satellite-missions/c-missions/
        capella-x-sar` (visited on 09/11/2020).

[25]   ESA. *Copernicus High Priority Candidates: ROSE-L*. 2020. URL: `https://www.esa.
        int/Applications/Observing_the_Earth/Copernicus/Copernicus_High_Priority_
        Candidates` (visited on 09/11/2020).

[26]   ESA. *eoPortal Directory: ALOS-2 (Advanced Land Observing Satellite-2; SAR mis-
        sion) / Daichi-2*. 2020. URL: `https://directory.eoportal.org/web/eoportal/
        satellite-missions/a/alos-2` (visited on 07/11/2020).

[27] ESA. *eoPortal Directory: Copernicus.* 2020. URL: https://directory.eoportal.org/web/eoportal/satellite-missions/c-missions/copernicus (visited on 07/10/2020).

[28] ESA. *eoPortal Directory: COSMO-SkyMed.* 2020. URL: https://directory.eoportal.org/web/eoportal/satellite-missions/c-missions/cosmo-skymed (visited on 06/11/2020).

[29] ESA. *eoPortal Directory: COSMO-SkyMed Second Generation.* 2020. URL: https://directory.eoportal.org/web/eoportal/satellite-missions/c-missions/cosmo-skymed-second-generation (visited on 06/11/2020).

[30] ESA. *eoPortal Directory: RCM (RADARSAT Constellation Mission).* 2020. URL: https://directory.eoportal.org/web/eoportal/satellite-missions/r/rcm (visited on 06/11/2020).

[31] ESA. *eoPortal Directory: SAOCOM (SAR Observation and Communications Satellite) Constellation.* 2020. URL: https://directory.eoportal.org/web/eoportal/satellite-missions/s/saocom (visited on 07/11/2020).

[32] ESA. *eoPortal Directory: Sentinel-1.* 2020. URL: https://directory.eoportal.org/web/eoportal/satellite-missions/c-missions/copernicus-sentinel-1 (visited on 07/10/2020).

[33] ESA. *eoPortal Directory: Sentinel-2.* 2020. URL: https://directory.eoportal.org/web/eoportal/satellite-missions/c-missions/copernicus-sentinel-2 (visited on 07/10/2020).

[34] ESA. *eoPortal Directory: Sentinel-3.* 2020. URL: https://directory.eoportal.org/web/eoportal/satellite-missions/c-missions/copernicus-sentinel-3 (visited on 06/11/2020).

[35] ESA. *ICEYE Constellation of SAR X-band microsatellites.* 2020. URL: https://directory.eoportal.org/web/eoportal/satellite-missions/i/iceye-constellation (visited on 09/11/2020).

[36] ESA. *PRISMA (Hyperspectral Precursor and Application Mission).* 2020. URL: https://directory.eoportal.org/web/eoportal/satellite-missions/p/prisma-hyperspectral (visited on 10/11/2020).

[37] ESA. *What is Galileo?* URL: https://www.esa.int/Applications/Navigation/Galileo/What_is_Galileo (visited on 02/01/2021).

[38] The European Commission's science EU Science Hub and knowledge service. *Monitoring Agricultural ResourceS (MARS).* 2016. URL: https://ec.europa.eu/jrc/en/mars (visited on 05/25/2020).

[39] *EUGENIUS website.* 2017. URL: https://www.eugenius-asso.eu/about1.html# (visited on 05/25/2020).

[40] FAO. *CHAPTER 2: CROP WATER NEEDS.* URL: http://www.fao.org/3/s2022e/s2022e02.htm (visited on 02/20/2021).

[41] FAO. *CHAPTER 3: DETERMINATION OF THE IRRIGATION SCHEDULE FOR CROPS OTHER THAN RICE*. URL: http://www.fao.org/3/t7202e/t7202e06.htm (visited on 02/20/2021).

[42] Farms.com. *Precision Agriculture Economics*. URL: https://www.farms.com/precision-agriculture/economics/ (visited on 03/25/2021).

[43] P Ferrazzoli. "SAR for agriculture: Advances, problems and prospects". In: *Retrieval of Bio-And Geo-Physical Parameters from SAR Data for Land Applications*. Vol. 475. 2002, pp. 47–56.

[44] Africa Ixmuca Flores-Anderson et al. "The SAR Handbook: Comprehensive Methodologies for Forest Monitoring and Biomass Estimation". In: (2019).

[45] Jonathan A Foley et al. "Solutions for a cultivated planet". In: *Nature* 478.7369 (2011), pp. 337–342.

[46] Food and Agriculture Organization of the United Nations. *Global agriculture towards 2050*. Last visit April 2020. 2009. URL: http://www.fao.org/fileadmin/templates/wsfs/docs/Issues_papers/HLEF2050_Global_Agriculture.pdf.

[47] Food and Agriculture Organization of the United Nations. *How to Feed the World in 2050*. Last visit April 2020. 2009. URL: http://www.fao.org/fileadmin/templates/wsfs/docs/expert_paper/How_to_Feed_the_World_in_2050.pdf.

[48] Food and Agriculture Organization of the United Nations. *Land Use, Irrigation and Agricultural Practices: 1961-2017*. Last visit April 2020. 2019. URL: http://www.fao.org/economic/ess/environment/data/land-use/en/.

[49] Food and Agriculture Organization of the United Nations. *FAOSTAT*. 2020. URL: http://www.fao.org/faostat/en/#data (visited on 05/25/2020).

[50] Food and Agriculture Organization of the United Nations. *Food and Agriculture Data*. Last visit April 2020. 2020. URL: http://www.fao.org/faostat/en/#data.

[51] Ministero delle politiche agricole alimentari e forestali. *Statistiche meteo-climatiche*. URL: https://www.politicheagricole.it/flex/FixedPages/Common/miepfy700_riferimentiAgro.php/L/IT?parm1=0326&%20parm2=1722&%20parm3=spra&%20name=R&%20period=10a&%20nomeParam=Precipitazione&wdLOR=c3485FB01-D49D-452A-B75D-B833BA601CF5 (visited on 02/20/2021).

[52] Angelo Frascarelli. "Impatto economico dell'agricoltura di precisione". In: *Consiglio Nazionale delle Ricerche* (2018).

[53] Angelo Frascarelli. *L'analisi economica dell'agricoltura di precisione: criteri generali e applicazione a un'azienda maidicola*. 2018. URL: https://agriregionieuropa.univpm.it/it/content/article/31/53/lanalisi-economica-dellagricoltura-di-precisione-criteri-generali-e (visited on 03/25/2021).

[54] Massimo Gargano. "SICCITA' INVERNALE, NUOVI RISCHI PER L'AGRICOLTURA". In: *ECOSCIENZA, Numero 4, Anno 2017*. ECOSCIENZA, 2017, p. 2.

[55] GEOGLAM. *About GEOGLAM*. 2020. URL: http://earthobservations.org/geoglam.php (visited on 05/25/2020).

[56] GEOGLAM. *GEO Global Agricultural Monitoring Flagship Initiative (GEOGLAM). Implementation Plan for the GEO Work Programme 2020-2022*. Last visit April 2020. URL: `http://earthobservations.org/geoglam_resources/1%20Home/Planning%20and%20Reporting/GEOGLAM%202020-2022%20WkPln.pdf`.

[57] Francesco Giannetti. *Agricoltura di precisione: vantaggi e svantaggi delle nuove tecnologie in agricoltura*. 2018. URL: `https://www.consulenteagricolo.it/agricoltura-di-precisione/` (visited on 03/25/2021).

[58] terra e vita Giuseppe Cillo. *Fertilizzazione, se Ã¨ precisa Ã¨ piÃ¹ efficace e si risparmia*. 2017. URL: `https://terraevita.edagricole.it/nova/nova-agricoltura-di-precisione/fertilizzazione-precisa-si-risparmia/` (visited on 02/20/2021).

[59] GreenPatrol. *GreenPatrol website*. 2017. URL: `https://www.greenpatrol-robot.eu` (visited on 03/18/2021).

[60] R Hadria et al. "Monitoring of irrigated wheat in a semi-arid climate using crop modelling and remote sensing data: Impact of satellite revisit time frequency". In: *International Journal of Remote Sensing* 27.6 (2006), pp. 1093–1117.

[61] David Herring. *Precision Farming*. 2001. URL: `https://earthobservatory.nasa.gov/features/PrecisionFarming` (visited on 05/25/2020).

[62] Simeng Huang. *Multi-Phase Mission Analysis and Design for Satellite Constellation with Low-Thrust Propulsion*. Ph.D. Thesis, Politecnico di Milano, Supervisor: Colombo, C. 2021. URL: `https://www.politesi.polimi.it/handle/10589/169779`.

[63] I.Stat. *Agricoltura*. 2020. URL: `http://dati.istat.it/` (visited on 12/17/2020).

[64] I.Stat. *Andamento dell'Economia Agricola, Anno 2019*. 2020. URL: `https://www.istat.it/it/files/2020/05/Andamento-%20economia-agricola-2019.pdf` (visited on 12/08/2020).

[65] I.Stat. *Prodotto interno lordo lato produzione*. 2020. URL: `http://dati.istat.it/Index.aspx?%20DataSetCode=DCCN_PILT` (visited on 12/08/2020).

[66] *IL PROGETTO - Progetto Saturno*. URL: `https://www.progettosaturno.it/il-progetto/` (visited on 05/25/2020).

[67] Global Forest Observation Initiative. *A Layman Interpretation Guide to L-band and C-band Synthetic Aperture Radar data*.

[68] ISTAT. *6Â° Censimento Generale dell'Agricoltura. UTILIZZO DELLA RISORSA IDRICA AI FINI IRRIGUI IN AGRICOLTURA*. 2014.

[69] ISTAT. *LE STATISTICHE DELL'ISTAT SULL'ACQUA. ANNI 2015-2018*. 2019.

[70] ISTAT. "STRUTTURA E CARATTERISTICHE DELLE UNITA' ECONOMICHE DEL SETTORE AGRICOLO, ANNO 2017". In: *Edizione 2019*. ISTAT, 2019, p. 18.

[71] Christopher R Jackson and John R Apel. "Synthetic aperture radar: marine user's manual". In: (2004).

[72]   Aleem Khaliq, Leonardo Peroni, and Marcello Chiaberge. "Land cover and crop classi-
       fication using multitemporal sentinel-2 images based on crops phenological cycle". In:
       *2018 IEEE Workshop on Environmental, Energy, and Structural Monitoring Systems
       (EESMS)*. IEEE. 2018, pp. 1–5.

[73]   Koetz et al. *SEN4CAP Sentinels for CAP monitoring approach*. 2019. URL: `https :
       //ec.europa.eu/jrc/sites/jrcsh/files/14-sen4cap.pdf`.

[74]   Chang-an LIU et al. "Research advances of SAR remote sensing for agriculture applica-
       tions: A review". In: *Journal of Integrative Agriculture* 18.3 (2019), pp. 506–525.

[75]   MathWorks. *poly2mask Documentation*. 2002. URL: `https://www.mathworks.com/
       help/images/ref/poly2mask.html` (visited on 06/10/2020).

[76]   MathWorks. *How the Genetic Algorithm Works*. 2021. URL: `https://www.mathworks.
       com/help/gads/how-the-genetic-algorithm-works.html` (visited on 03/14/2020).

[77]   MathWorks. *What is the Genetic Algorithm?* 2021. URL: `https://www.mathworks.
       com/help/gads/what-is-the-genetic-algorithm.html` (visited on 03/14/2020).

[78]   Alex McBratney et al. "Future directions of precision agriculture". In: *Precision agri-
       culture* 6.1 (2005), pp. 7–23.

[79]   SW McCandless Jr and CR Jackson. "Principles of Synthetic Aperture Radar, Chapter
       1". In: *US Department of Commerce: National Oceanic and Atmospheric Administration,*
       (2005), pp. 1–23.

[80]   Pisante. Michele and Giuseppe Cillo. *Agricoltura di precisione: sfide e opportunitÃ*.
       2018. URL: `https://agriregionieuropa.univpm.it/it/content/article/31/
       53/agricoltura-di-precisione-sfide-e-opportunita` (visited on 03/25/2021).

[81]   Alberto Moreira. "Synthetic aperture radar (SAR): Principles and applications". In: *The
       4th Advance Training Course in Land Remote Sensing* (2013), pp. 1–5.

[82]   Emily Myers et al. "Assessing the impact of satellite revisit rate on estimation of corn
       phenological transition timing through shape model fitting". In: *Remote Sensing* 11.21
       (2019), p. 2558.

[83]   EUROPEAN DATA JOURNALISM NETWORK. *1.6 million farmers receive almost 85
       percent of the EU's agricultural subsidies*. 2019. URL: `https://www.europeandatajournalism.
       eu/eng/News/Data-news/1.6-million-farmers-receive-almost-85-percent-of-
       the-EU-s-agricultural-subsidies` (visited on 02/20/2021).

[84]   NASA earth observatory. *Data Requirements for Precision Farming*. 2001. URL: `https:
       //earthobservatory.nasa.gov/features/PrecisionFarming/precision_farming5.
       php` (visited on 06/10/2020).

[85]   Sung Wook Paek et al. "Small-satellite synthetic aperture radar for continuous global
       biospheric monitoring: A review". In: *Remote Sensing* 12.16 (2020), p. 2546.

[86]   P Paris et al. "Rapporto nazionale pesticidi nelle acque. Dati 2015- 2016". In: *Edizione
       2018: Rapporti 282/2018*. ISPRA Italia, 2018, p. 100.

[87] GH Peters and Prabhu Pingali. *Tomorrow's Agriculture: Incentives, Institutions, Infrastructure and Innovations-Proceedings of the Twenty-fouth International Conference of Agricultural Economists: Incentives, Institutions, Infrastructure and Innovations-Proceedings of the Twenty-fouth International Conference of Agricultural Economists.* Routledge, 2018.

[88] T Riedel. *Biosphere-Agricultural Applications with SAR Data.*

[89] Michael Robertson, Peter Carberry, and Lisa Brennan. *Economic benefits of precision agriculture Case studies from Australian grain farms.* 2008. URL: `https://grdc.com.au/resources-and-publications/grdc-update-papers/tab-content/grdc-update-papers/2008/02/economic-benefits-of-precision-agriculture-case-studies-from-australian-grain-farms` (visited on 03/25/2021).

[90] Kverneland Group Italia S.r.l. *QUALI VANTAGGI ECONOMICI DALL'AGRICOLTURA DI PRECISIONE?* 2020.

[91] SA Sarmap. "Synthetic Aperture Radar and SARscape: SAR Guidebook". In: *Sarmap SA: Purasca, Switzerland* (2009), p. 274.

[92] *SatAgro website.* 2020. URL: `https://www.satagro.pl/#start` (visited on 05/25/2020).

[93] R Schrijver, K Poppe, and C Daheim. "Precision agriculture and the future of farming in Europe". In: *Science and Technology Options Assessment. Brussels. http://www. ep. europa. eu/stoa* (2016).

[94] Remco Schrijver, Krijn Poppe, and Cornelia Daheim. "L'agricoltura di precisione e il futuro dell'agricoltura in Europa. Studio prospettico scientifico". In: *EPRS, Servizio Ricerca del Parlamento europeo. Unità Prospettiva scientifica (STOA)* (2016).

[95] *Sen4CAP - Sentinels for Common Agriculture Policy.* 2017. URL: `http://esa-sen4cap.org/` (visited on 05/25/2020).

[96] TD Setiyono et al. "Rice yield estimation using synthetic aperture radar (SAR) and the ORYZA crop growth model: development and application of the system in South and South-east Asian countries". In: *International Journal of Remote Sensing* 40.21 (2019), pp. 8093–8124.

[97] Jiali Shang et al. "Application of multi-frequency synthetic aperture radar (SAR) in crop classification". In: *Advances in geoscience and remote sensing.* IntechOpen, 2009.

[98] terra e vita Simone Martarello. *Agricoltura di precisione: "Tutti possono cambiare passo".* 2020. URL: `https://terraevita.edagricole.it/nova/nova-agricoltura-di-precisione/agricoltura-di-precisione-ibf/` (visited on 02/23/2021).

[99] Henning Skriver et al. "Crop classification using short-revisit multitemporal SAR data". In: *IEEE Journal of Selected Topics in Applied Earth Observations and Remote Sensing* 4.2 (2011), pp. 423–431.

[100] Marco Sozzi et al. "Benchmark of satellites image services for precision agricultural use". In: *Proceedings of the AgEng Conference, Wageningen, The Netherlands.* 2018, pp. 8–11.

[101] Zheng Sun, Di Wang, and Geji Zhong. "A review of crop classification using satellite-based polarimetric SAR imagery". In: *2018 7th International Conference on Agro-geoinformatics (Agro-geoinformatics)*. IEEE. 2018, pp. 1–5.

[102] EGNOS User Support. *EGNSS4CAP app employs EGNOS to support farmers with the Common Agricultural Policy*. 2020. URL: `https://egnos-user-support.essp-sas.eu/new_egnos_ops/news-events/news/egnss4cap-app-employs-egnos-support-farmers-common-agricultural-policy` (visited on 03/18/2021).

[103] *talkingalkingfields Products*. Last visit April 2020. 2017. URL: `www.talkingfields.de`.

[104] David A Vallado. *Fundamentals of astrodynamics and applications*. Vol. 12. Springer Science & Business Media, 2001.

[105] Roxana Vintila et al. "Monitoring crop status at the field scale using high revisit frequency satellite observations". In: *Proc. ISPMSRS "Int. Symp. Physical Measurements & Signatures Remote Sens.* 2005, pp. 1682–1750.

[106] John G Walker. *Continuous whole-earth coverage by circular-orbit satellite patterns*. Tech. rep. Royal Aircraft Establishment Farnborough (United Kingdom), 1977.

[107] European Commission website. *A European Green Deal: Striving to be the first climate-neutral continent*. 2021. URL: `https://ec.europa.eu/info/strategy/priorities-2019-2024/european-green-deal_en` (visited on 03/14/2020).

[108] James R Wertz, David F Everett, and Jeffery J Puschell. *Space mission engineering: the new SMAD*. Microcosm Press, 2011.

[109] JR Wertz. *Orbit & Constellation Design & Management, second printing ed. El Segundo*. 2009.

[110] Mike G Wooding et al. "Satellite Radar in Agriculture. Experience with ERS-1." In: *ESA Scientific Publications. ISBN 92-9092-339-3.* (1995).

[111] Pablo J Zarco-Tejada, N Hubbard, and Ph Loudjani. "Precision agriculture: An opportunity for EU farmer–Potential support with the CAP 2014-2020". In: *Joint Research Centre (JRC) of the European Commission* (2014).

[112] Xiaoyang Zhang, Mark A Friedl, and Crystal B Schaaf. "Sensitivity of vegetation phenology detection to the temporal resolution of satellite data". In: *International Journal of Remote Sensing* 30.8 (2009), pp. 2061–2074.

Nomenclature

Acronyms

ADCS Attitude Dynamics and Control System

ASI   Agenzia Spaziale Italiana

BOL   Beginning Of Life

CAP   Common Agricultural Policy

CONAE Comision Nacional de Actividades Espaciales

DOC   Denominazione di Origine Controllata

DORIS Doppler Orbitography and Radiopositioning Inegrated by Satellite

EOL   End Of Life

EPS   Electric Power System

ESA   European Space Agency

EU   European Union

EVI   Enhanced Vegetation Index

FAO   Food and Agriculture Organization

GDP   Gross Domestic Product

GEOGLAM Group on Earth Observations Global Agricultural Monitoring

GHG   Greenhouse gasses

GIS   Geographic Information System

GNSS   Global Navigation Satellite System

GPS   Global Positioning System

IGT   Indicazione Geografica Tipica

ISPRA Istituto Superiore per la Protezione e la Ricerca Ambientale

ISTAT Istituto Nazionale di Statistica

JAXA Japan Aerospace Exploration Agency

JRC   Joint Research Centre

LAI   Leaf Area Index

LEO   Low Earth Orbit

LPIS   Land Parcel Identification System

LRR   Laser Retroreflector

MARS Monitoring Agricultural ResourceS

MIMICS Michigan Microwave Canopy Scattering)

MWR Microwave Radiometer

NA   Not Available

NASA National Aeronautic and Space Administration

NDVI Normalized Difference Vegetation Index

NRC   National Resource Council

OBDH On-board Data Handling

OLCI Land Cover Instrument

PA   Precision Agriculture

PRF   Pulse Repetition Frequency

PRIMA Piattaforma Italiana Multi Applicativa

PRISMA PRecursore IperSpettrale della Missione Applicativa

RCM   RADARSAT Constellation Mission

RF   Radio Frequency

SAR   Synthetic Aperture Radar

SLAR Side Looking Aperture Radar

SRP   Solar Radiation Pressure

SSO   Sun-synchronous Orbit

TAS-I Thales Alenia Space Italia S.p.A.

TT&C Telemetry, Tracking and Command

UAA Utilised Agricultural Area

VRA Variable Rate Applications

WTM Water Cloud Model

List of Symbols

P_Ω Orbit nodal period [s]

α_{ecl} Fraction of orbital revolution under eclipse [rad]

β Signal beamwidth [Hz]

$\ddot{\mathbf{r}}$ Satellite acceleration vector in Cartesian coordinates [km^2/s^2]

$\ddot{r}_i$ Modulus of i coordinate of satellite acceleration in Cartesian coordinates

$\Delta\Omega_{S/C}$ Relative RAAN between a pair of satellites [rad]

$\Delta u_{S/C}$ Relative argument of latitude between a pair of satellites [rad]

Δv Change in velocity for station-keeping and end-of-life manoeuvres [km/s]

Δv_{EoL} Change in velocity for end-of-life disposal of constellations [km/s]

Δv_{keep} Change in velocity for station-keeping [km/s]

$\Delta\lambda_{rev}$ Ground track angular spacing [deg]

δ_R SAR resolution in range direction [m]

δ_{AT} SAR resolution in along track direction [m]

$\dot{\Omega}$ Right ascension of the ascending node variation [deg/s]

$\dot{\omega}$ Pericenter anomaly variation [deg/s]

$\dot{\Omega}_{SS}$ Right ascension of the ascending node variation for a Sun-synchronous orbit [deg/s]

$\dot{M}$ Mean anomaly variation [deg/s]

$\dot{M}_0$ Initial mean anomaly variation [deg/s]

η SAR antenna efficiency

$\frac{m_{SC}}{C_D A}$ Ballistic coefficient [kg/m^2]

$\hat{\mathbf{i}}$ First unit vector in Cartesian coordinates

$\hat{\mathbf{j}}$ Second unit vector in Cartesian coordinates

$\hat{\mathbf{k}}$ Third unit vector in Cartesian coordinates

λ SAR Wavelength [cm]

$\mathbf{a}_{J_2}$ J_2 effect's perturbation acceleration in Cartesian coordinates $[m/s^2]$

$\mathbf{lb}_i$ Lower bound for the design variables used in the optimisation

$\mathbf{r}$ Satellite position vector in Cartesian coordinates [km]

$\mathbf{ub}_i$ Upper bound for the design variables used in the optimisation

$\mathbf{x}_{RGT}$ Optimisation design vector, repeated-ground track case

$\mathbf{x}_{SSORGT}$ Optimisation design vector, Sun-synchronous repeated-ground track case

μ Earth gravitational parameter $[km^3/s^2]$

$\omega_\oplus$ Earth angular speed [rad/s]

ϕ_{site} Latitude of launch site [rad]

Ψ Constellation miss distance [rad]

ψ Satellite pair miss distance [rad]

ρ Atmospheric density

σ Radar target cross section

τ_i Uncompressed initial duration

θ SAR access angle [deg]

θ_{MAX} SAR antenna maximum access angle [deg]

θ_{min} SAR antenna minimum access angle [deg]

ζ Random value

a Orbit semi-major axis [km]

A_C Free space attenuation

a_f Final semi-major axis after altitude decay [km]

a_n Semi-major axis of normal orbit [km]

a_{i-J_2} Modulus of i coordinate of acceleration due to J_2 perturbation effect in Cartesian coordinates $[m/s^2]$

A_{mr} Attenuation of troposphere

A_{PHY} Attenuation introduced by line/waive guide [K]

A_{real} Field real area [ha]

A_{SAR} SAR antenna area $[m^2]$

A_{SAR}^{min} Minimum SAR antenna area $[m^2]$

B Bandwidth [Hz]

c Speed of light [m/s]

cov Coverage parameter

D_R SAR antenna dimension in range direction [m]

D_{AT} SAR antenna dimension in along track direction [m]

d_{gross} Crop gross irrigation depth [cm]

d_{net} Crop approximate net irrigation depth [cm]

e Orbit eccentricity

ea Efficiency of water irrigation application

F Angular separation [PU]

F Noise factor

f_R Pulse repetition frequency [Hz]

G SAR antenna gain

h Satellite altitude from ground [km]

h_{max} Constellation maximum height [km]

h_{min} Constellation minimum height [km]

i Orbit inclination [rad]

J_2 First zonal harmonics coefficient

J_i Cost function

j_{SSORGT} Design variables used in optimisation, Sun-synchronous case

k_B Boltzmann constant

$k_{day2rep}$ Number of days before orbit's ground track repeats itself [days]

$k_{rev2rep}$ Number of orbital revolutions before orbit's ground track repeats itself

l Square side [m]

lch_h Cost of orbit injection [km]

lch_i Payload capability [rad]

m_{SC} Spacecraft mass [kg]

$N_{acqui,i}^{max}$ Satellites maximum number of SAR acquisitions

$N_{acqui,i}^{TOT}$ Constellation total number of SAR acquisitions

N_{irr} Number of irrigation applications over the growing period

n_{SA} Number of elements that comprises the synthetic aperture

N_{SC} Number of satellites

$N_{squares}$ Number of squares

opp Constellation collision opportunity parameter

opp_{lb} opp lower boundary

opp_{ub} opp upper boundary

P Number of orbital planes

P_k Orbit anomalistic period [s]

P_r SAR antenna power received [W]

P_t SAR antenna power transmitted [W]

$P_{\theta G}$ Nodal Period of Greenwich [s]

R SAR target distance [km]

r Modulus of satellite position vector in Cartesian coordinates [km]

r_i Modulus of i coordinate of satellite position vector in Cartesian coordinates [km]

r_p Perigee radius of disposal orbit [km]

$R_\oplus$ Earth radius

SNR Signal to noise ratio

T Effective noise temperature [K]

T_0 Reference temperature [K]

T_A Atmospheric temperature [K]

T_C Free space temperature [k]

T_E Sidereal day [s]

T_s Time over which the synthetic aperture is formed [s]

T_y Sidereal year [s]

t_{cov} Time to get to the maximum coverage [days]

T_{crop} Crop growing period duration [days]

t_{ecl} Eclipse time [s]

t_{irr} Crop Irrigation Interval [days]

$T_{LN/WG}$ Line/waive guide physical temperature [K]

T_{LNA} Low-noise amplifier temperature [K]

T_{mr} Mean radiating temperature [K]

T_{PHY} Physical temperature of line/waive guide [K]

t_{rev} Constellation revisit time [days]

t_{SAR} SAR acquisition time [s]

$target_{cov,i}$ Target coverage in zone i

v Satellite's velocity [km/s]

W_g SAR ground swath [km]

W_{need} Crop water need during the growing period [mm]

Acknowledgements